AD-A082 005 NIELSEN ENGINEERING AND RESEARCH INC MOUNTAIN VIEW CALIF F/G 20/4
THE RAPID PREDICTION OF AIRCRAFT STORE LOADING DISTRIBUTIONS AT--ETC(U)
OCT 79 A J CRISALLI, S S STAHARA, M J HEMSCH F44620-75-C-0047
UNCLASSIFIED NEAR-TR-204 AFOSR-TR-79-1282 NL

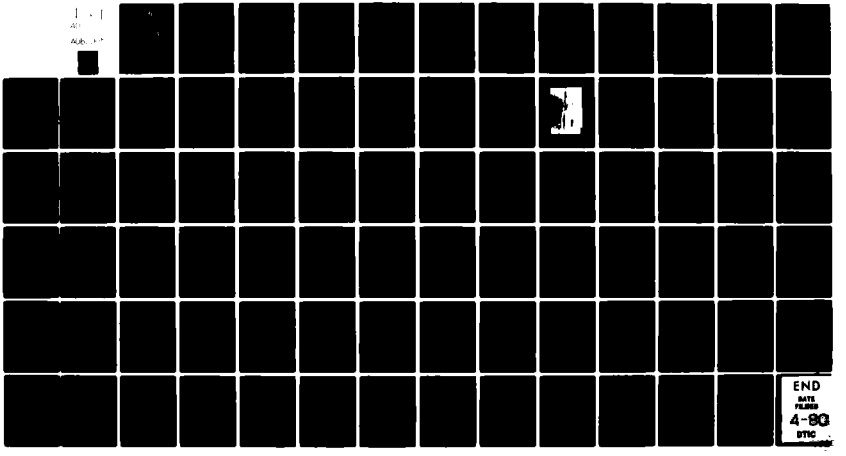

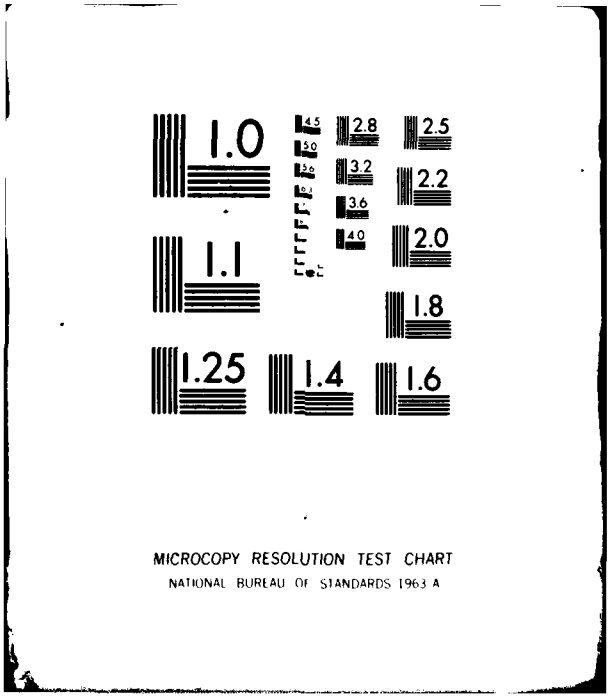
1.0
1.1
1.25
1.4
1.6
1.8
2.0
2.2
2.5
2.8
3.2
3.6
4.0
4.5
5.0
5.6
MICROCOPY RESOLUTION TEST CHART
NATIONAL BUREAU OF STANDARDS 1963 A

AFOSR-TR- 79-1232

LEVEL II

12

AD A082005

THE RAPID PREDICTION OF AIRCRAFT STORE LOADING DISTRIBUTIONS AT TRANSONIC SPEEDS

by

A. J. Crisalli, S. S. Stahara,
and M. J. Hemsch

DTIC
ELECTE
MAR 1 4 1980
S D
C

NEAR TR 204
October 1979

Approved for public release;
distribution unlimited.

Prepared under Contract No. F44620-75-C-0047

for

AIR FORCE OFFICE OF SCIENTIFIC RESEARCH
Washington, D.C. 20332

by

NIELSEN ENGINEERING & RESEARCH, INC.
510 Clyde Avenue, Mountain View, CA 94043
Telephone (415) 968-9457

79 12 18 33

UNCLASSIFIED Unclassified
SECURITY CLASSIFICATION OF THIS PAGE (When Data Entered)

REPORT DOCUMENTATION PAGE	READ INSTRUCTIONS BEFORE COMPLETING FORM
1. REPORT NUMBER: AFOSR-TR-79-1282	2. GOVT ACCESSION NO.
3. RECIPIENT'S CATALOG NUMBER	
4. TITLE (and Subtitle): THE RAPID PREDICTION OF AIRCRAFT STORE LOADING DISTRIBUTIONS AT TRANSONIC SPEEDS. Part II.	5. TYPE OF REPORT & PERIOD COVERED: FINAL rept. 1 Jan 75 - 30 Sep 79
	6. PERFORMING ORG. REPORT NUMBER: NEAR TR-204
7. AUTHOR(s): ANTHONY J. CRISALLI, STEPHEN S. STAHARA, MICHAEL J. HEMSCH	8. CONTRACT OR GRANT NUMBER(s): F44620-75-C-0047
9. PERFORMING ORGANIZATION NAME AND ADDRESS: NIELSEN ENGINEERING & RESEARCH, INC, 510 CLYDE AVE, MOUNTAIN VIEW, CA 94043	10. PROGRAM ELEMENT, PROJECT, TASK AREA & WORK UNIT NUMBERS: 2307A1, 61102F, A1
11. CONTROLLING OFFICE NAME AND ADDRESS: AIR FORCE OFFICE OF SCIENTIFIC RESEARCH/NA, BLDG 410, BOLLING AIR FORCE BASE, D C 20332	12. REPORT DATE: Oct 79
	13. NUMBER OF PAGES: 79
14. MONITORING AGENCY NAME & ADDRESS (if different from Controlling Office)	15. SECURITY CLASS. (of this report): UNCLASSIFIED
	15a. DECLASSIFICATION/DOWNGRADING SCHEDULE

16. DISTRIBUTION STATEMENT (of this Report)

Approved for public release; distribution unlimited.

17. DISTRIBUTION STATEMENT (of the abstract entered in Block 20, if different from Report)

18. SUPPLEMENTARY NOTES

19. KEY WORDS (Continue on reverse side if necessary and identify by block number)

TRANSONIC FLOW
WING-BODY/PYLON/STORE COMBINATIONS
EXTERNAL STORE LOADING DISTRIBUTIONS

20. ABSTRACT (Continue on reverse side if necessary and identify by block number)

An account is provided of the progress made in the development of an engineering predictive method for determining loading distributions on external stores located in the three-dimensional transonic flow field of a parent aircraft. Attention has been directed toward developing accurate but rapid methods for predicting store loadings in transonic flow fields generated by wing-body/pylon combinations representative of modern fighter-bomber aircraft. Detailed evaluations, based on extensive comparisons with experimental data obtained from a parallel wind-tunnel test phase of the program, are presented for two store

DD FORM 1 JAN 73 1473 EDITION OF 1 NOV 65 IS OBSOLETE

UNCLASSIFIED 37978

SECURITY CLASSIFICATION OF THIS PAGE (When Data Entered)

loading prediction methods. Results are provided for various wing-body/pylon/store configurations for flow conditions throughout the transonic regime. The theoretical loading-prediction methods are based on nonuniform crossflow slender-body theory for $M_\infty < 1$ and nonuniform crossflow source-doublet theory for $M_\infty > 1$. The three-dimensional nonuniform parent-generated flow fields in which the stores are immersed were approximated by three-dimensional paneling method solutions. This was done in this initial application since both loading-prediction methods employed depend only on the lateral velocity components of the wing-body/pylon flow field; and prior work under this program indicated that linear three-dimensional paneling method solutions are capable of providing remarkably accurate predictions of the parent-generated upwash and sidewash for the configurations and transonic flow conditions considered. The results indicate that while the overall accuracy of such an engineering loading-prediction method is reasonable, discrepancies due to large gradient effects (not necessarily transonic) induced by the pylon leading and trailing edges, and possibly from wing trailing-edge shocks, require further development of the loading-prediction method. These improvements, as well as several improvements associated with the parent flow-field prediction method, are discussed.

TABLE OF CONTENTS

Accession For
NTIS GRA&I
DDC TAB
Unannounced
Justification
By
Distribution/
Availability Codes
Dist | Avail and/or special
A

AIR FORCE OFFICE OF SCIENTIFIC RESEARCH (AFSC)
NOTICE OF TRANSMITTAL TO DDC
This technical report has been reviewed and is approved for public release IAW AFR 190-12 (7b).
Distribution is unlimited.
A. D. BLOSE
Technical Information Officer

THE RAPID PREDICTION OF AIRCRAFT STORE LOADING DISTRIBUTIONS AT TRANSONIC SPEEDS

by

A. J. Crisalli, S. S. Stahara,
and M. J. Hemsch

1. INTRODUCTION

The purpose of this report is to describe in detail the progress made in the development of a rapid technique for the prediction of loading distributions on external aircraft stores at transonic speeds. In a previous report (ref. 1), the progress made on the development of an engineering predictive method for determining three-dimensional transonic flow fields about wing-body/pylon combinations was determined, and represented the first step in the determination of store trajectories released from aircraft operating at transonic speeds. The second step is the development of a suitable method for the calculation of store loading distributions in those flow fields. The third step is the actual determination of the trajectories of the stores by integrating the six-degree-of-freedom equations of motion subject to the computed aerodynamic loads.

The purpose of this report is to review the work on the second step of the transonic store problem as performed under AFOSR Contract No. F44620-75-C-0047. Both the experimental and theoretical predictive techniques will be analyzed and evaluated by comparing them with the experimental data for stores in both attached or separated positions relative to a simplified parent aircraft configuration representative of modern fighter-bombers. Suggestions for improvements of the current methodology will then be presented.

2. EXPERIMENTAL WORK

The experimental data used in the evaluation of the transonic store loading predictive techniques discussed in this report were taken from the AEDC 4T wind-tunnel test described in detail in volume I of the three

volume data report provided in references 2-4. These tests included both flow-field and store loading-distribution data. Data from a previous wind-tunnel test (ref. 5), which did not involve stores, was used to evaluate the flow-field predictive methods (ref. 1). Here we provide a brief description of the wind-tunnel tests described in references 2-4 with emphasis on the store loading-distribution data.

Figure 1 shows the body-fixed coordinate system which is used both throughout this report and the wind-tunnel test report. Figure 2 shows planform and cross-sectional views, including key geometrical locations, of the wing-body/pylon/store model which was used throughout the wind-tunnel tests and in the evaluation of the predictive techniques discussed in this report. Figure 3 shows a photograph of the wing-body model in combination with a wing-mounted pylon and an instrumented pressure store which is sting-mounted on the Captive Trajectory System (CTS) in the AEDC 4T tunnel. Loading distributions on the store were calculated by integrating the experimentally-measured surface pressures. Note that there are no fins on the model stores.

In the wind-tunnel test described in references 2-4 the wing-body in combination with various pylon and store arrangements was tested at four free-stream Mach numbers, M_∞ = 0.925, 0.950, 1.050 and 1.10 and three angles of attack $\alpha = 0^o$, 2^o, and 5^o. The experimental procedure involved attaching pylon and store models to the wing-body combination in two separate systematic model-buildup test series. At each stage of the first series, flow velocities and static pressures were taken for the wing-body/pylon configuration in those regions normally occupied by an attached or initially-separated store. Additionally, force/moment/surface pressure measurements were taken on the wing-body model. To provide outer flow-field information, flow velocities and static pressure measurements were taken on a cylindrical control surface as far removed from the tunnel centerline as possible.

The second model-buildup test series involved a special pressure-instrumented store that was mounted on the Captive Trajectory System and positioned in normal store-attached locations and also at various distances away from the pylon in order to simulate a separated store. At each stage of this sequence, detailed pressure distributions on the

instrumented store were obtained from a single row of pressure taps by rolling the store through 360° at 10° roll-angle increments. Figure 4 shows detailed views of the instrumented pressure store and the dummy store together with their dimensions and other geometric details, including the locations of the 19 pressure orifices of the instrumented store.

Figure 5 shows a cross-sectional view of the various wing-body/pylon/store configurations for which store surface-pressure data were obtained at various Mach numbers and angles of attack. The first configuration [fig. 5(a)] consists of the store alone. The second configuration [fig. 5(b)] as used for the $M_\infty = 1.10$ tests consists of the instrumented store located in the normal "store-attached" position and three store-detached positions under the fuselage pylon. The third configuration [fig. 5(c)] consists of the instrumented store located in the normal "store-attached" position and three store-detached positions under the wing pylon. A side view of the four positions of the instrumented pressure store for the wing-pylon/store configuration used for $M_\infty = 1.10$ is shown in figure 6. In order to study the increasing lateral influence on the store of shock waves emanating from the wing leading edge of the wing-body at higher supersonic free-stream Mach numbers, the vertical locations below the fuselage and wing pylons of the pressure store at $M_\infty = 0.925$, 0.950, and 1.050 were selected to differ from those for $M_\infty = 1.10$ in that the interval of separation between the first three positions is one store radius for the first three Mach numbers and one store diameter for $M_\infty = 1.10$. Note that the instrumented store in position 1 ("store-attached") was actually at a small distance (less than 0.10 inch) from the pylon in order to insure no contact with the pylons as the store was rolled.

In the following section the theoretical method will be briefly reviewed and then evaluated by comparing the experimental values of the normal- and side-force distributions with the theoretical predictions. A more detailed discussion of the wind-tunnel tests including flow-field data, data uncertainties and wind-tunnel wall effects can be found in the flow-field report, reference 1, and the data reports, references 2-5.

3. COMPUTATION OF STORE-LOADING DISTRIBUTIONS BASED ON NONUNIFORM CROSSFLOW THEORY AND THREE-DIMENSIONAL LINEAR PANELING-METHOD SOLUTIONS

3.1 Introduction

The three-dimensional linear method for calculating store-loading distributions initially developed in references 6 and 7 is based on employing linear paneling method solutions for the flow field due to the parent. The lateral force distributions on a store which is separated from the parent (i.e., the wing-body/pylon combination) are determined by first calculating the flow field in the vicinity of the parent aircraft at the store position but with the store absent. The force distribution on the store is then determined by slender-body theory for $M_\infty < 1$ or source-doublet theory for $M_\infty > 1$ by utilizing the nonuniform crossflow velocity components at the locus of points corresponding to the position that the longitudinal axis of the store would occupy in the flow. Thus, the ability to predict with suficient accuracy the flow field without store in the vicinity of the wing-body/pylon combination is the essential first step in the computation of store loadings and trajectories.

In reference 1 it was found from exensive comparisons with tunnel data that three-dimensional linear-theory paneling methods yielded satisfactory predictions of upwash and sidewash in the vicinity of wing-body/pylon combinations at angles of attack up to 5° (higher angles of attack were not tested) and free-stream Mach numbers, $M_\infty = 0.925$, 0.950, and 1.050. It was also determined that these predictions became less satisfactory as $M_\infty \to 1.0$. Nevertheless, even at $M_\infty = 0.950$ and 1.050 the upwash and sidewash prediction displayed reasonable agreement with the experimental data.

The effectiveness, as shown in reference 1, of paneling methods in providing reasonable upwash and sidewash predictions over a range of transonic free-stream Mach numbers, angles of attack, and wing-body/pylon combinations implies that such linear methods should be investigated as the basis of an economical procedure for the prediction of loadings of stores placed in these flow fields. The methodology previously developed for the subsonic free-stream situation and used in this study is

described in reference 5. That method employs nonuniform slender-body theory to determine store lateral loads. The analogous procedure previously developed for the supersonic free-stream case and also used in this report is described in reference 7. That method employs more accurate but computationally more expensive line-sources and line-doublets placed on the body axis to compute store lateral loads.

3.2 Comparison of Predicted Store Loadings with Data, $M_\infty = 0.925$

Figures 7 to 14 display comparisons of the experimental data with the subsonic theoretical prediction method. Those predictions are based on nonuniform crossflow slender-body theory used together with subsonic paneling-method solutions for the flow field due to the parent alone. Results are given for the normal- and side-force distributions along the pressure store, previously illustrated in figure 4, for free-stream Mach number $M_\infty = 0.925$ and angles of attack $\alpha = 0^\circ$ and 5°. Both the fuselage-store and wing-store configurations are included in the comparisons. The comparisons are indexed with corresponding page and figure numbers in Table I.

Figures 7 to 10 display the normal- and side-force comparisons for the fuselage-store configurations, for which the two store positions used in the comparisons are illustrated in the sketch below.

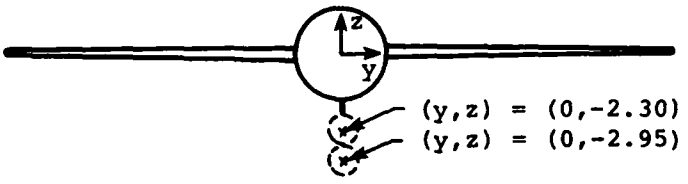

Figures 11 to 14 display the corresponding normal- and side-force comparisons for the wing-store configuration; the two store positions used in those comparisons are shown in the sketch below.

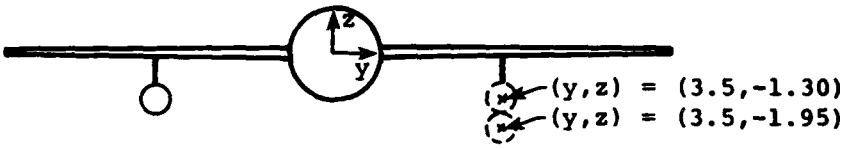

In the above sketches, the two positions of the instrumented store are indicated by the dotted circles. The solid circle denotes a "dummy" store for which no calculations were performed. The first store location corresponds to a store-attached position. The second location corresponds to a store position directly under the attached position but removed vertically from it a distance of one store diameter. The (y,z) locations of the store axial centerlines are also indicated in the diagram. The x location of the store nosetip is the same for both vertical positions, i.e., x = 11.218 inches for the fuselage store and x = 11.967 inches for the wing store.

A scan of the loading comparisons shown in figures 7 to 14 indicates that the theoretical predictions display quite reasonable agreement with the data. At this lowest subsonic Mach number tested, the least satisfactory agreement occurs in the region of the shoulder of the store and along the aft portion of he store in the vicinity of the pylon trailing edges. In these regions there are strong variations in the data which are not properly accounted for by the linear prediction. Further discusion of this point is presented in sections 3.3 and 3.4.

3.3 Comparison of Predicted Store Loadings with Data, $M_\infty = 0.950$

Figures 15 to 22 display similar comparisons of the experimental data with the theoretical predictions of the normal- and side-force distributions along the store for free-stream Mach number $M_\infty = 0.950$ and angles of attack $\alpha = 0^\circ$ and 5°. As in the previous section, both the fuselage-store and wing-store configurations are included in the predictions. The comparisons are indexed with corresponding page and figure numbers in Table I.

A scan of those comparisons (figs. 15-22) yields the same conclusions that were drawn for the $M_\infty = 0.925$ case. Linear theory shows generally reasonable agreement with experiment with the least satisfactory agreement occurring in the loading distributions in the region of the store shoulder and also on the aft portion of the store near the pylon trailing edges.

3.4 Discussion of Theoretical Comparisons for $M_\infty = 0.925$ and $M_\infty = 0.950$

The comparison presented in figures 7-22 are remarkably similar to those previously obtained in the initial application of the loading method for purely subsonic flows (see, for example, fig. 15 of ref. 8). We note that the overall forces are small compared to the peak local forces.

The major discrepancies shown in figures 7-22 between theory and data occur near the shoulder of the store ($x = 13.5$ in. for the wing location and $x = 12.7$ in. for the fuselage location) and near the trailing edge of the pylon ($x = 16.8$ in. for the wing pylon and $x = 16.4$ in. for the fuselage pylon). It is interesting to note that these locations correspond to rapid changes in the first derivative of the axial distributions of the upwash and sidewash (see figs. 49-63 of ref. 1). This behavior is illustrated in figure 23 for two of the configurations tested, both at the same (y,z) location but with different axial locations of the nose tip.

Since slender-body theory predicts linear dependence of loading on both the rate of change with axial distance of the store radius $\frac{da}{dx}$ and local upwash dw/dx, only the data for the cylindrical portion of the store (where $\frac{da}{dx} = 0$) are shown for clarity. Note that the data for the two positions agree very well from $x = 15.8$ in. to the store base, indicating that the flow field without the store present is dominating the store loading. To check the ability of slender-body theory to predict the store loading given an accurate flow-field prediction, the w-versus-x curve shown in figure 23(a) was numerically differentiated. The values of dw/dx obtained, multiplied by a constant, are shown in figure 23(b). The constant was chosen to give the same peak loading. The agreement is good except for the region just aft of the shoulder of the second-position store and downstream of the peak positive loading.

Apparently the steep gradients in upwash are too difficult for slender-body theory to handle, and it appears that the more general source-doublet method is required to account accurately for this effect. Finally, we note that although the paneling method solutions used to simulate the flow field for the comparisons provide only purely subsonic solutions while the data indicate that limited regions of supersonic flow and shocks are present near the store, it is not yet clear to what extent it is necessary to account for these flow features to obtain accurate store loads. It is clear, however, that loading predictions based on slender-body theory cannot treat sharp gradients due to either sudden store surface geometry changes or rapid changes in the parent-generated flow field. The latter could be caused either by shocks or by the presence of abrupt geometry changes, such as associated with pylon tips.

3.5 Comparison of Predicted Store Loadings with Data, $M_\infty = 1.050$

Theoretical predictions of the normal- and side-force distributions found by using nonuniform crossflow line-source and line-doublet theory coupled with supersonic paneling method solutions for the flow field due to the parent alone were compared with data at $M_\infty = 1.050$ for the same wing-body/pylon/store configurations and angles of attack as for the $M_\infty = 0.925$ and $M_\infty = 0.950$ situations. In all of these cases, the theoretical loading predictions exhibit a highly oscillatory behavior.* This is illustrated in figures 24 to 27 which provide comparisons of the theoretical results with data for store-attached (figs. 24,25) and store-separated (figs. 26,27) positions at $\alpha = 0^\circ$ and 5°. These comparisons are indexed in Table I. The fuselage-store comparisons for this Mach number are not presented since the results are similar to those for the wing store.

The oscillatory behavior of the predictions at $M_\infty = 1.050$ is clearly unsatisfactory. The causes of this behavior together with means of improving the predictions for supersonic free-stream Mach numbers near 1 are discussed in the next section.

*Similar oscillations were observed for the previous supersonic store work (ref. 7).

3.6 Discussion of Theoretical Comparisons for $M_\infty = 1.050$

The theoretical normal- and side-force distributions shown in figures 24 to 27 depend directly upon the corresponding theoretical flow-field upwash and sidewash predictions for the parent with store absent. The extent to which the oscillatory behavior of the loading predictions is due to the flow-field behavior is important to ascertain. Figure 28 displays comparisons of the theoretical predictions and data for the upwash and sidewash angles for a typical case, i.e., wing-store attached position, $\alpha = 0^o$. Also shown in that figure is a smooth curve faired through the experimental data which will be discussed shortly. We observe that the flow-field data display a smoother behavior than the flow-field paneling method predictions. It is of interest, therefore, to determine loading predictions on the basis of experimental flow-field data as opposed to paneling method flow fields which were used to predict the results shown in figs. 24 to 27. The loading distributions which result from employing experimental upwash and sidewash distributions are shown in figures 29 to 32. By comparing the distributions in figures 29 to 32, in sequence, with those of figures 24 to 27, we note that a significant improvement is apparent. In particular, the highly oscillatory behavior displayed in figures 24 to 27 has been dampened.

Although a notable improvement is obtained by the use of the smoother experimental flow-field data in computing store loadings, the predictions shown in figures 29 to 32 are still not completely satisfactory. In an attempt to improve this situation further, a smoothed curve as mentioned above was faired through the flow-field upwash data of figure 28(a). The faired curve, which is even smoother than the data, was then used as the basis for computing the normal-force distribution. Although the resulting normal-force distribution shown in figure 33 is smoother than the corresponding distribution in figure 29(a), the agreement with data is actually less satisfactory.

The above investigation illustrates that the oscillatory behavior of the store-loading predictions is closely coupled to any oscillatory behavior of the flow-field. However, the store-loading predictions are quite sensitive to any smoothing of the input flow-field, and a rational means of accomplishing this is necessary. Further development is required in this area.

4. SUMMARY AND CONCLUSIONS

The main conclusion to emerge from this report is that, for free-stream Mach numbers $M_\infty = 0.925$ and 0.950 and angles of attack $\alpha = 0^\circ$ and 5°, the use of subsonic three-dimensional linear paneling method flow-field solutions together with nonuniform-crossflow slender-body theory on the external store yields economical and reasonable predictions of the normal- and side-force distributions on stores without fins for a variety of wing-body/pylon/store combinations considered. The least satisfactory agreement occurs in the same regions in which rapid changes in upwash and sidewash are present in the flow field without the store present. Nevertheless, in view of the economy and rapidity of the linear flow-field methods, the results are considered quite reasonable even at the higher subsonic Mach number considered, $M_\infty = 0.950$.

In the case $M_\infty = 1.050$, the linear theory predictions of the normal- and side-force distributions, based on supersonic three-dimensional linear paneling-method flow-field solutions together with nonuniform-crossflow supersonic source-doublet theory on the external store, exhibit a highly oscillatory behavior. It appears that the oscillations in the loading predictions can be significantly reduced if the corresponding flow-field predictions upon which the loading predictions are based are smoothed in some rational fashion. Since the choice of the smoothing has a crucial effect on the loading predictions, and because it is difficult to perform rationally such solution smoothings a posteriori, a more satisfactory basis would be the development and use of a three-dimensional supersonic paneling method which eliminates the resonance effect leading to these flow-field oscillations.

At this point, it is useful to compare some of the data for the range of Mach numbers tested to determine the importance of transonic effects. Figure 34 shows the upwash for $M_\infty = 0.925$, 0.950, and 1.050 for a typical wing-body/pylon configuration with no store present for $\alpha = 0^\circ$ and 5°. Note that the Mach number effect is small except in the region near the pylon trailing edge ($x = 16.8$ in.) and is stronger for $\alpha = 0^\circ$ than for 5° as would be expected due to the slowing of the flow under the lifting wing.

The loading distributions when a store is inserted into the flow in such a manner that its longitudinal axis corresponds to the survey locations of figure 34 are displayed in figure 35. Note that the transonic effects are quite strong in the region of the pylon trailing edge as would be expected from inspection of figure 34. We make the further observation with reference to the data displayed in figures 34a and 35a, that although the measured gradients in the local flow-field upwash near the pylon leading (x = 13.5 in.) and trailing (x = 16.8 in.) edges are greatest for the M_∞ = 1.050 case, the measured normal-force gradient is largest for the M_∞ = 0.950 flow. For the loading distribution theories employed here and in the previous store work (refs. 6-8), i.e., the nonuniform slender-body crossflow theory for $M_\infty < 1$ and nonuniform crossflow source-doublet theory for $M_\infty > 1$, this effect would not be predicted. It is probable that the cause of this observed phenomena is due to local transonic effects appearing on the relatively large store employed - which would be greatest at a strong supercritical oncoming Mach number, but would disappear at lower or higher Mach numbers. That this is almost certainly the cause is apparent from the measured results displayed in figures 34b and 35b. They show that this phenomena disappears when the angle of attack is changed from $\alpha = 0^\circ$ to 5°. This change acts to slow the flow substantially on the pressure side of the wing and significantly reduce the local transonic effects on the store.

Finally, we note that figures 34 and 35 indicate that a rapid nonlinear store-loading calculation is required which is capable of treating mixed subsonic-supersonic flows and steep gradients of the flow variables. It should be noted that predictions of the location of steep gradients is especially important if lifting surfaces such as store tail fins are located in the vicinity of those gradients.

In summary, the results presented in this report and in reference 1 indicate that the following work is needed:

1. Improvement of the linear supersonic paneling method to provide accurate store-loading distributions without oscillations.

2. Development of a method for computing store-loading distributions in the presence of mixed subsonic-supersonic flows and steep gradients of the flow-field variables.

3. Development of an engineering method for improving the linear paneling method prediction of the location of the wing-pylon-trailing edge shock.

In order to extend the methods to treat realistic store geometries, further analytical and theoretical work is needed to handle the effects of store boattails and fins.

ACKNOWLEDGEMENTS

Support for the research reported in this investigation was provided by the Air Force Office of Scientific Research under Contract No. F44620-75-C-0047 with Dr. James D. Wilson as Technical Monitor. Support for the wind-tunnel test program was provided by the Air Force Flight Dynamic Laboratory with Mr. Calvin L. Dyer as Technical Monitor. Special thanks are given to Janice Walters for extensive programming support.

REFERENCES

1. Crisalli, A. J., Stahara, S. S., Nielsen, J. N., and Spreiter, J. R.: The Development of Rapid Predictive Methods for Three-Dimensional Transonic Flow Fields About Fighter Bomber Aircraft. NEAR TR 198, July 1979.

2. Stahara, S. S. and Crisalli, A. J.: Data Report for a Test Program to Study Transonic Flow Fields About Wing-Body Pylon/Store Combinations, Volume I - Summary Report, Tunnel Empty Flow Survey Data, Wing-Body Force/Moment/Surface Pressure Data, and Pressure Store/Force/Moment/Surface Pressure Data. NEAR TR 163, May 1978.

3. Stahara, S. S. and Crisalli, A. J.: Data Report for a Test Program to Study Transonic Flow Fields About Wing-Body/Pylon/Store Combinations, Volume II - Flow Field Survey Data for Configurations 21 and 22. NEAR TR 163, May 1978.

4. Stahara, S. S. and Crisalli, A. J.: Data Report for a Test Program to Study Transonic Flow Fields About Wing-Body/Pylon/Store Combinations, Volume III - Flow Field Survey Data for Configurations 24, 1 25 and 26. NEAR TR 163, May 1978.

5. Perkins, S. C., Jr., Stahara, S. S., and Hemsch, M. J.: Data Report for a Test Program to Study Transonic Flow Fields About Aircraft with Application to External Stores. NEAR TR 138, July 1977.

6. Goodwin, F. K. and Dillenius, M. F. E.: Extension of the Method for Predicting Six-Degree-of-Freedom Store Separation Trajectories at Speeds up to the Critical Speed to Include a Fuselage with Noncircular Cross Section, Volume I - Theoretical Methods and Comparisons with Experiment. AFFDL-TR-74-130, Nov. 1974.

7. Dillenius, M. F. E., Goodwin F. K., and Nielsen, J. N.: Prediction of Supersonic Store Separation Characteristics, Volume I - Theoretical Methods and Comparisons with Experiment. AFFDL-TR-76-41, May 1976.

8. Goodwin, F. K., Dillenius, M. F. E., and Nielsen, J. N.: Prediction of Six-Degree-of-Freedom Store Separation Trajectories at Speeds up to the Critical Speed, Volume I - Theoretical Methods and Comparisons with Experiment. AFFDL-TR-72-83, Oct. 1974.

TABLE 1.- COMPARISONS OF LINEAR THEORY WITH DATA FROM REFERENCE 2

1	2	3	4	5	6	7	8	9
Configuration		M_∞	α (deg)	y (in.)	z (in.)	$\frac{dC_N}{dx_s}$ (page no.)	$\frac{dC_y}{dx_s}$ (page no.)	Figure
WB/FP/S		0.925	0	0	-2.297	21	22	7
↓		↓	5	0	-2.297	23	24	8
↓		↓	0	0	-2.947	25	26	9
↓		↓	5	0	-2.947	27	28	10
WB/WP/S		↓	0	3.5	-1.30	29	30	11
↓		↓	5	3.5	-1.30	31	32	12
↓		↓	0	3.5	-1.950	33	34	13
↓		↓	5	3.5	-1.950	35	36	14
WB/FP/S		0.950	0	0	-2.297	37	38	15
↓		↓	5	0	-2.297	39	40	16
↓		↓	0	0	-2.947	41	42	17
↓		↓	5	0	-2.947	43	44	18
WB/WPS		↓	0	3.5	-1.30	45	46	19
↓		↓	5	3.5	-1.30	47	48	20
↓		↓	0	3.5	-1.950	49	50	21
↓		↓	5	3.5	-1.950	51	52	22
SB/FP/S		1.050	0	3.5	-1.30	54	55	24
↓		↓	5	3.5	-1.30	56	57	25
↓		↓	0	3.5	-1.950	58	59	26
↓		↓	5	3.5	-1.950	60	61	27

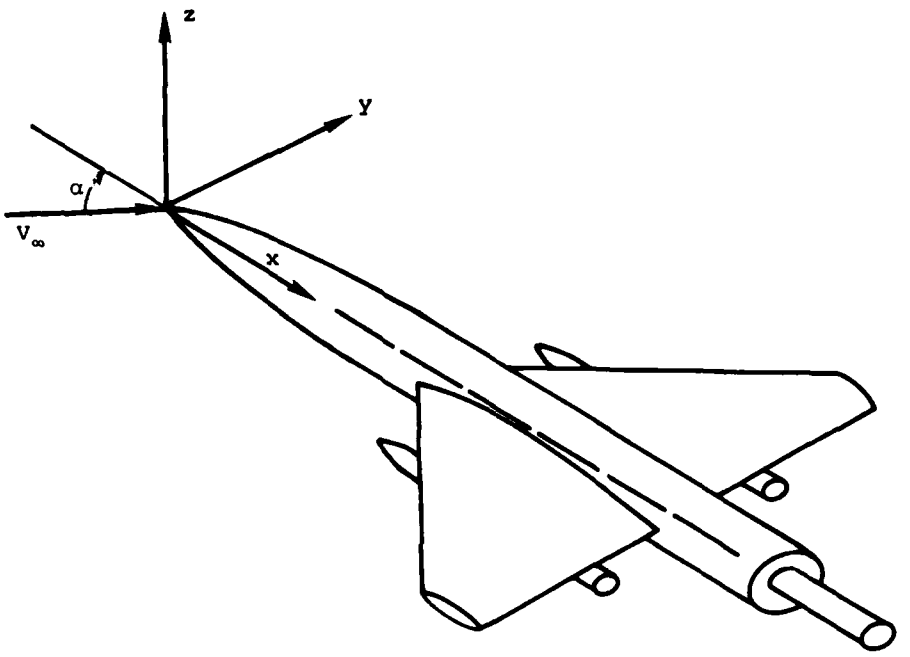

Figure 1.- Body-fixed coordinate system for inner flow field surveys.

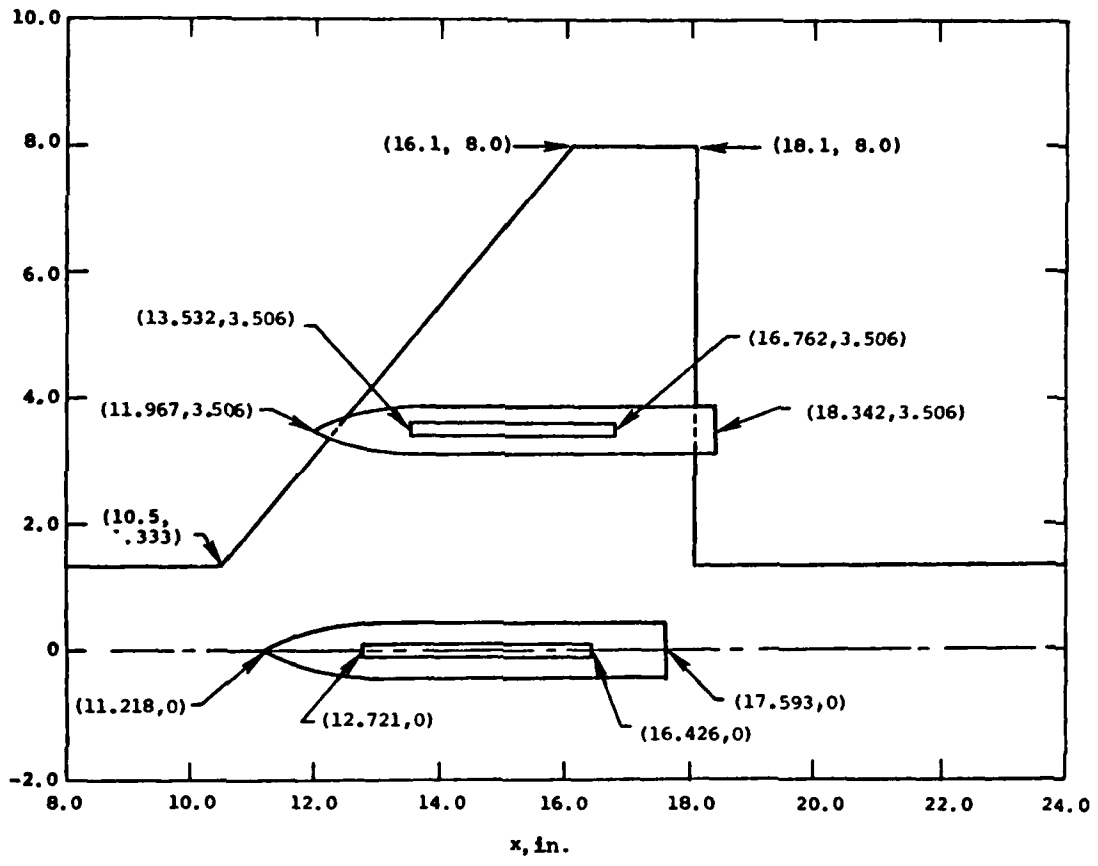

(a) Planform view, including (x,y) coordinates.

Figure 2.- Wing-body with pylons and stores, including measured body-fixed coordinates.

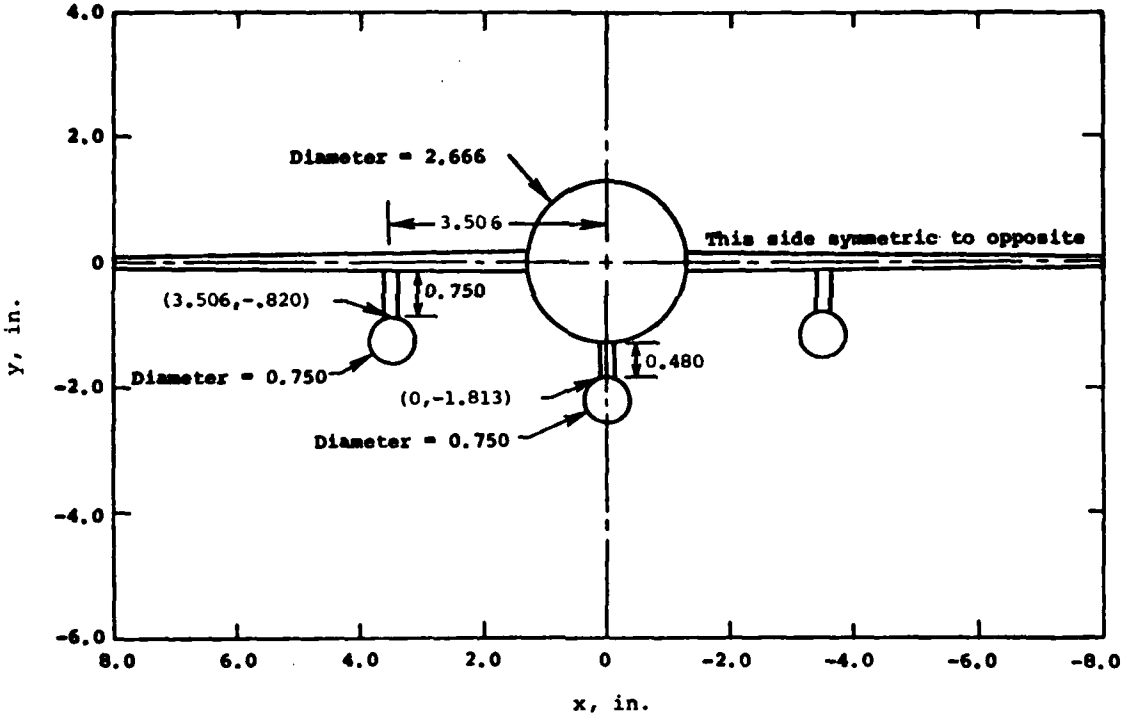

(b) Cross-sectional view (viewed from front of model), including (y,z) coordinates.

Figure 2.- Concluded.

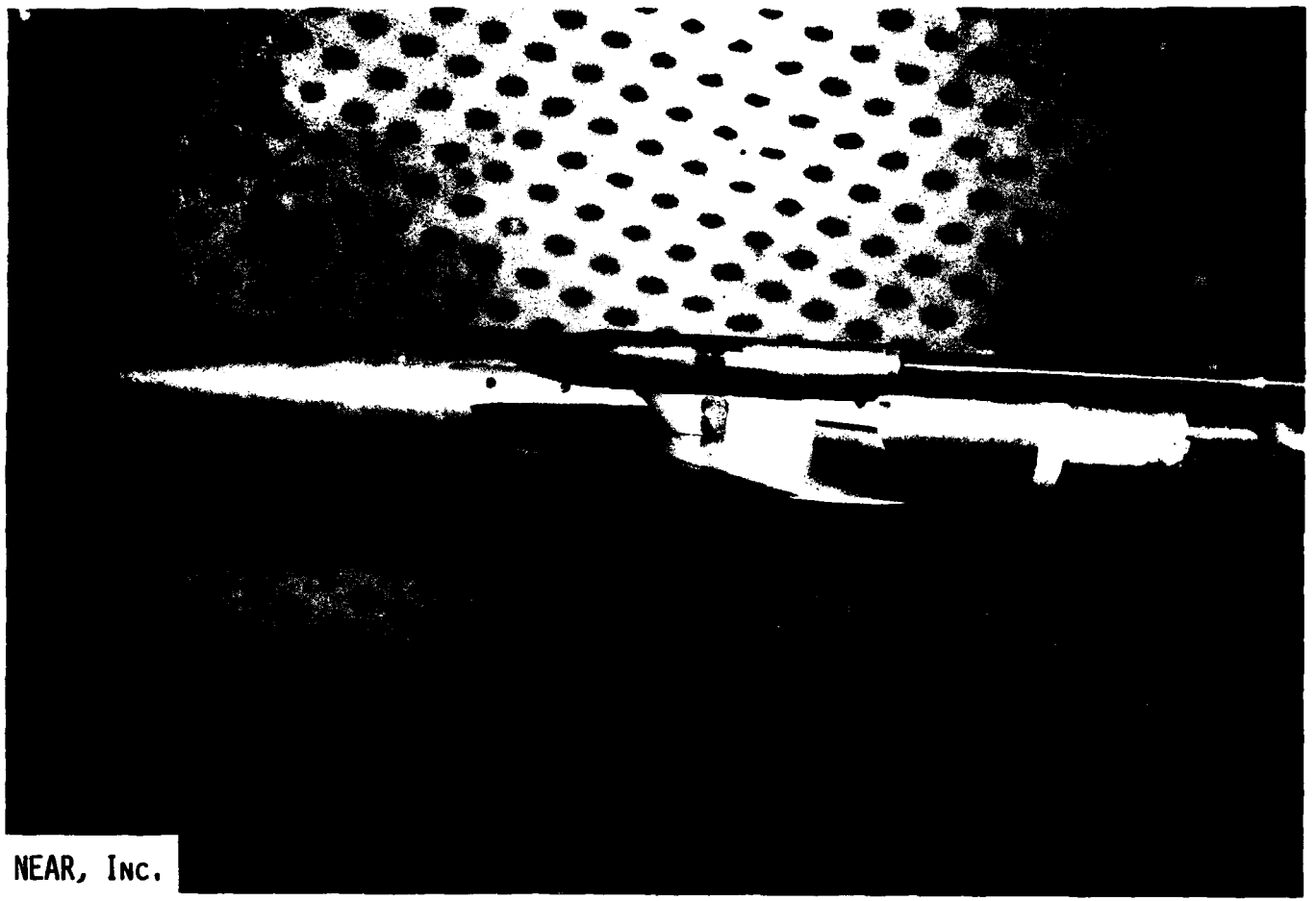

Figure 3.- Wing-body in combination with wing pylon and instrumented pressure store in store separated position.

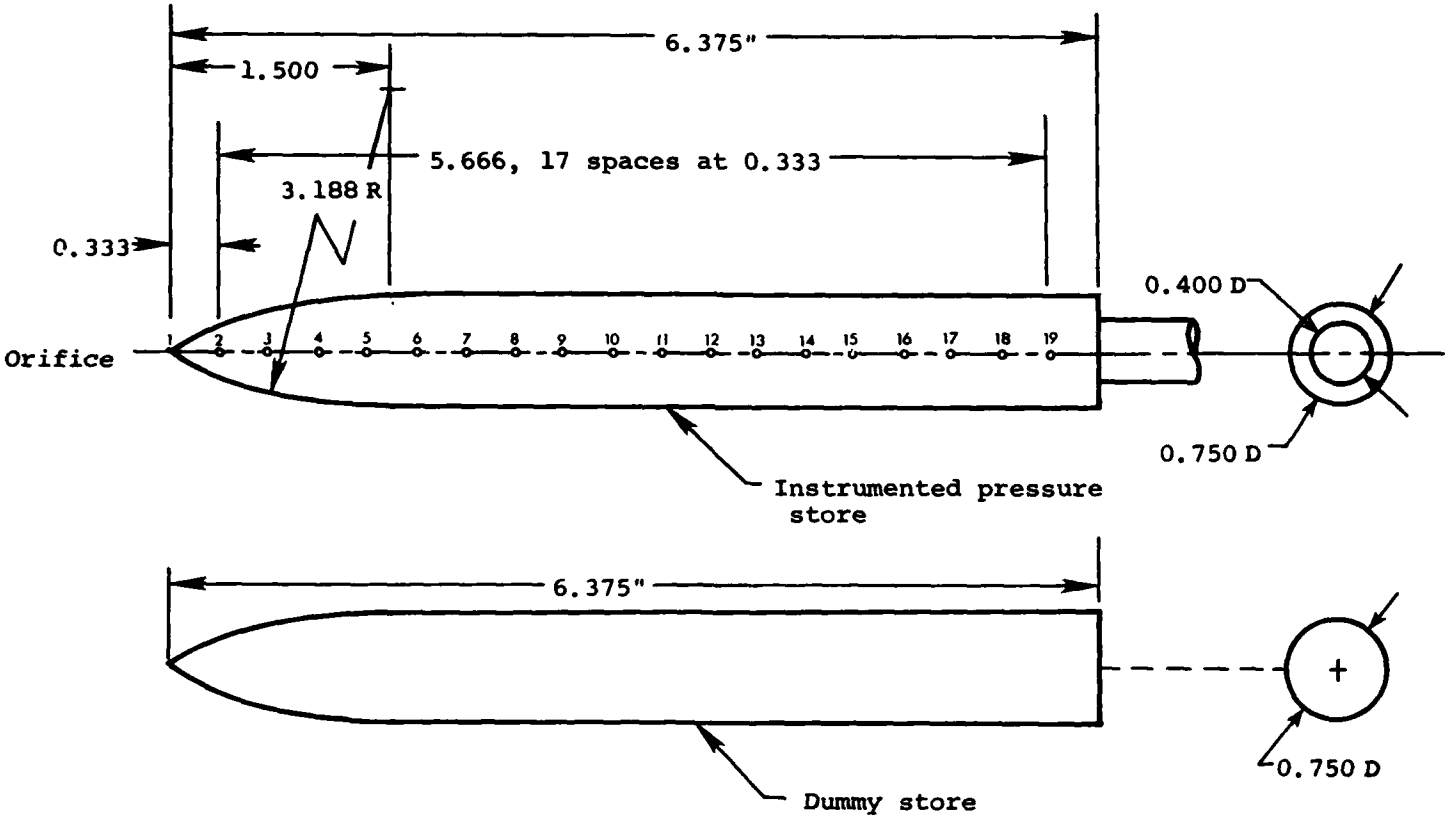

Figure 4.- Instrumented pressure store and dummy store.

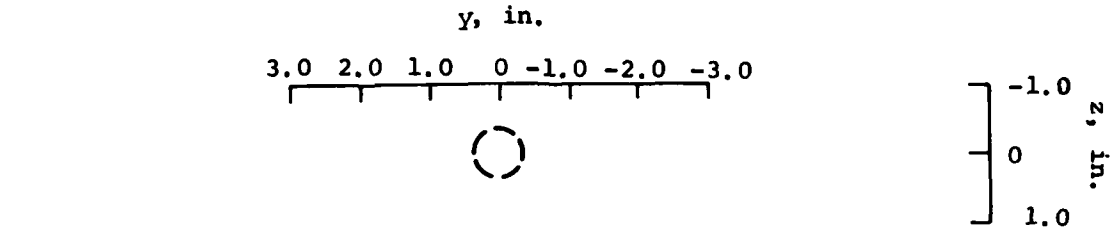

(a) Store-alone configuration.

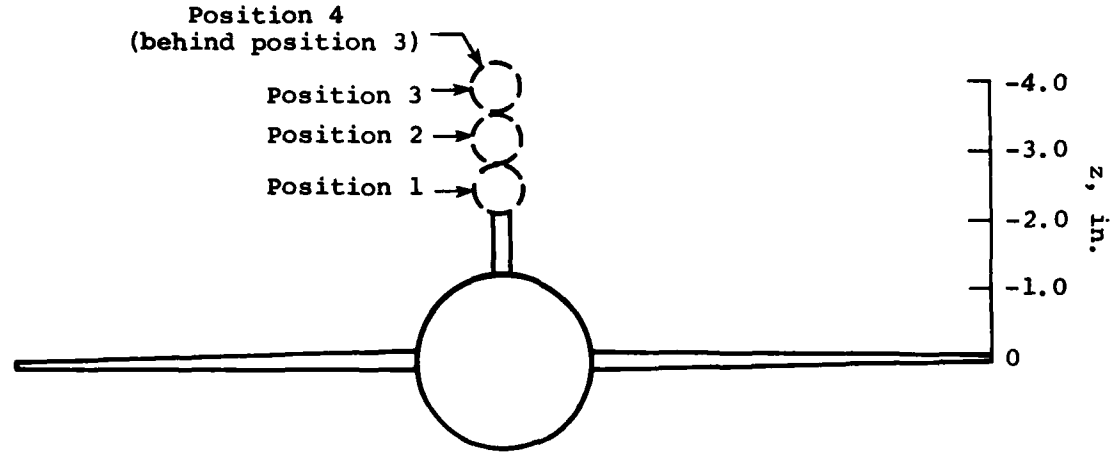

(b) Configurations with store near fuselage pylon.

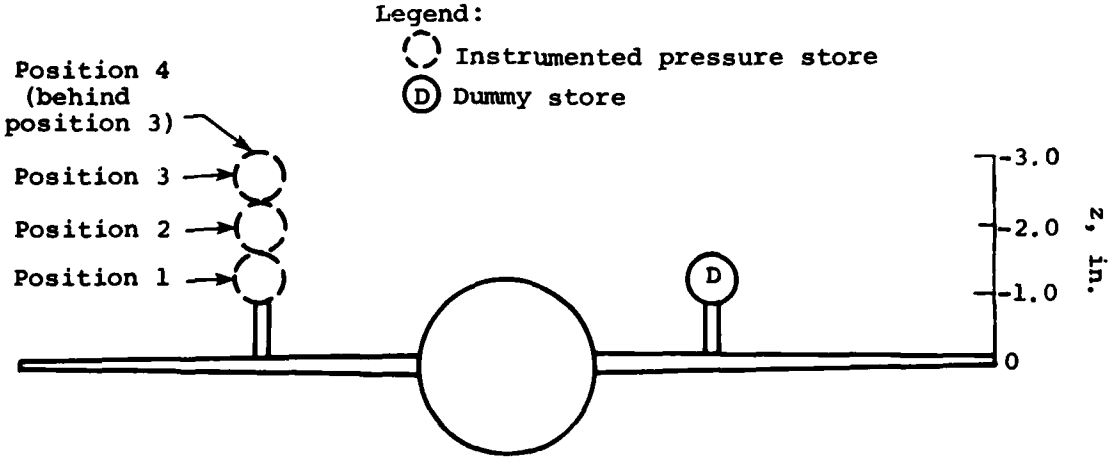

(c) Configurations with store near wing pylon.

Figure 5.- Illustration of wing-body/pylon/store configurations viewed from rear of model. Positions shown correspond to the M_∞ = 1.10 tests.

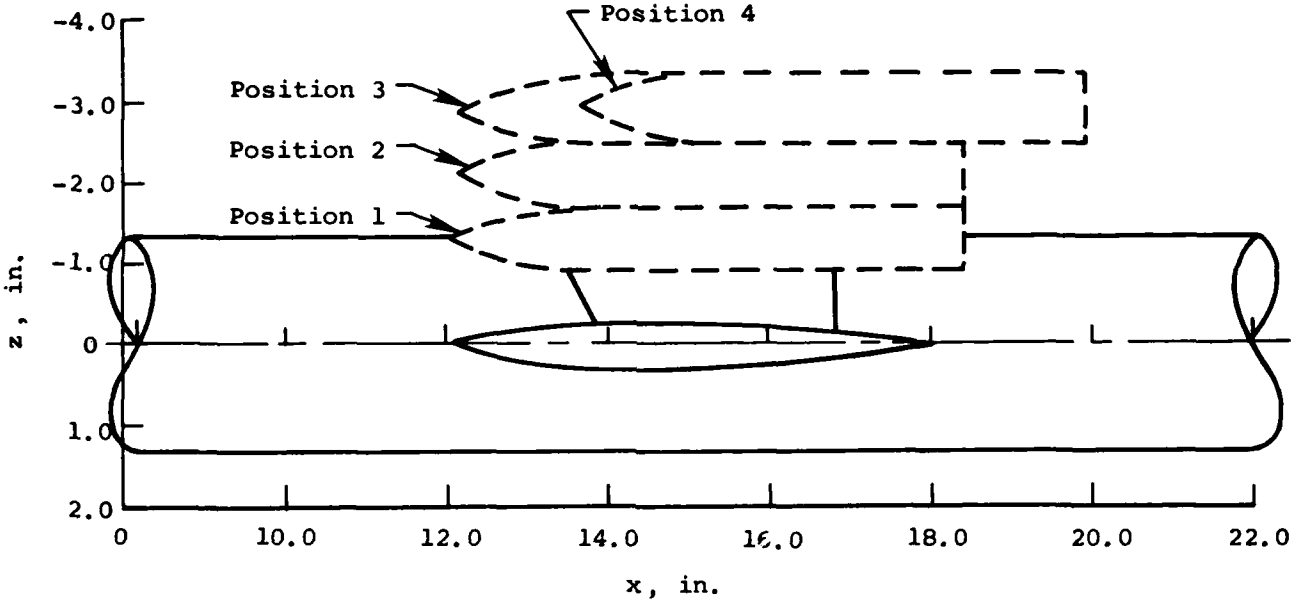

Figure 6.- Side view of four positions of instrumented pressure store for configuration shown in figure 5(c). Positions shown correspond to the $M_\infty = 1.10$ tests.

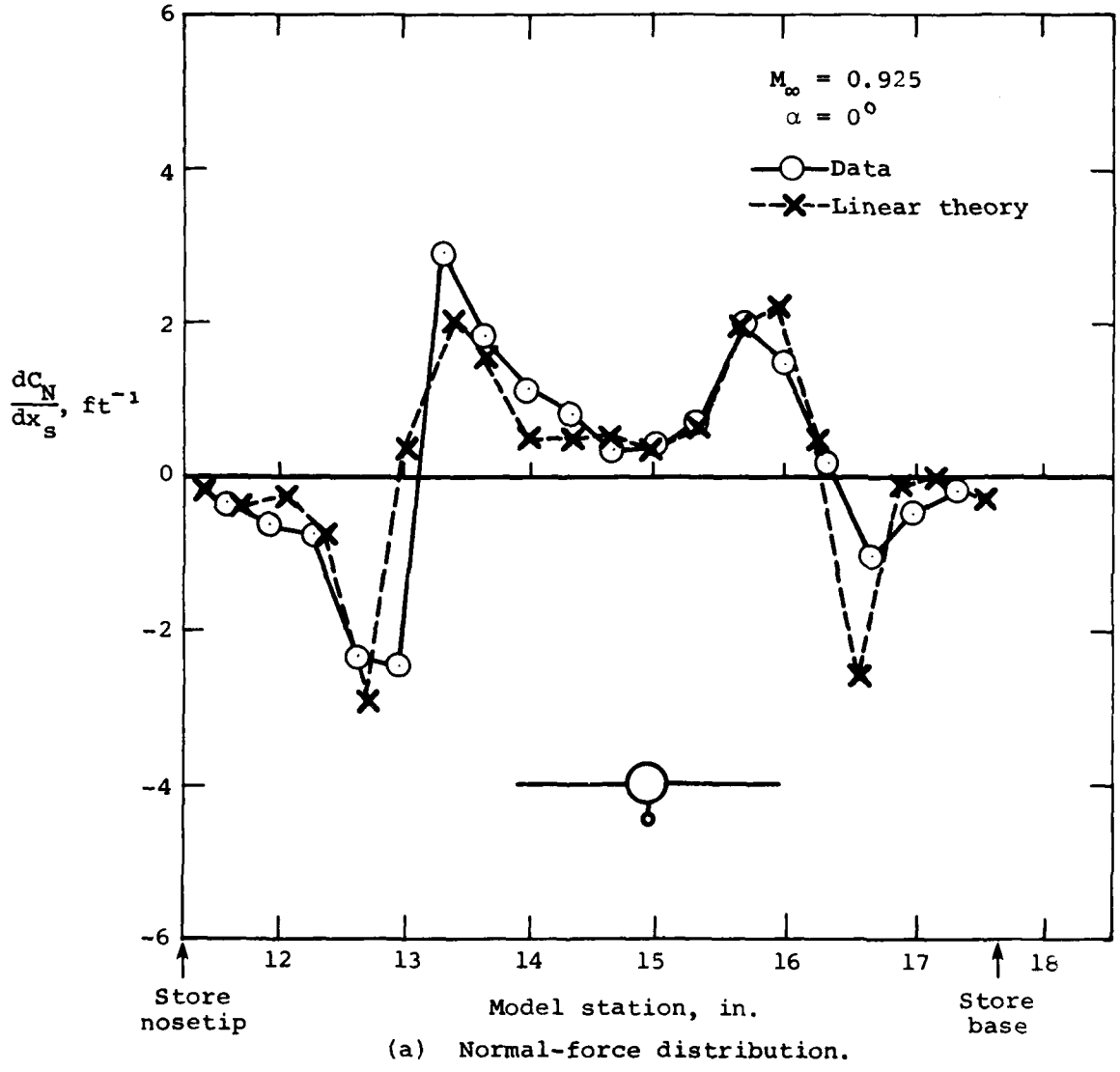

(a) Normal-force distribution.

Figure 7.- Comparison of measured and theoretical loading distributions for store attached to fuselage pylon; $M_\infty = 0.925$, $\alpha = 0^\circ$, $(y_s, z_s) = (0, -2.297$ in.).

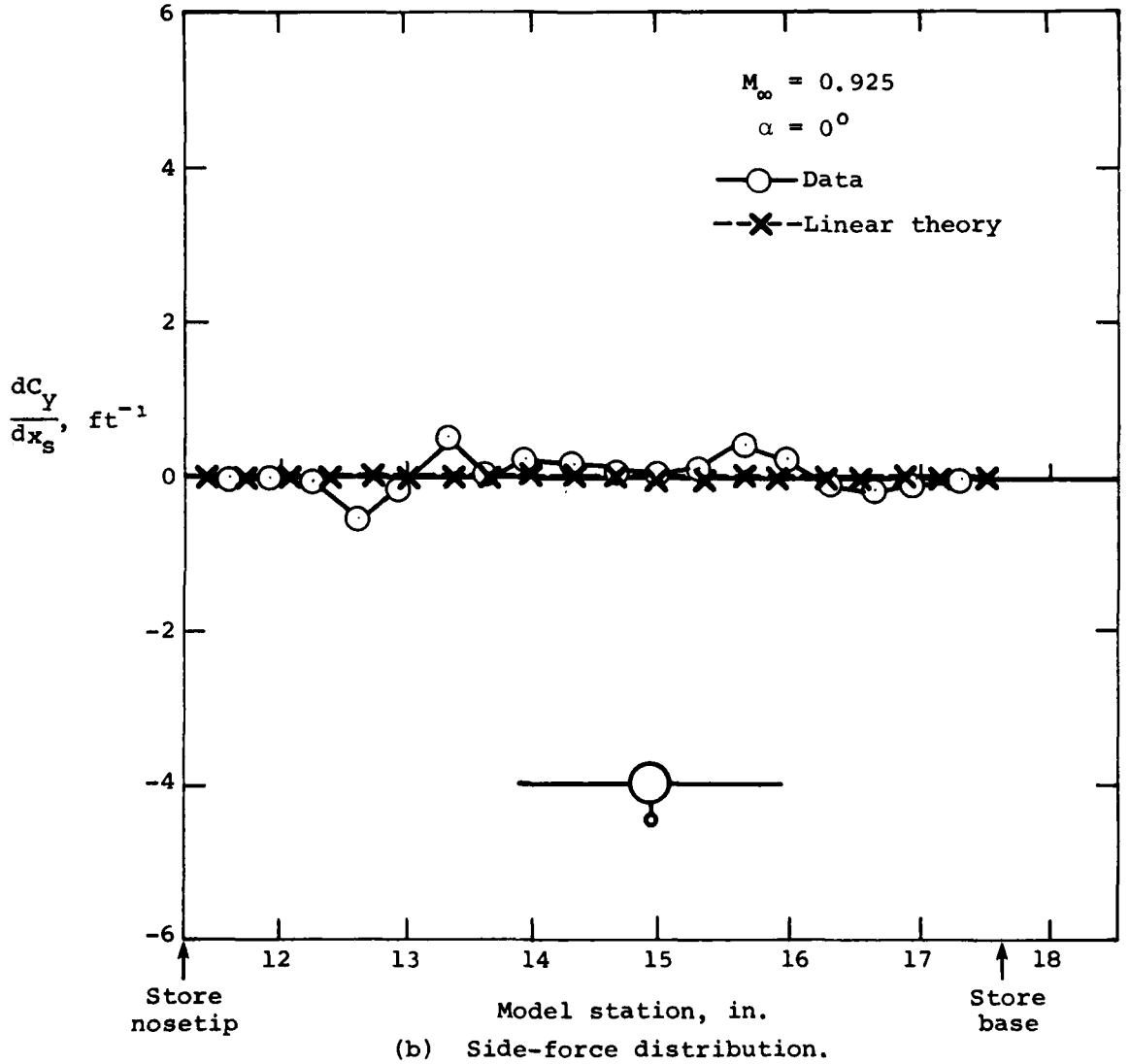

(b) Side-force distribution.

Figure 7.- Concluded.

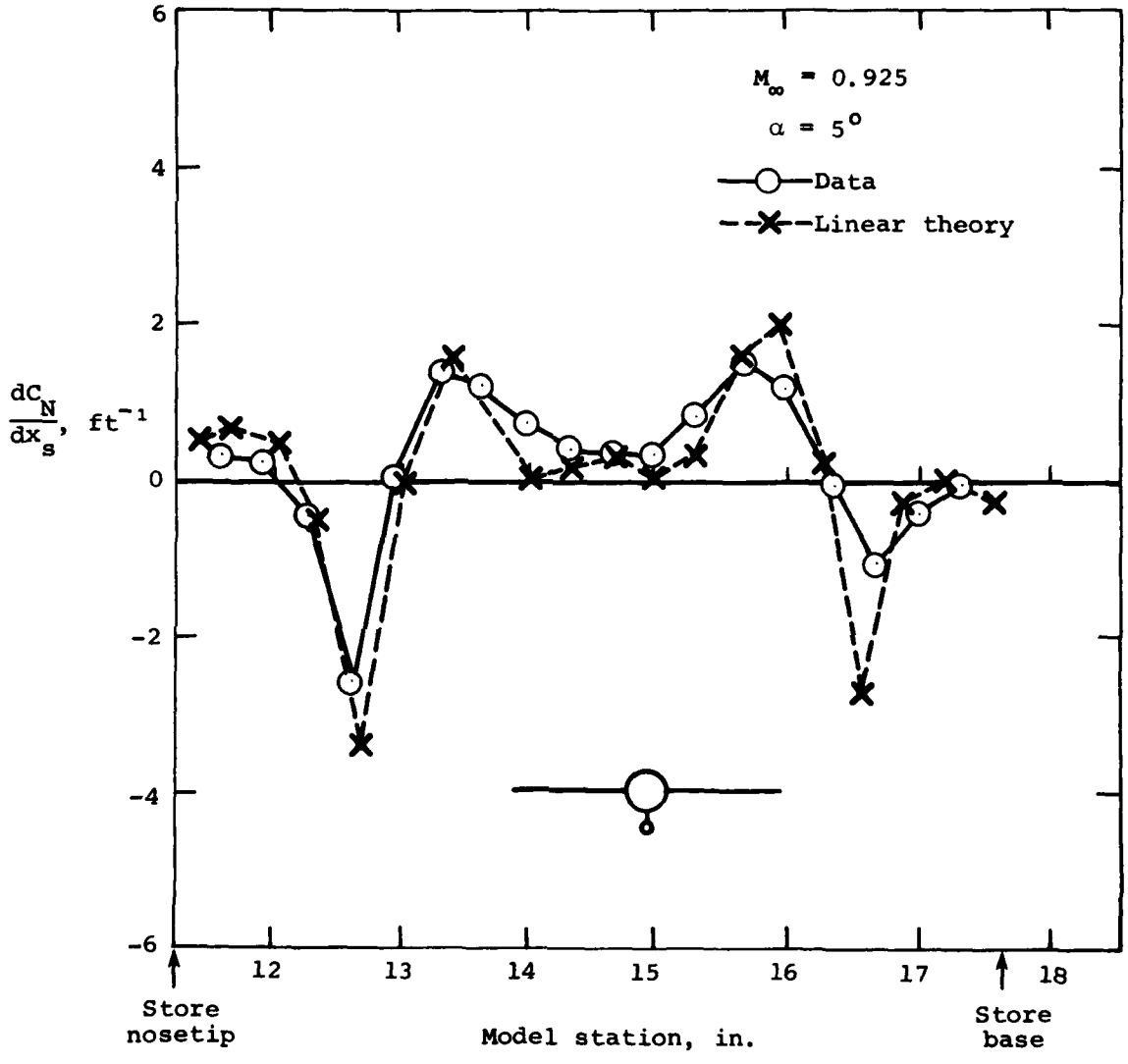

(a) Normal-force distribution.

Figure 8.- Comparison of measured and theoretical loading distributions for store attached to fuselage pylon; M_∞ = 0.925, α = 5°, (y_s, z_s) = (0, -2.297 in.).

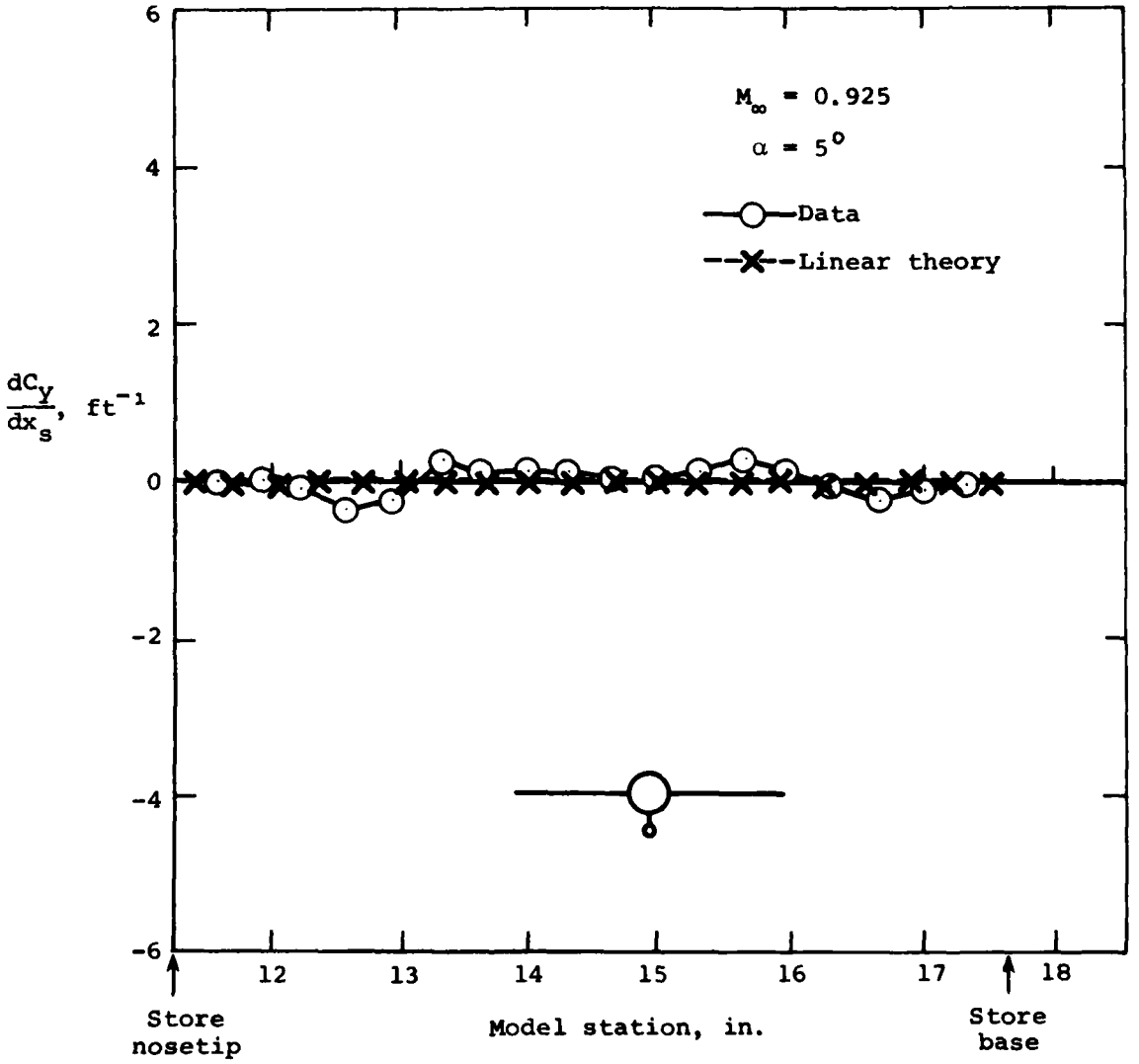

(b) Side-force distribution.

Figure 8.- Concluded.

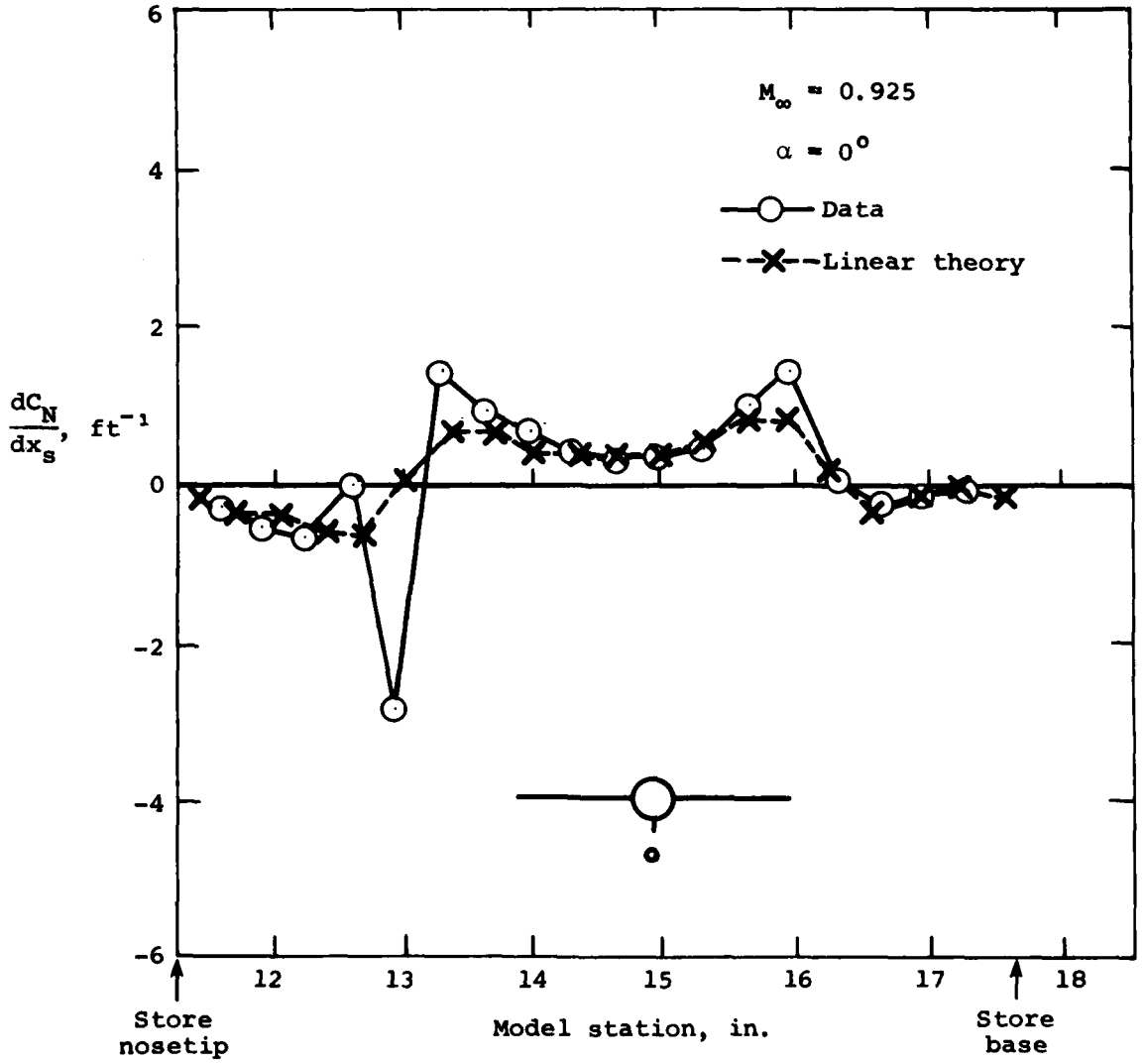

(a) Normal-force distribution.

Figure 9.- Comparison of measured and theoretical loading distributions for store separated from fuselage pylon; M_∞ = 0.925, α = 0°, (y_s, z_s) = (0, -2.947 in.).

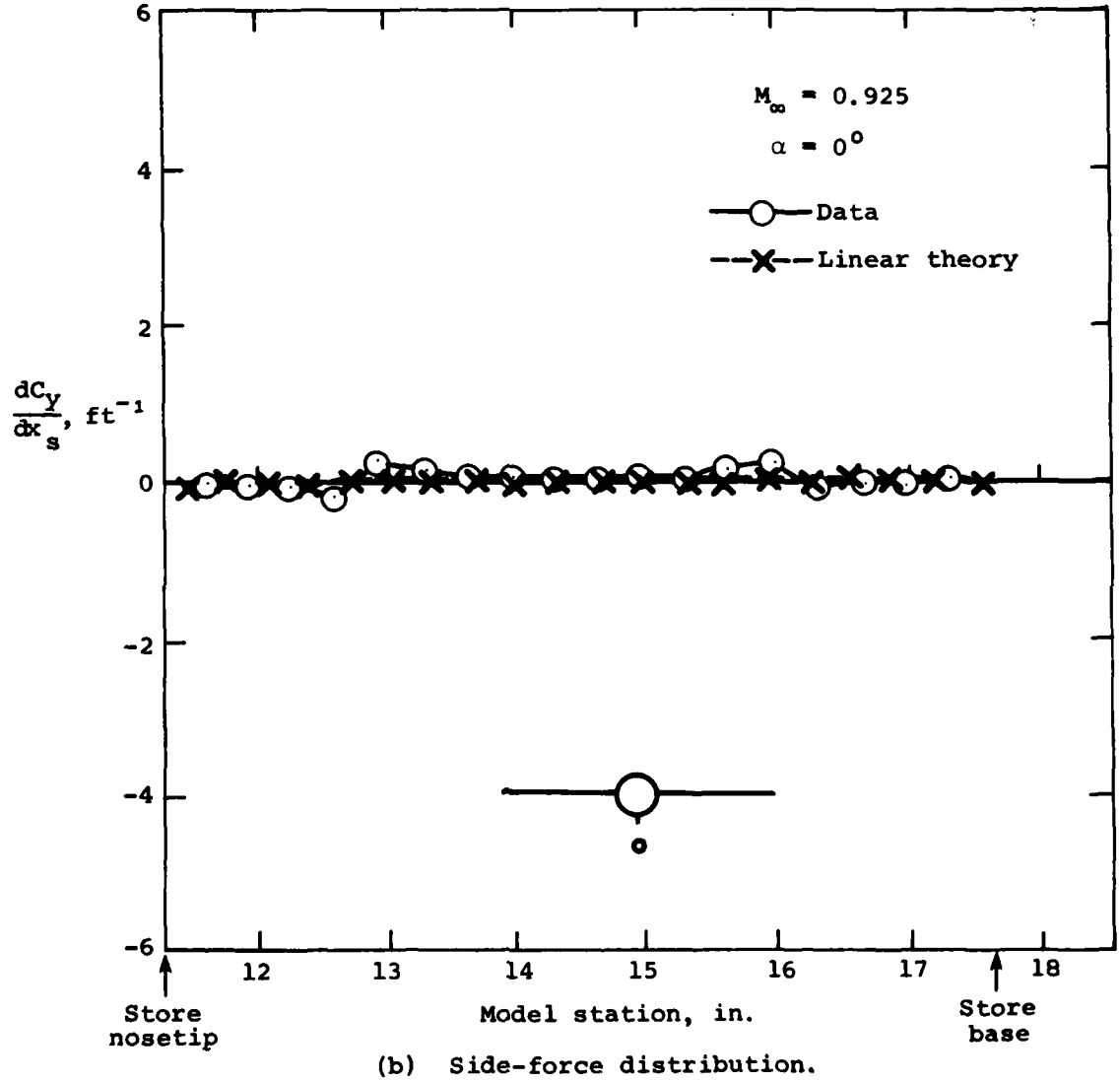

(b) Side-force distribution.

Figure 9.- Concluded.

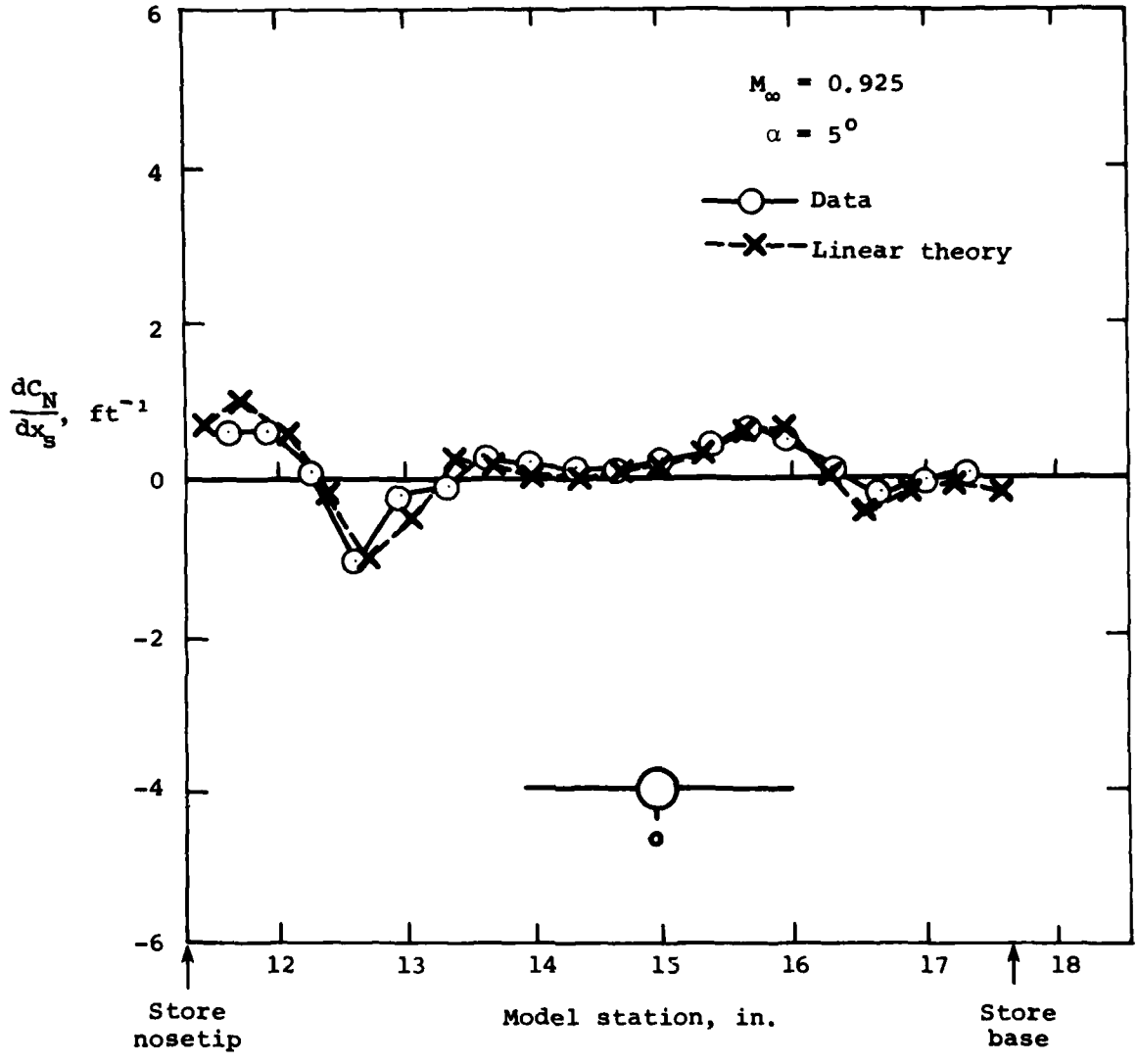

(a) Normal-force distribution.

Figure 10.- Comparison of measured and theoretical loading distributions for store separated from fuselage pylon; $M_\infty = 0.925$, $\alpha = 5^\circ$, $(y_s, z_s) = (0, -2.947$ in.).

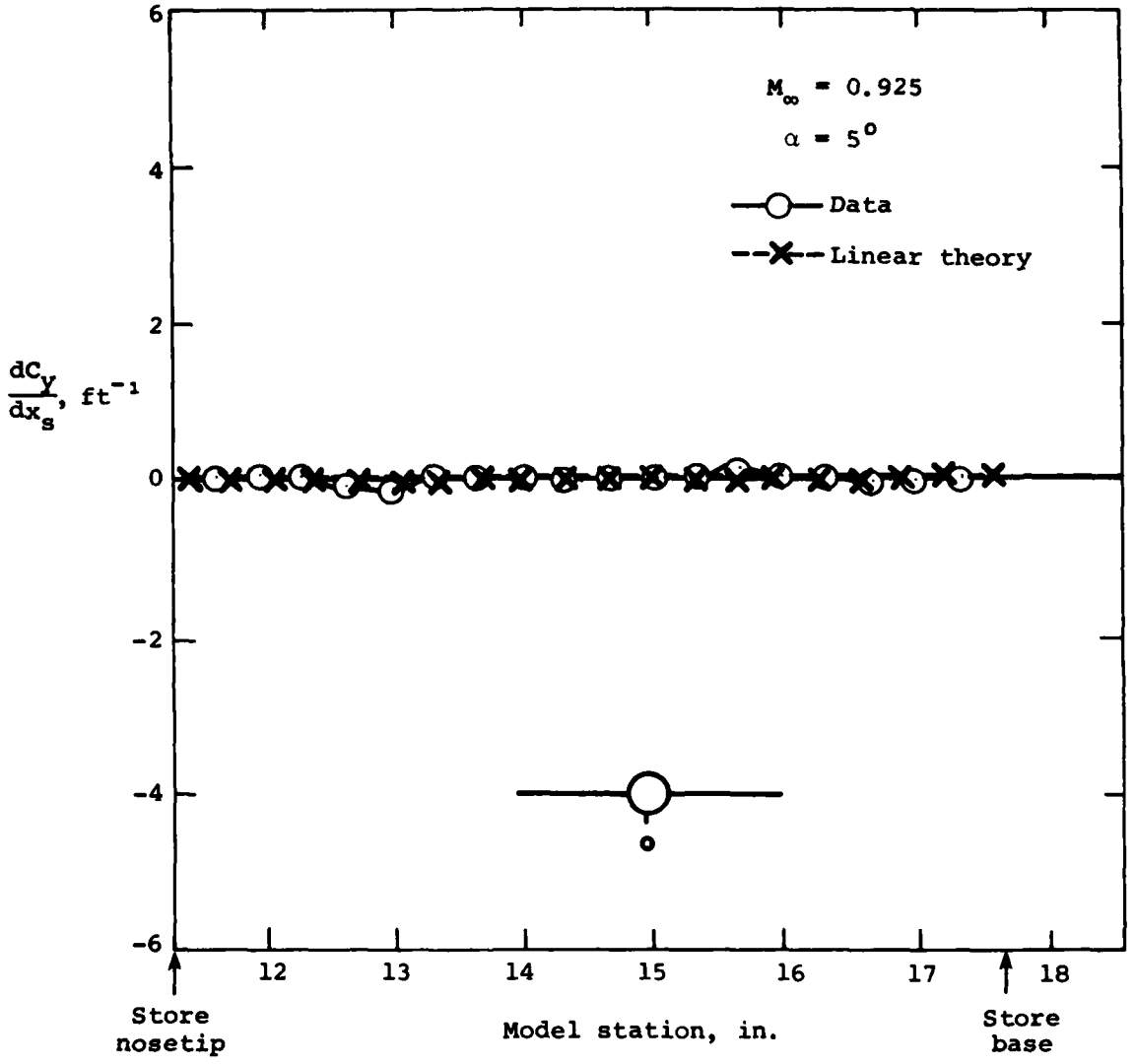

(b) Side-force distribution.

Figure 10.- Concluded.

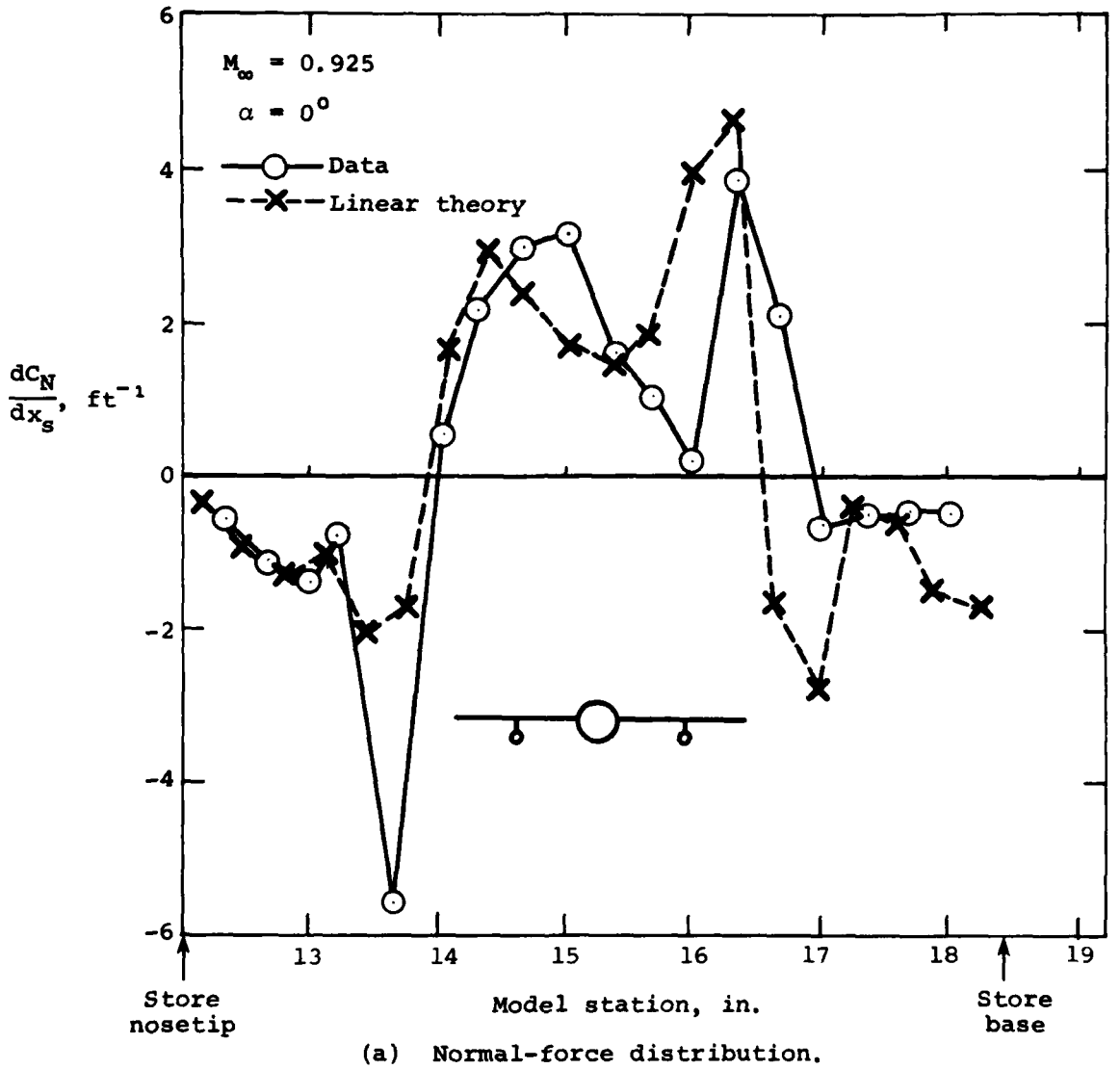

(a) Normal-force distribution.

Figure 11.- Comparison of measured and theoretical loading distributions for store attached to wing pylon; M_∞ = 0.925, α = 0°, (y_s, z_s) = (3.5 in., -1.3 in.).

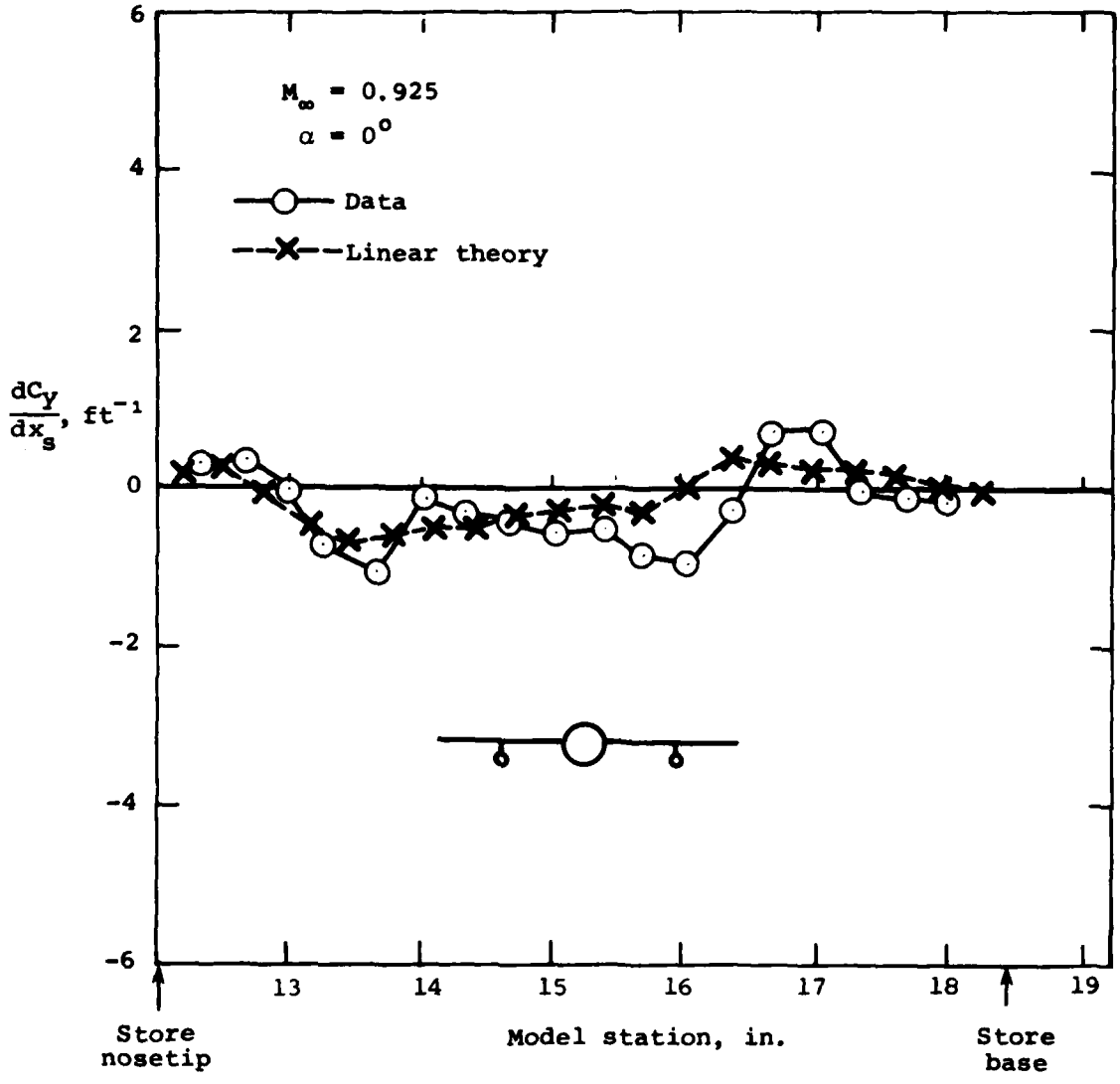

(b) Side-force distribution.

Figure 11.- Concluded.

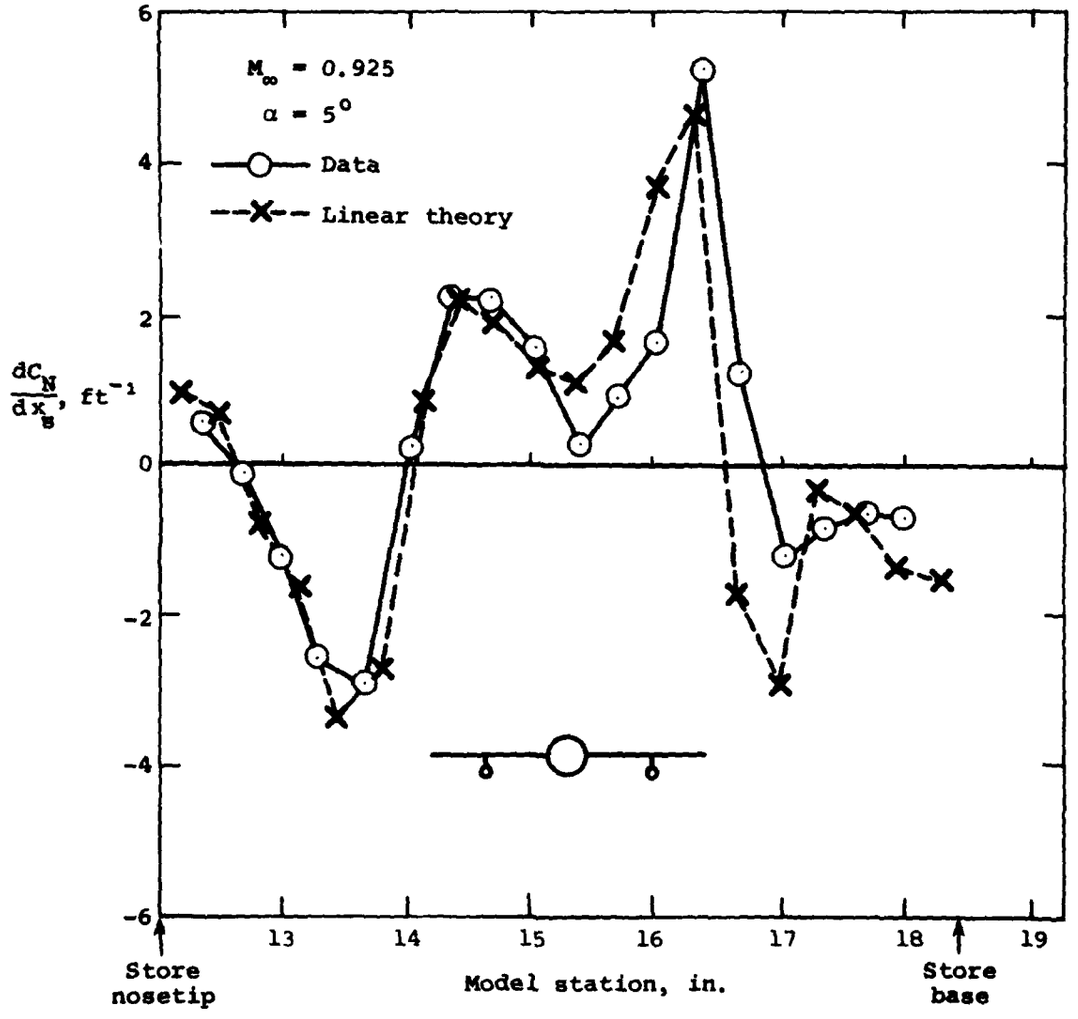

(a) Normal-force distribution.

Figure 12.- Comparison of measured and theoretical loading distributions for store attached to wing pylon; M_∞ = 0.925, α = 5°, (y_s, z_s)=(3.5 in., -1.3 in.).

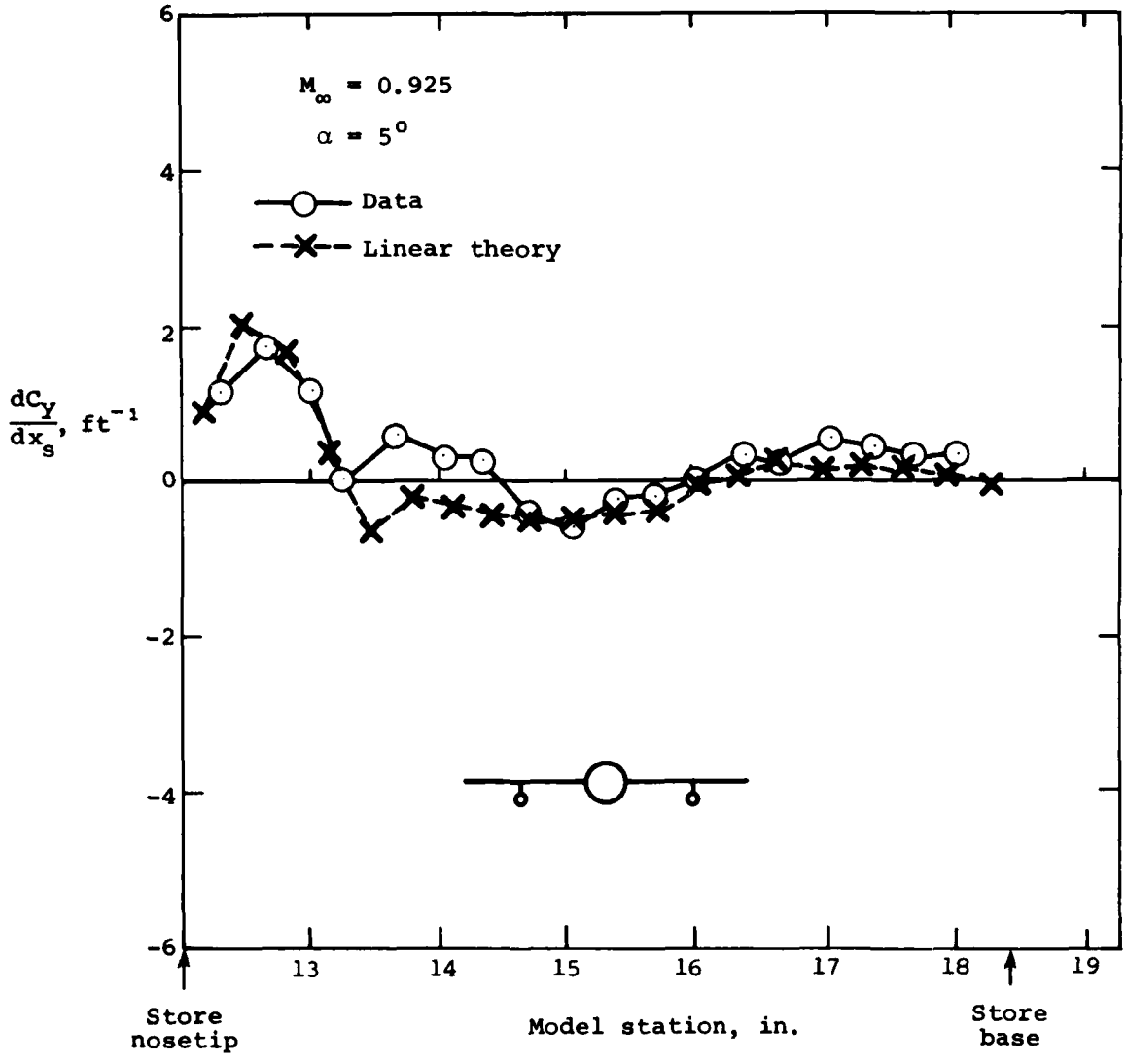

(b) Side-force distribution.

Figure 12.- Concluded.

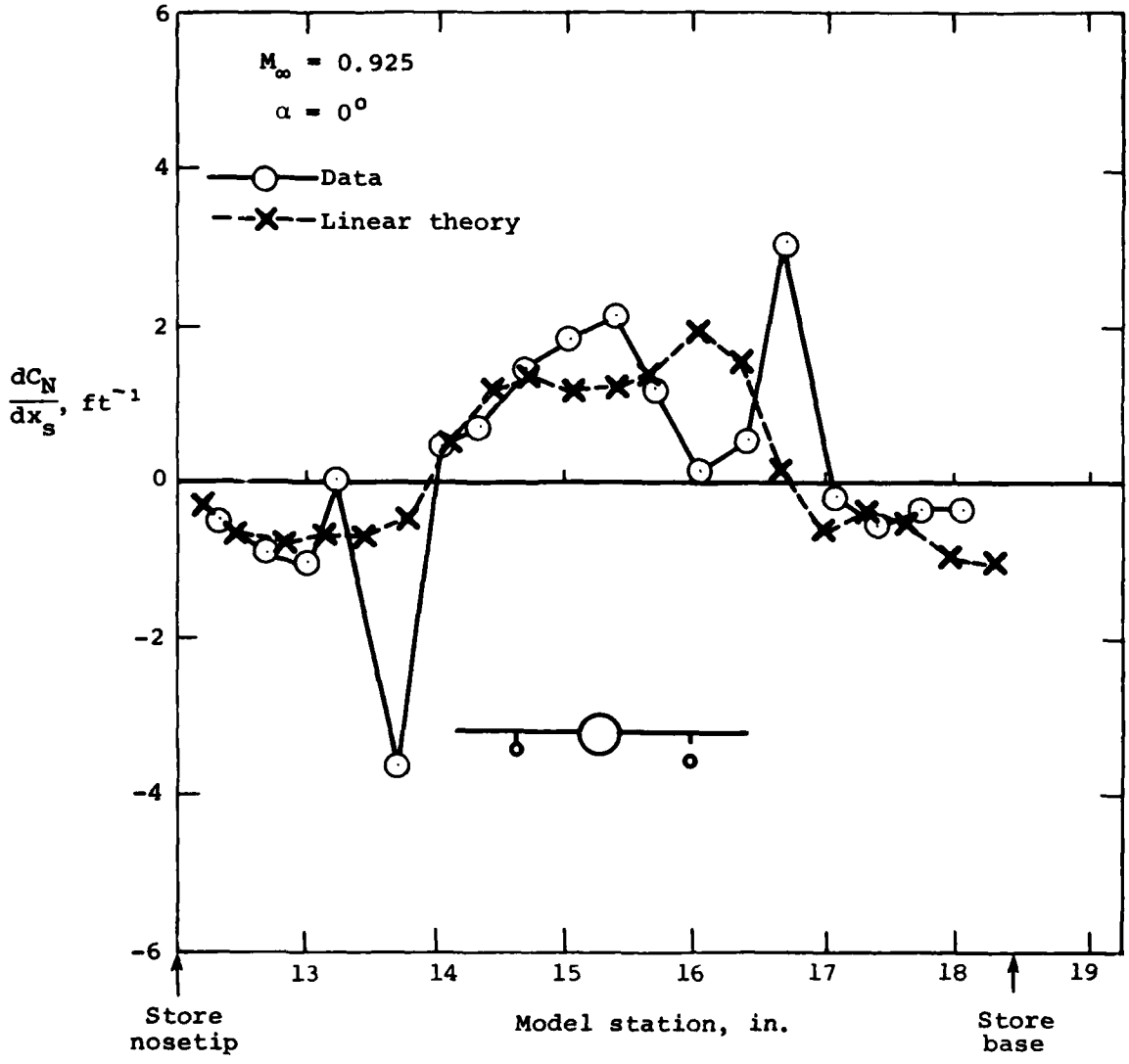

(a) Normal-force distribution.

Figure 13.- Comparison of measured and theoretical loading distributions for store separated from wing pylon; M_∞ = 0.925, α = 0°, (y_z, z_s) = (3.5 in., -1.95 in.).

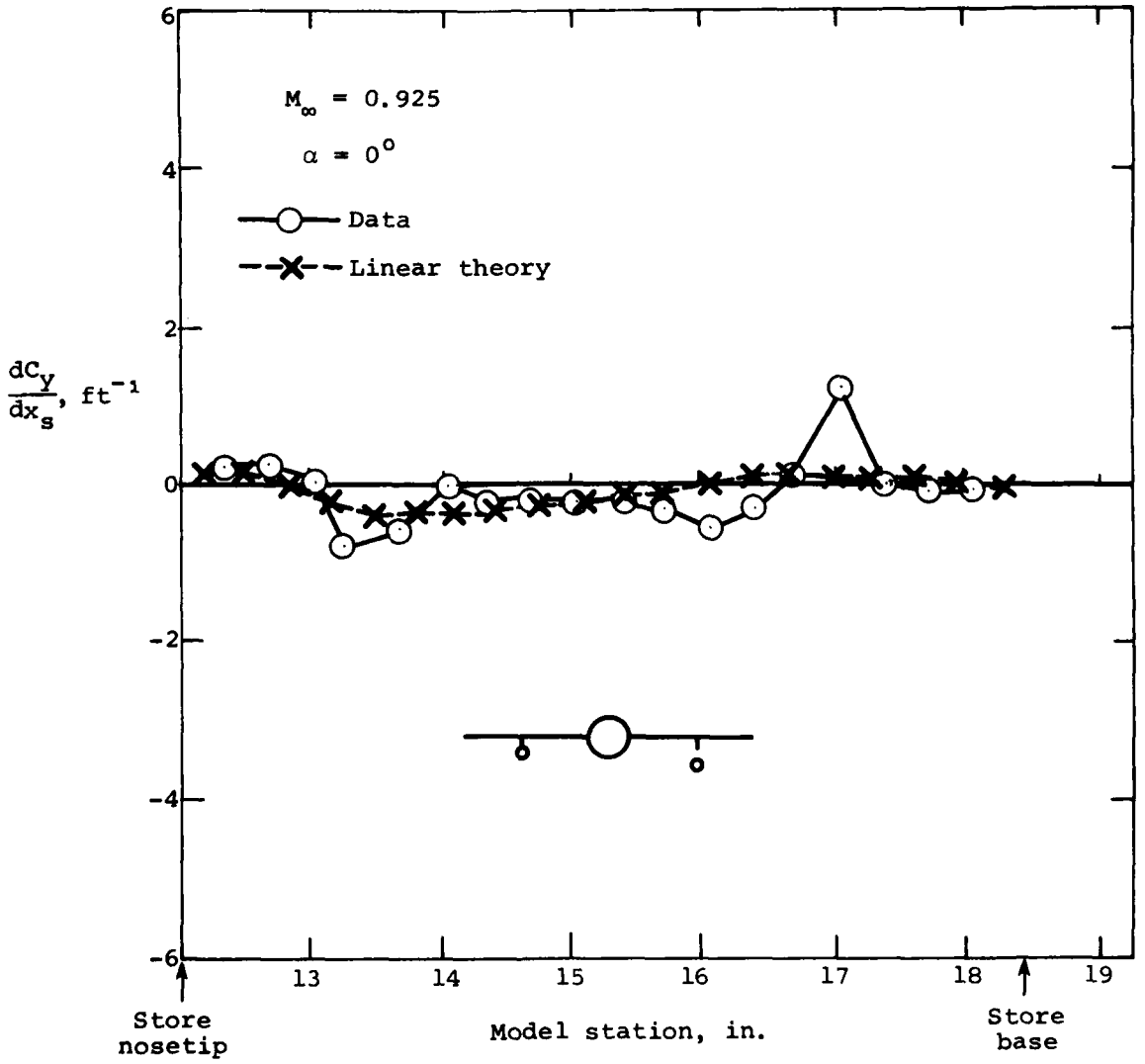

(b) Side-force distribution.

Figure 13.- Concluded.

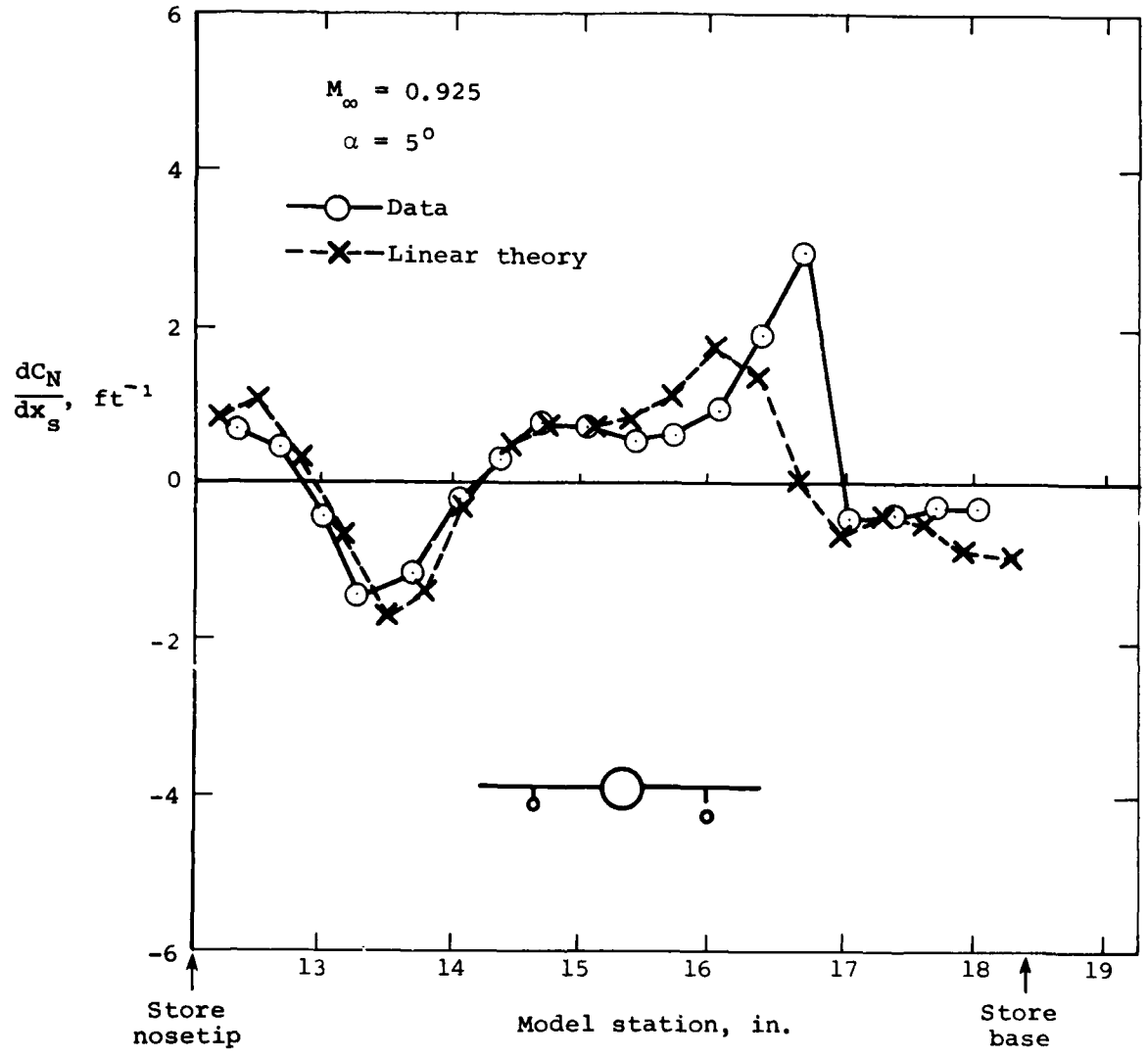

(a) Normal-force distribution.

Figure 14.- Comparison of measured and theoretical loading distributions for store separated from wing pylon: $M_\infty = 0.925$, $\alpha = 5^o$, $(y_s, z_s) = (3.5$ in., -1.95 in.).

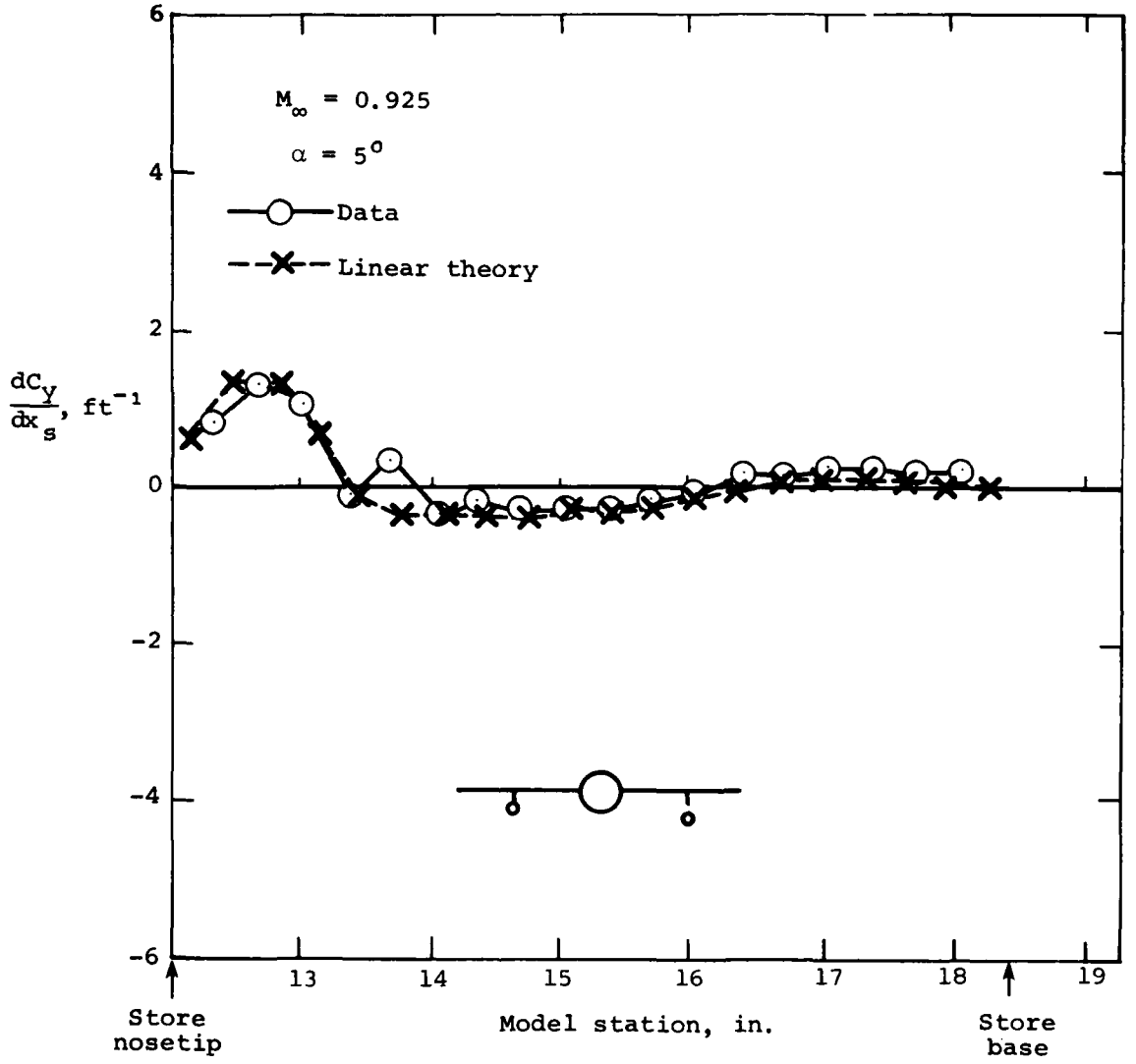

(b) Side-force distribution.

Figure 14.- Concluded.

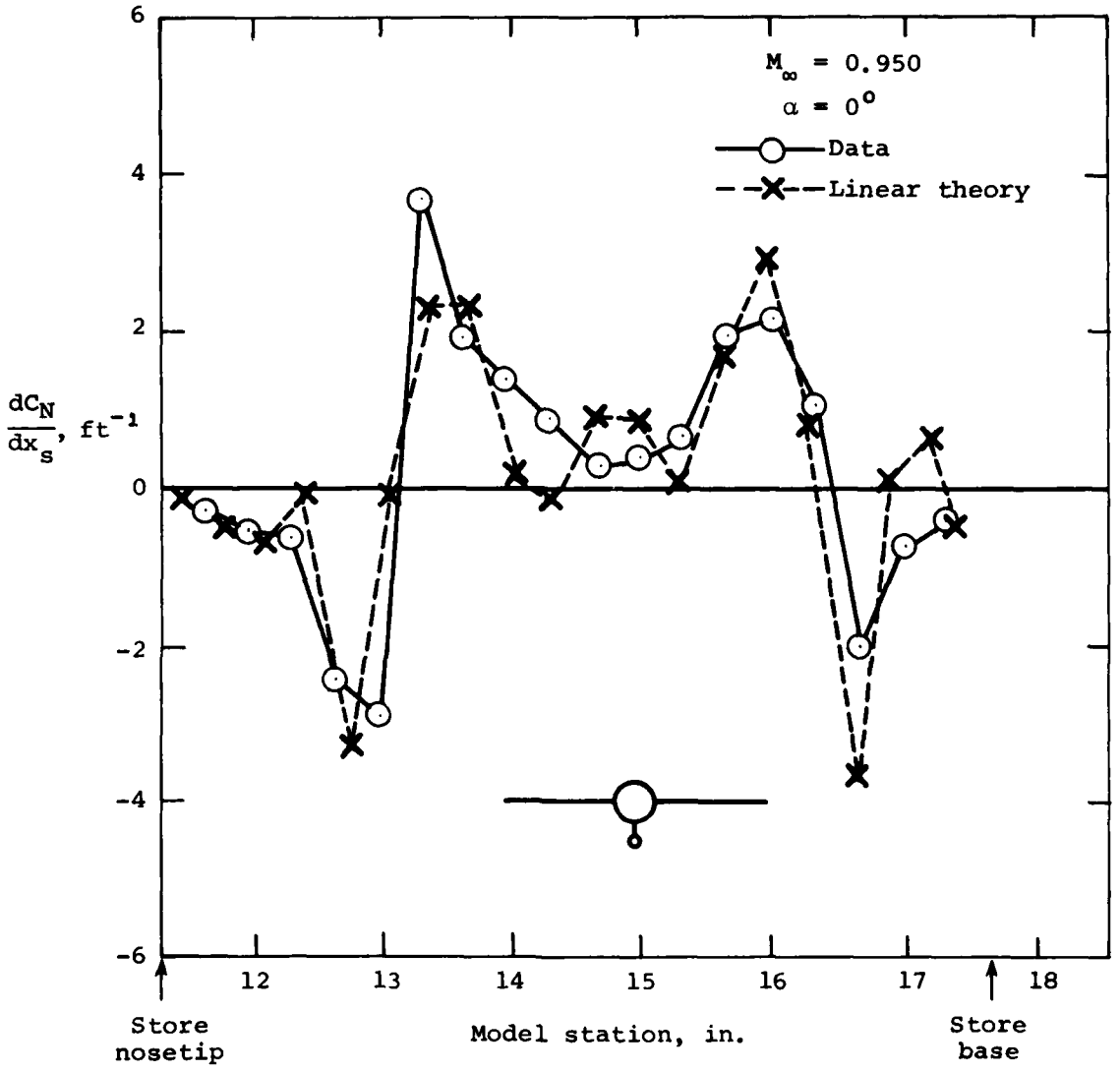

(a) Normal-force distribution.

Figure 15.- Comparison of measured and theoretical loading distributions for store attached to fuselage pylon; M_∞ = 0.950, α = 0°, (y_s, z_s) = (0,-2.297 in.).

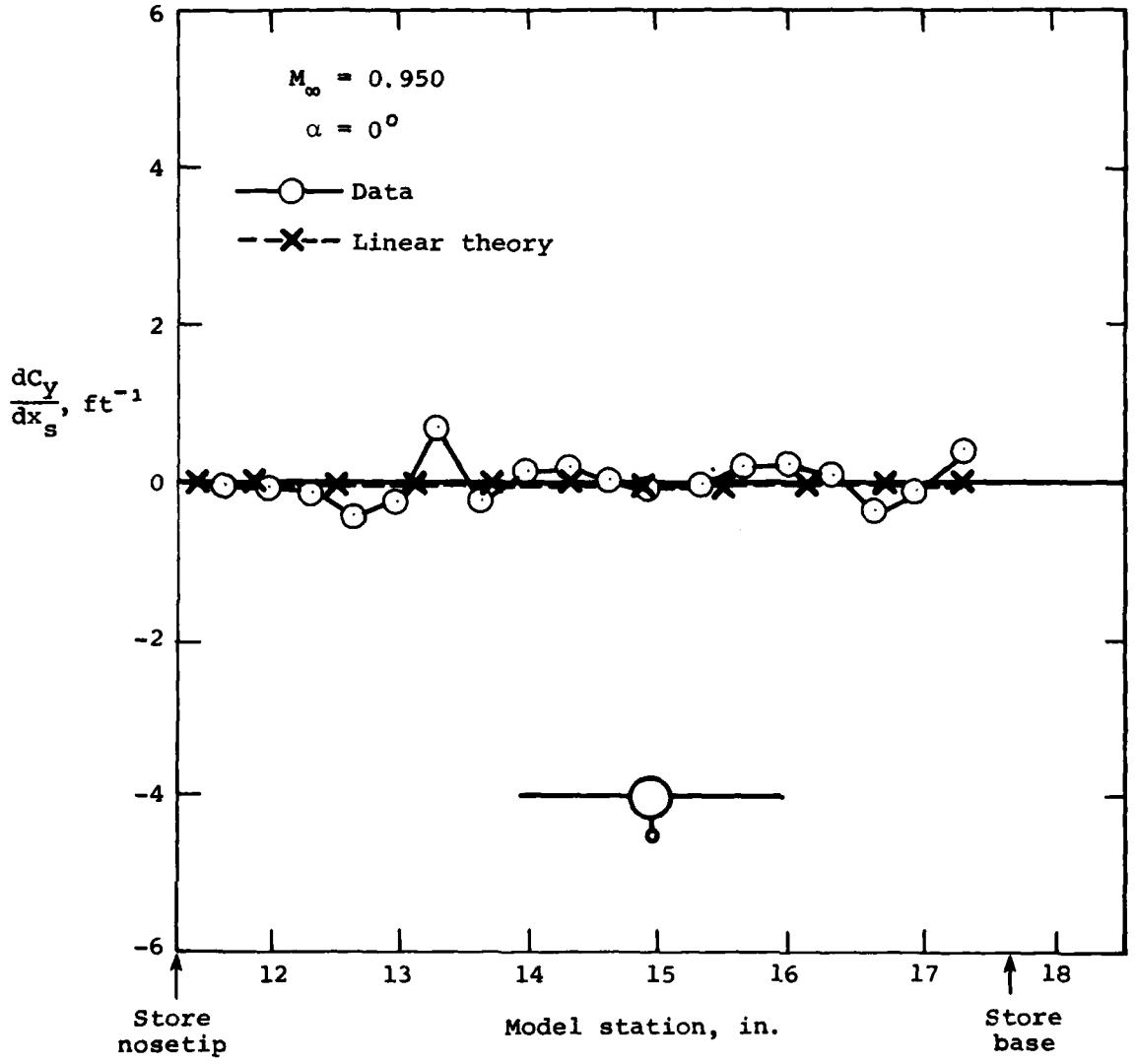

(b) Side-force distribution.

Figure 15.- Concluded.

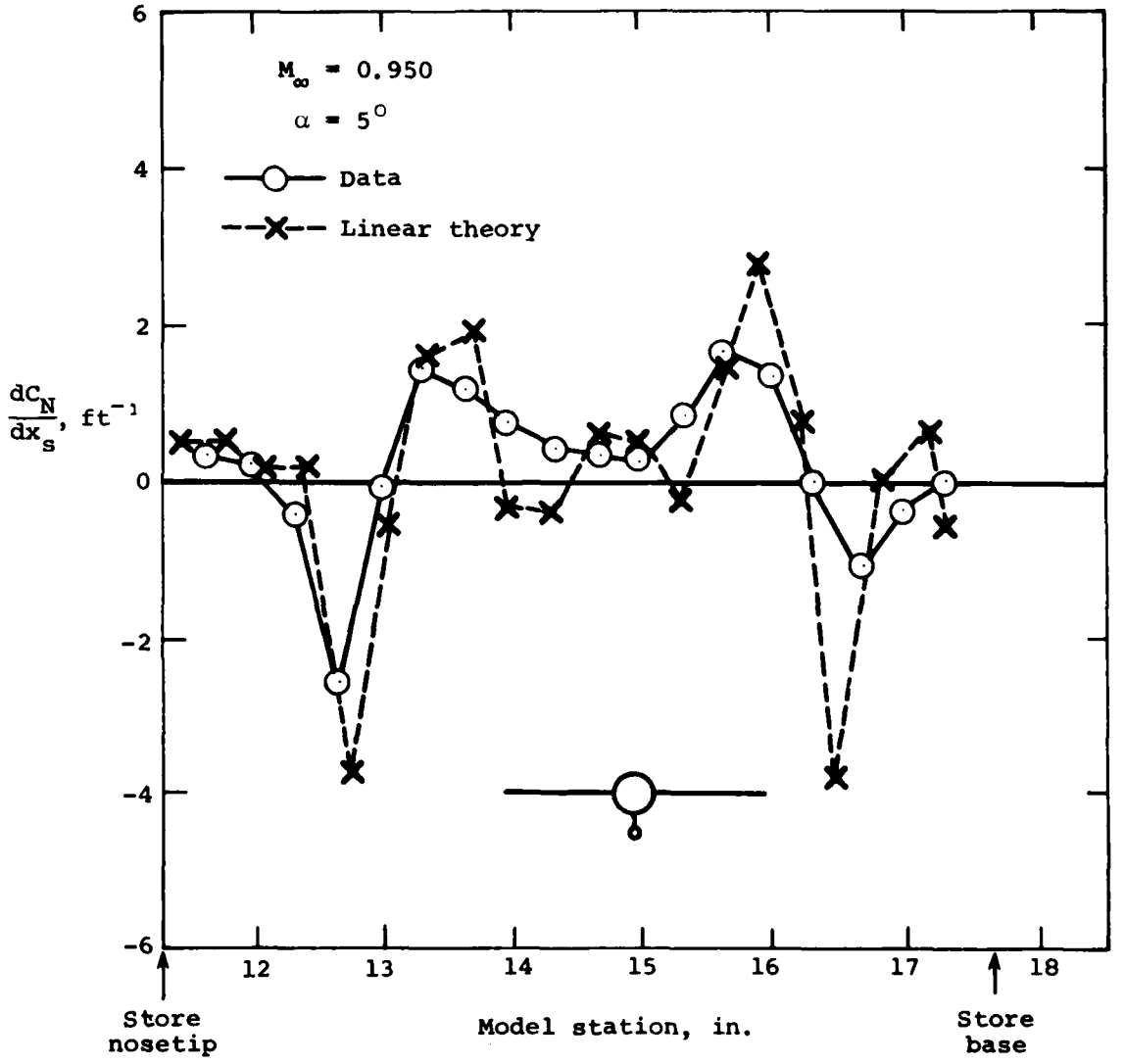

(a) Normal-force distribution.

Figure 16.- Comparison of measured and theoretical loading distribution for store attached to fuselage pylon; M_∞ = 0.950, α = 5°, (y_s, z_s) = (0, -2.297 in.).

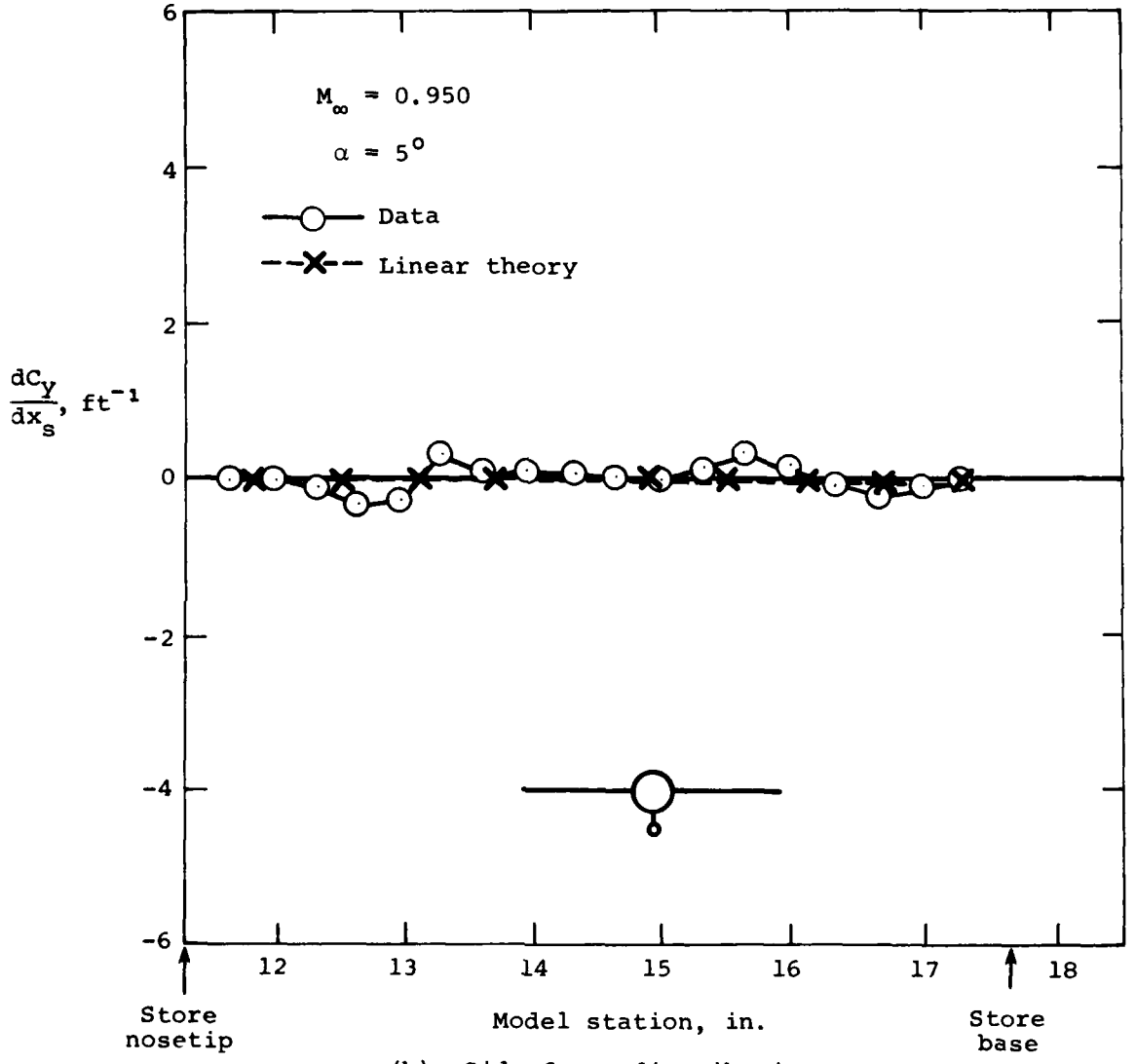

(b) Side-force distribution.

Figure 16.- Concluded.

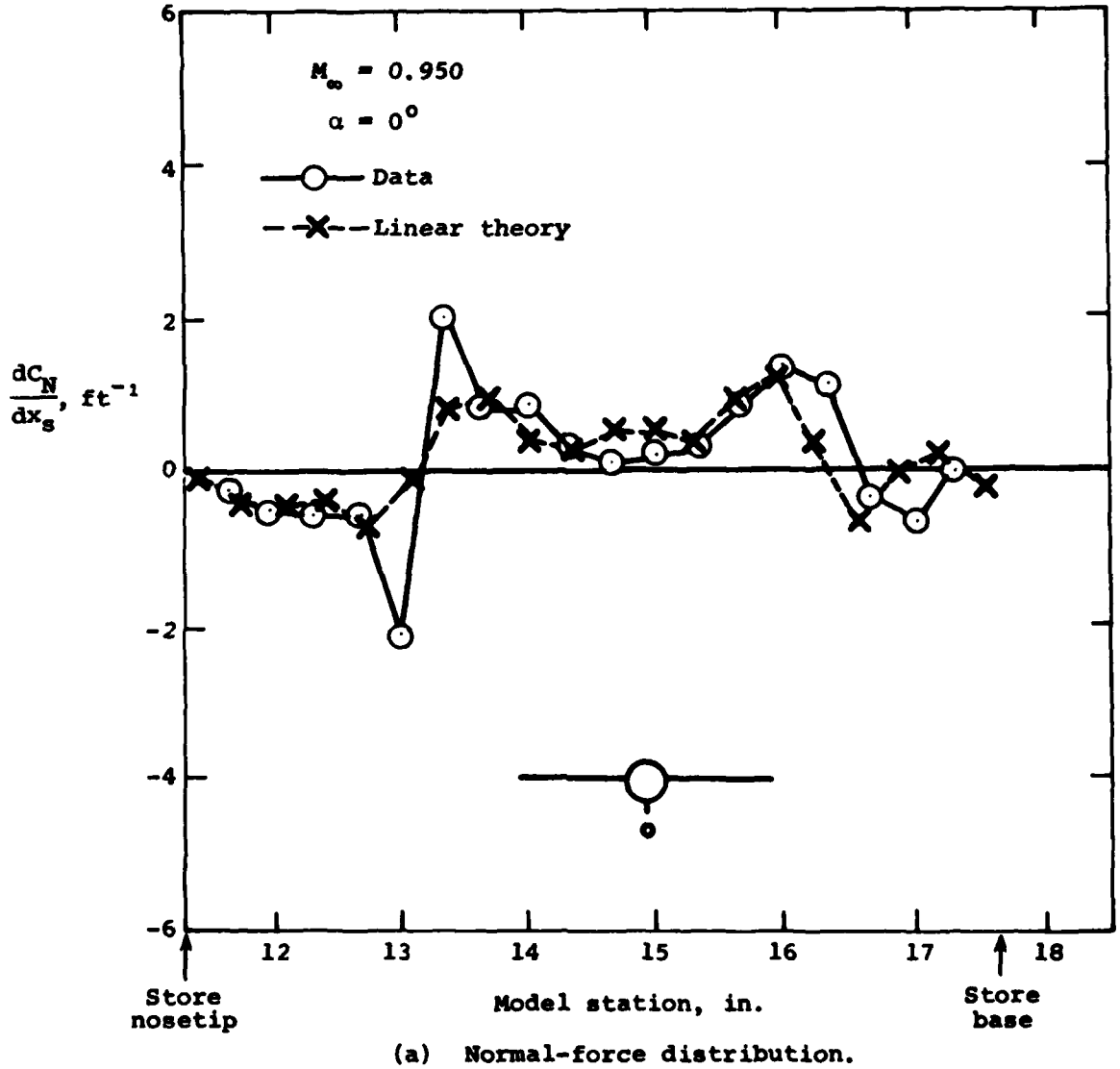

(a) Normal-force distribution.

Figure 17.- Comparison of measured and theoretical loading distributions for store separated from fuselage pylon; M_∞ = 0.950, α = 0°, (y_s, z_s) = (0, -2.947 in.).

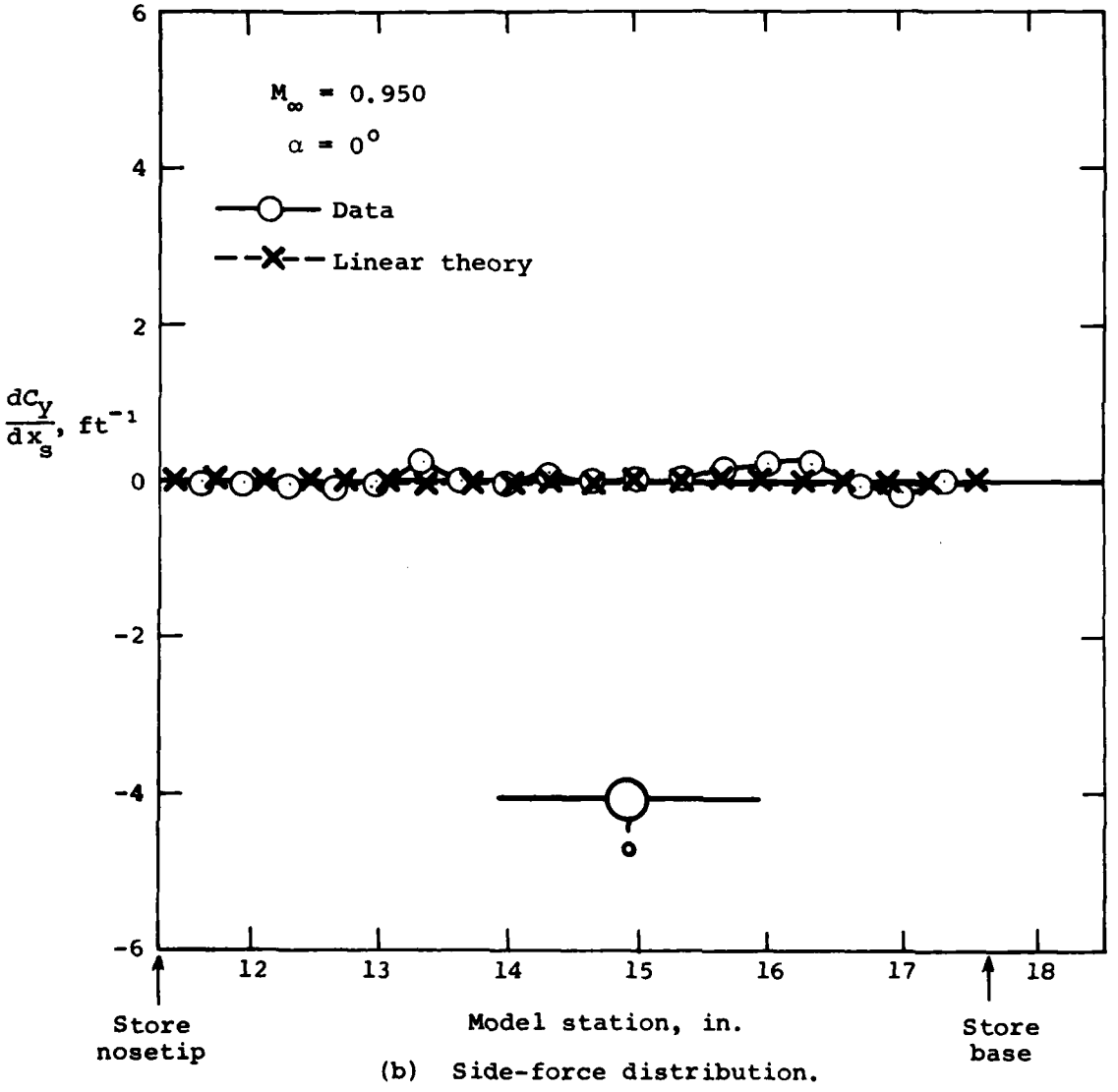

(b) Side-force distribution.

Figure 17.- Concluded.

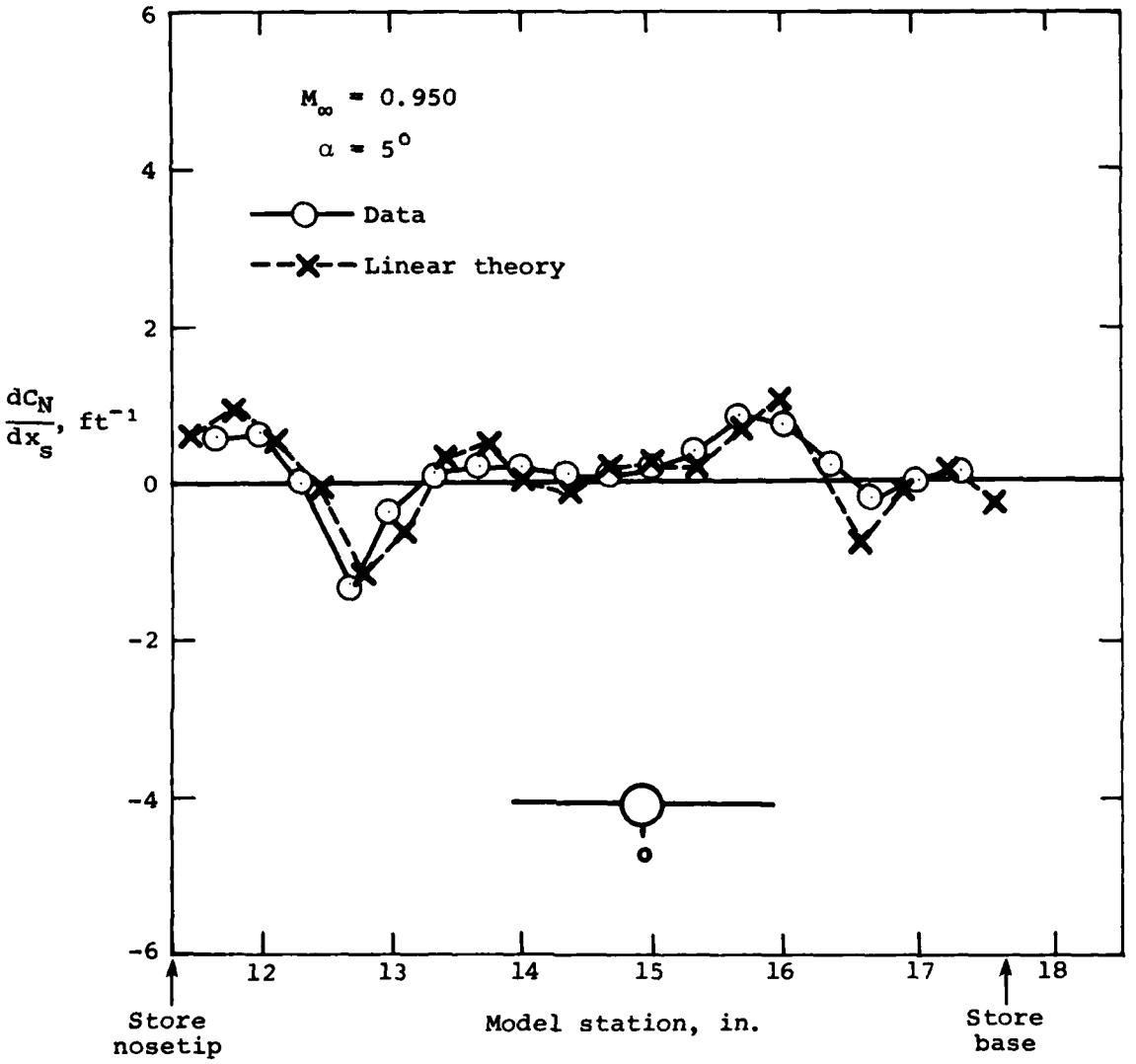

(a) Normal-force distribution.

Figure 18.- Comparison of measured and theoretical loading distributions for store separated from fuselage pylon; M_∞ = 0.950, α = 5°, (y_s, z_s) = (0, -2.947 in.).

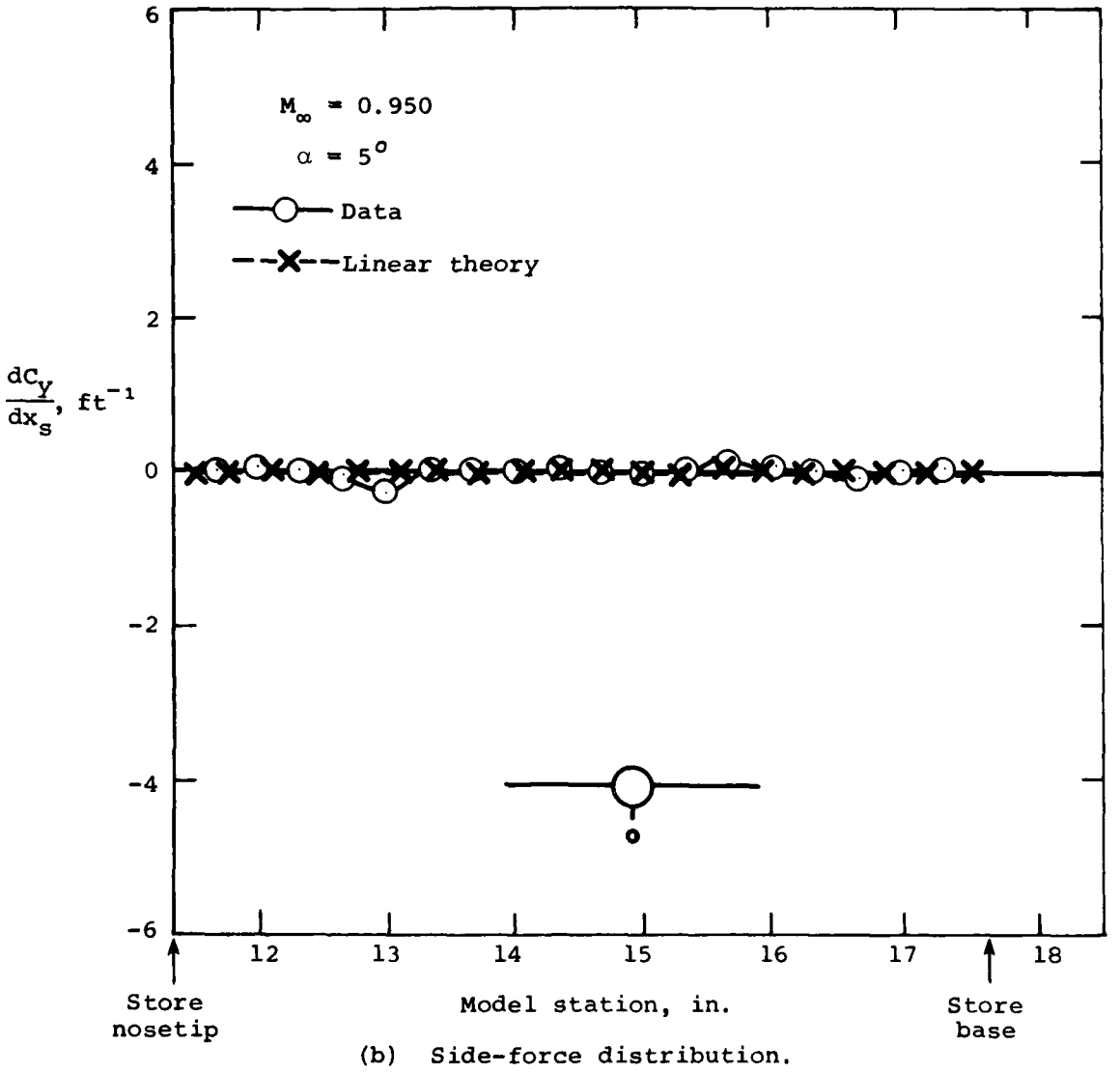

(b) Side-force distribution.

Figure 18.- Concluded.

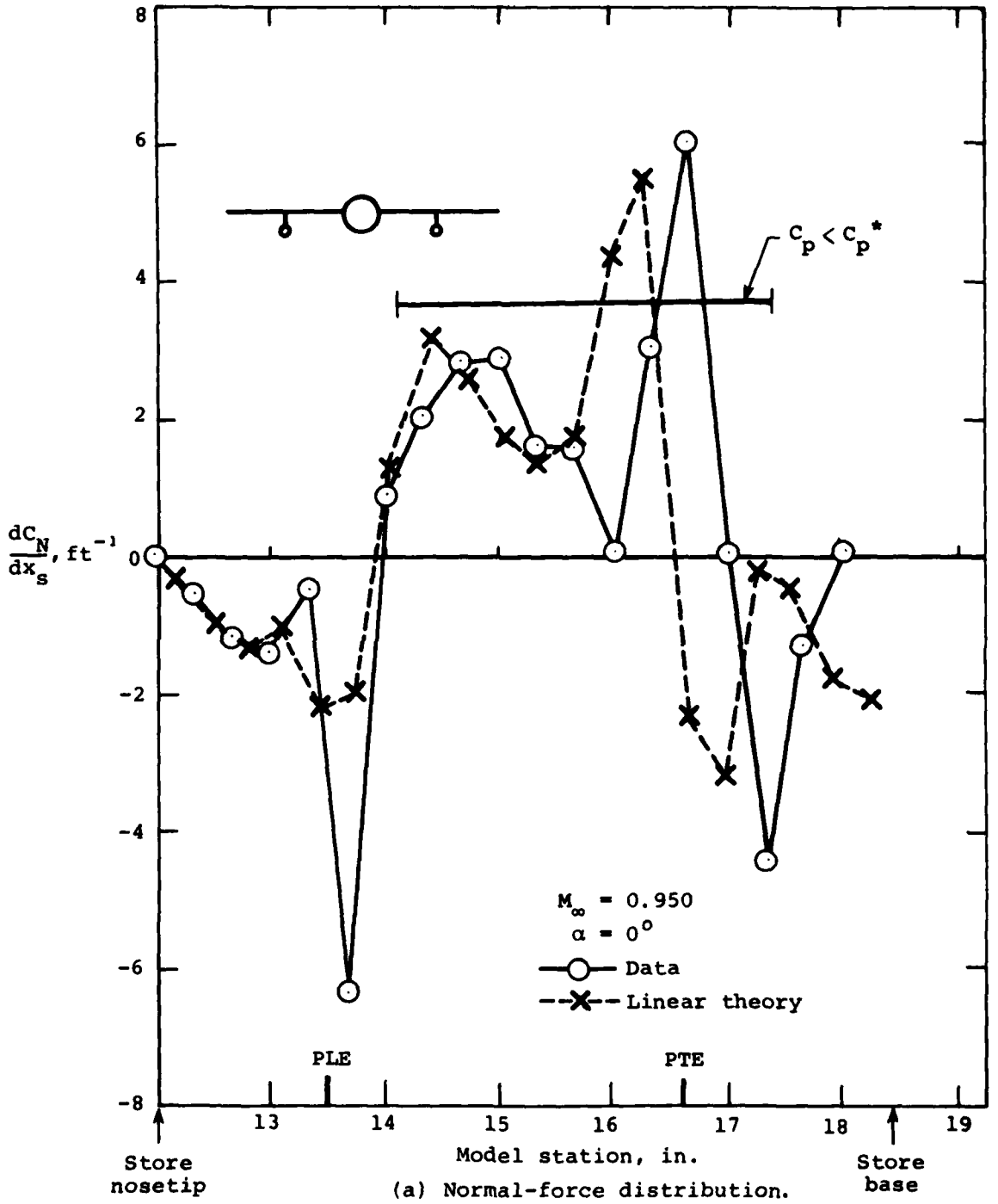

(a) Normal-force distribution.

Figure 19.- Comparison of measured and theoretical loading distributions for store attached to wing pylon; M_∞ = 0.950, α = 0 , (y_s, z_s) = (3.5 in., -1.3 in.).

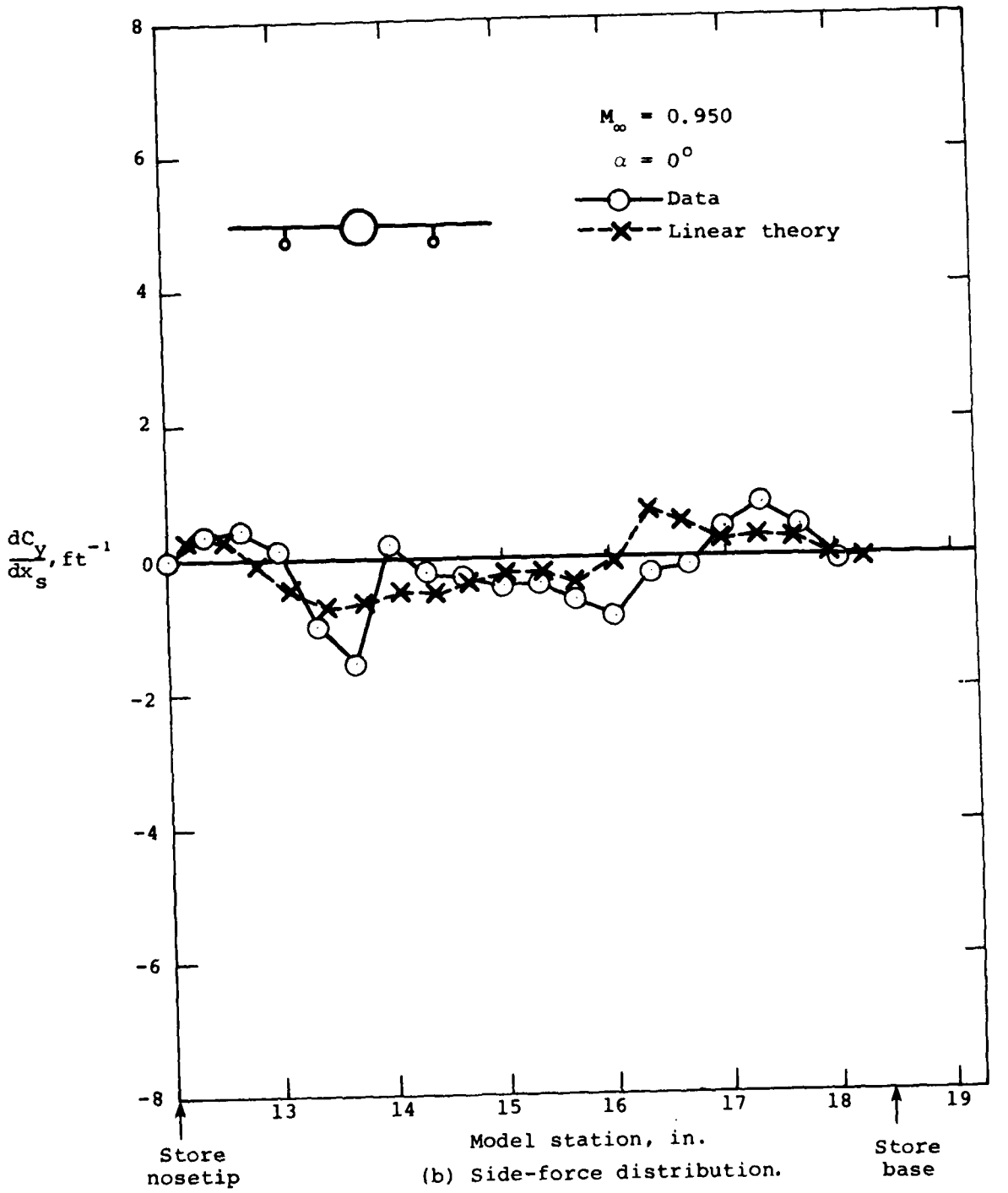

(b) Side-force distribution.

Figure 19. - Concluded.

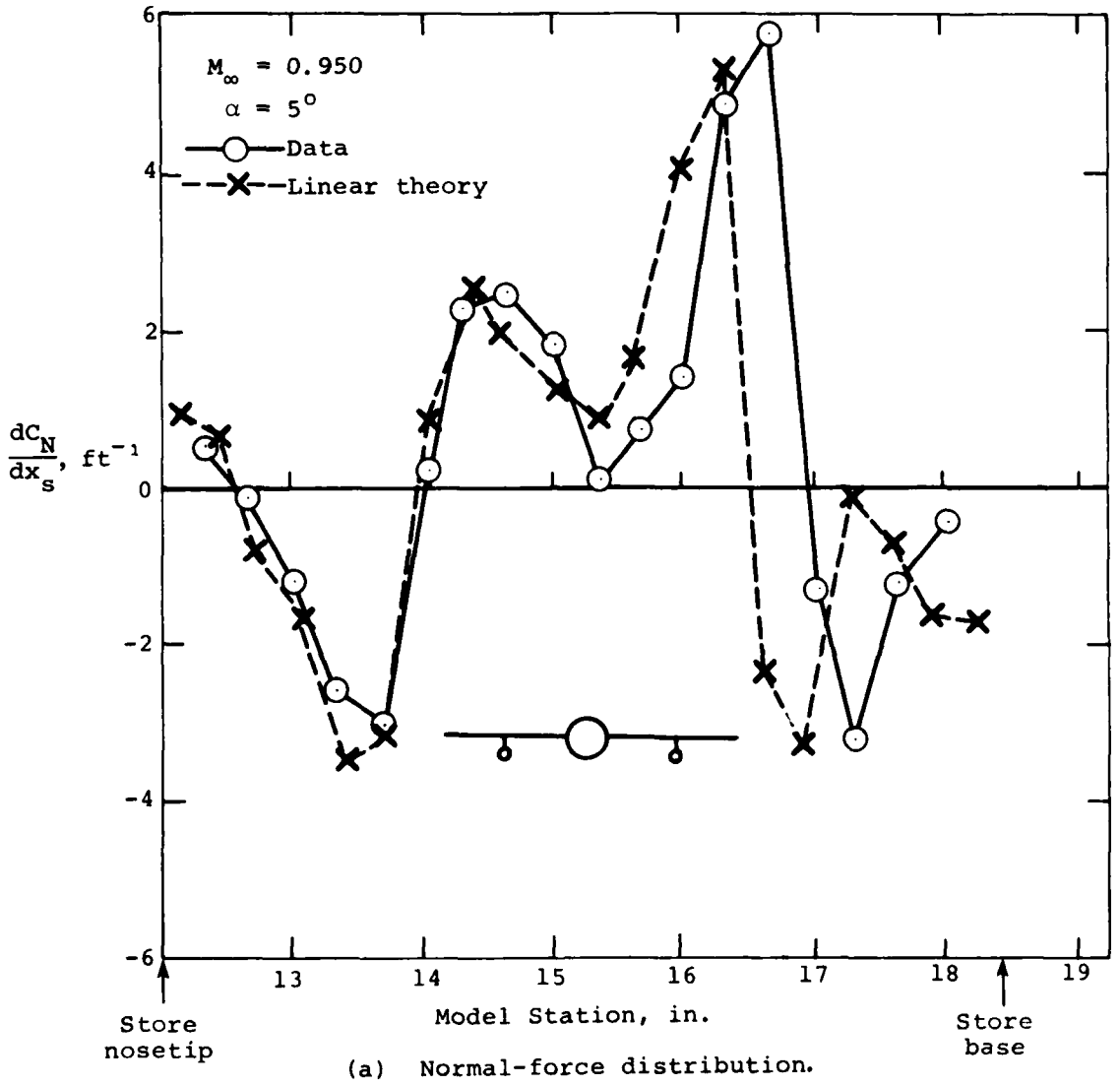

(a) Normal-force distribution.

Figure 20.- Comparison of measured and theoretical loading distributions for store attached to wing pylon; $M_\infty = 0.950$, $\alpha = 5^o$, $(y_s, z_s) = (3.5$ in., -1.3 in.$)$.

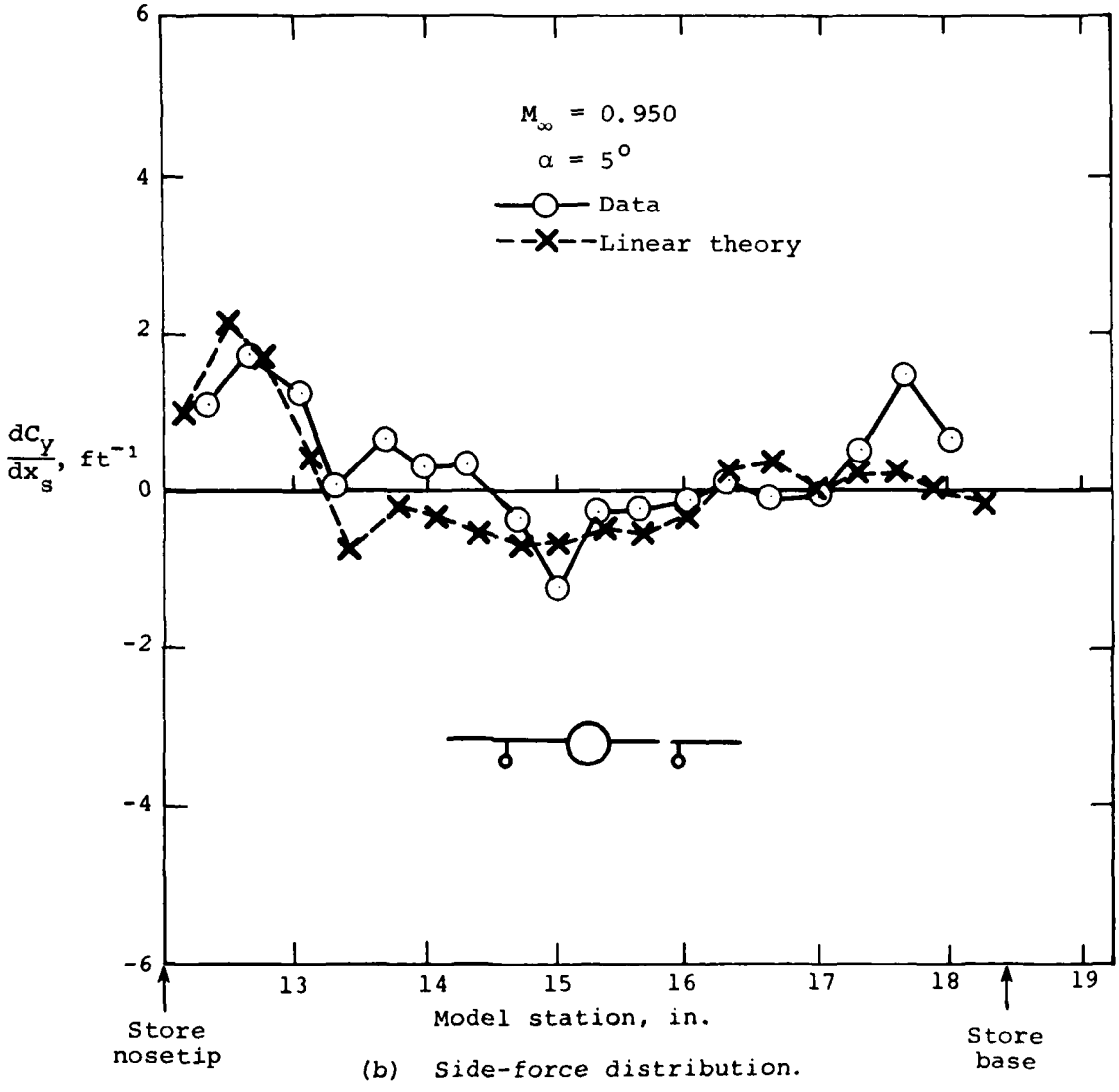

(b) Side-force distribution.

Figure 20.- Concluded.

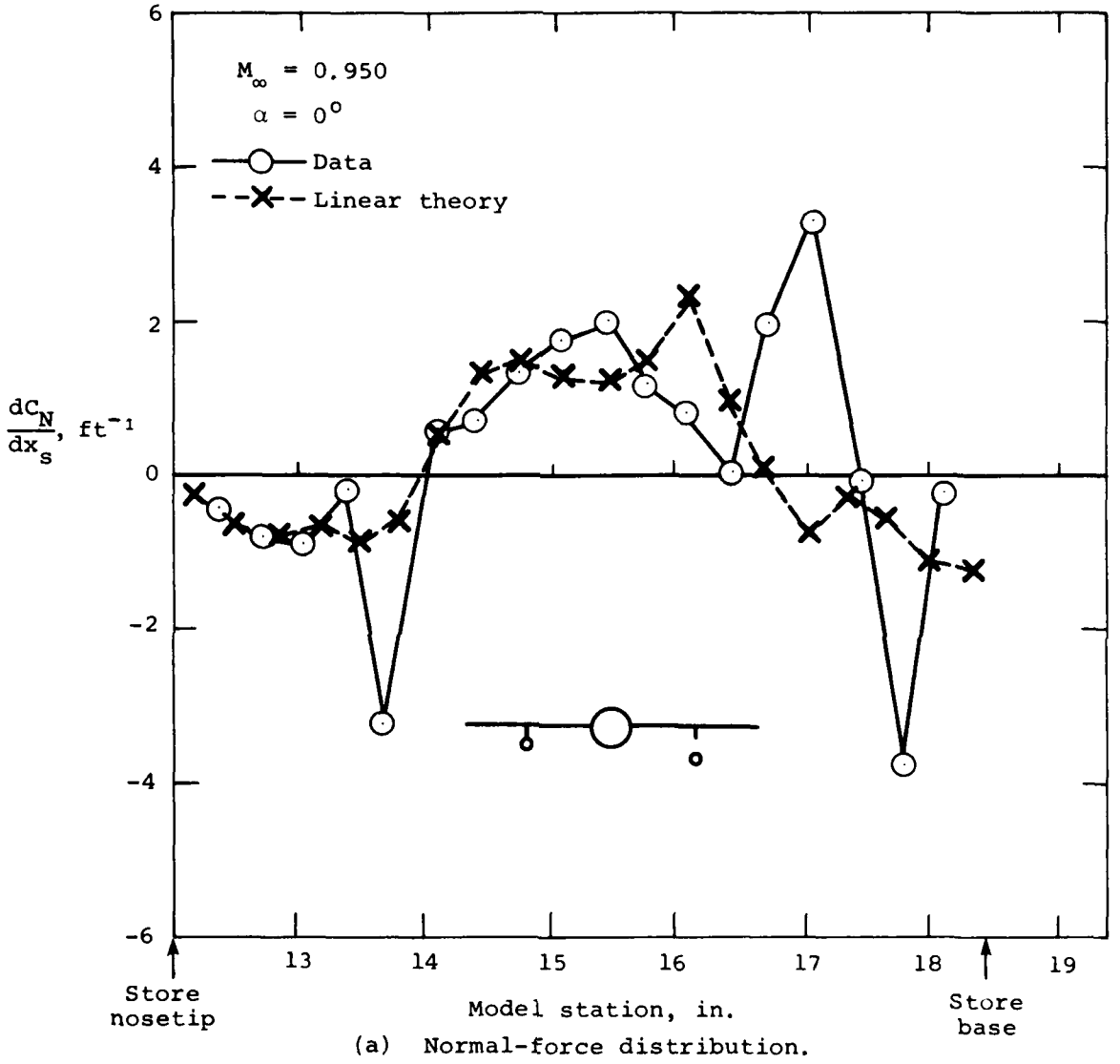

(a) Normal-force distribution.

Figure 21.- Comparison of measured and theoretical loading distributions for store separated from wing pylon; M_∞ = 0.950, $\alpha = 0^\circ$, (y_s, z_s) = (3.5 in., -1.95 in.).

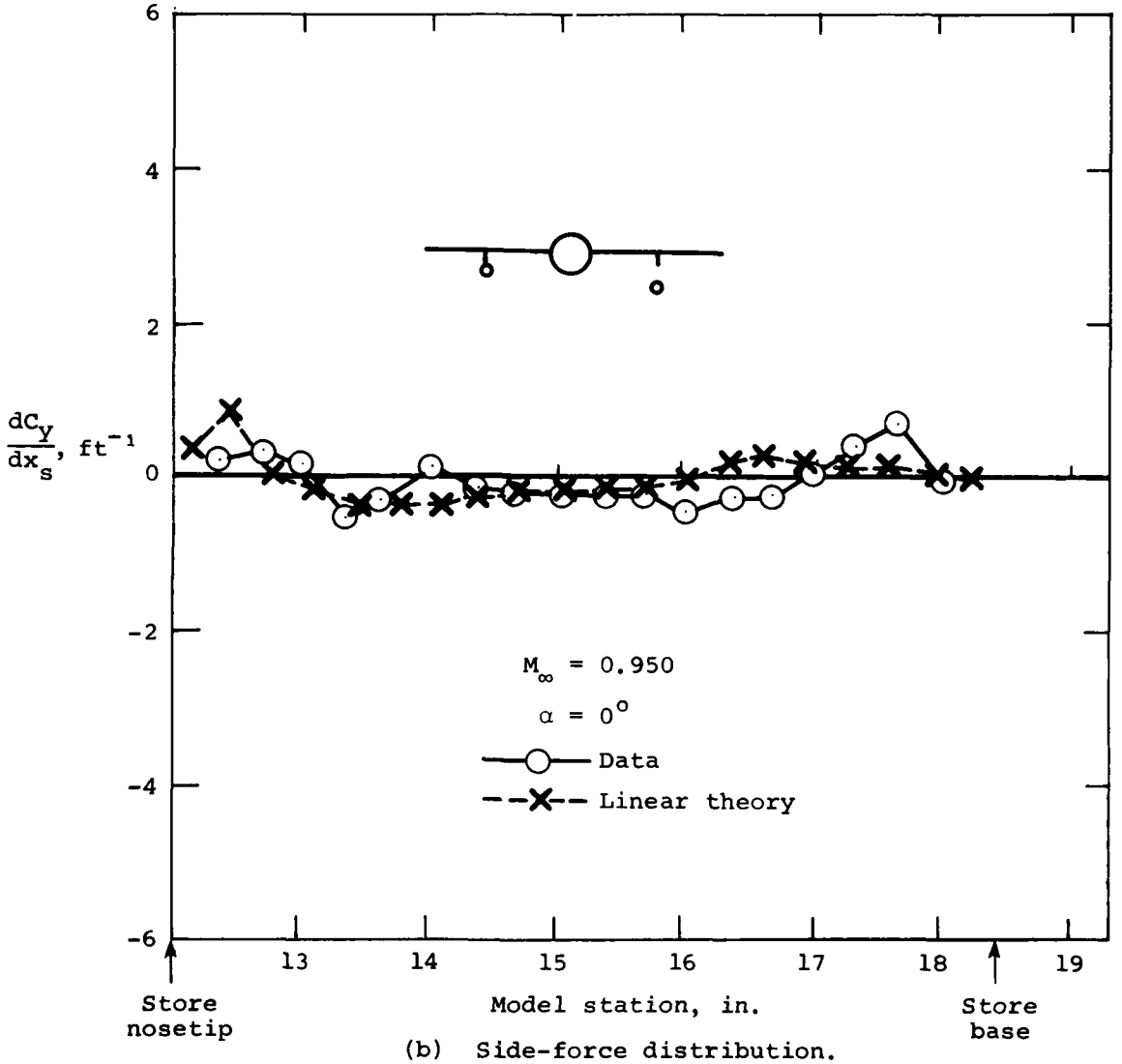

(b) Side-force distribution.

Figure 21.- Concluded.

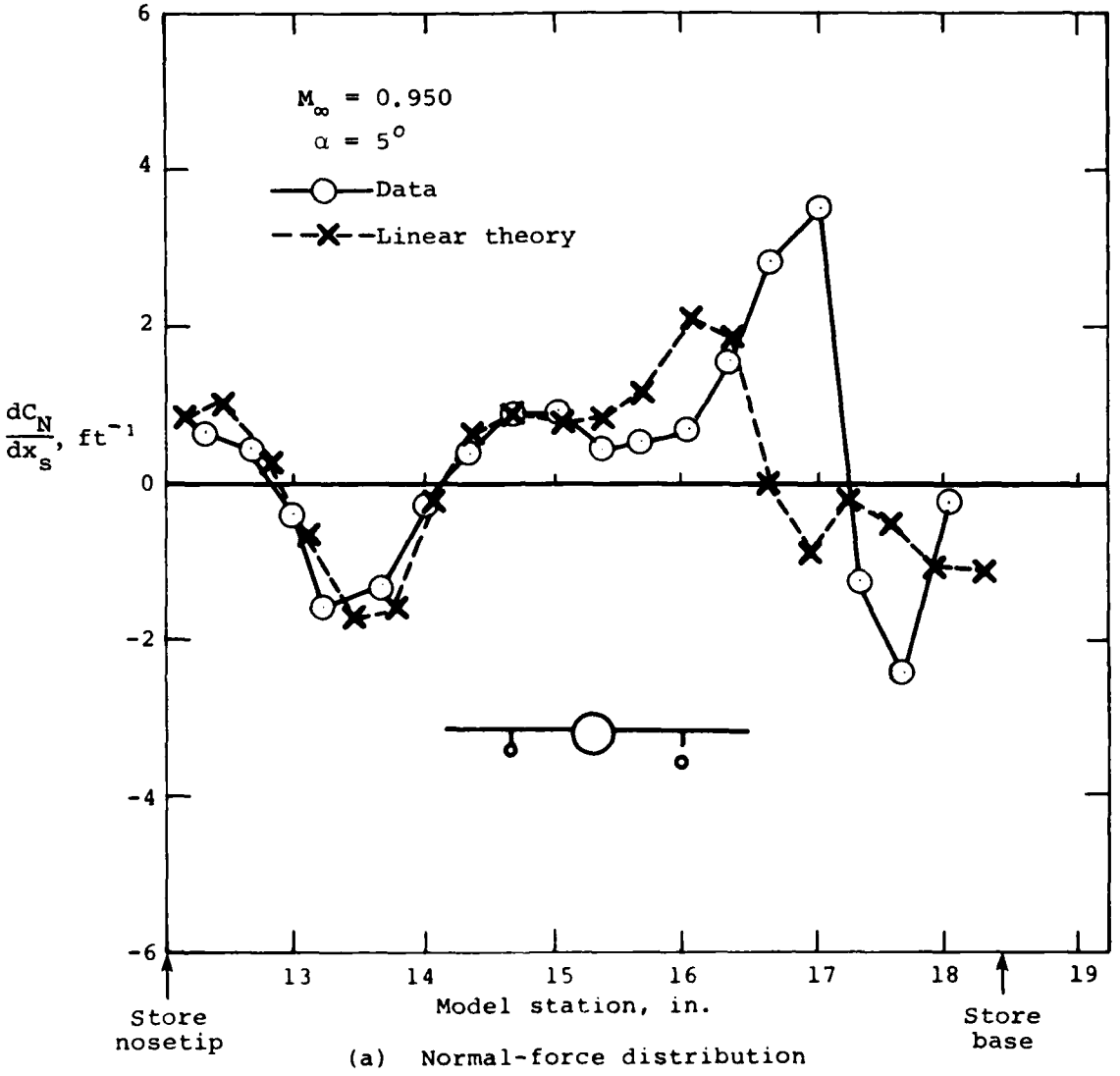

(a) Normal-force distribution

Figure 22.- Comparison of measured and theoretical loading distributions for store separated from wing pylon; $M_\infty = 0.950$, $\alpha = 5°$, (y_s, z_s) = (3.5 in., -1.950 in.).

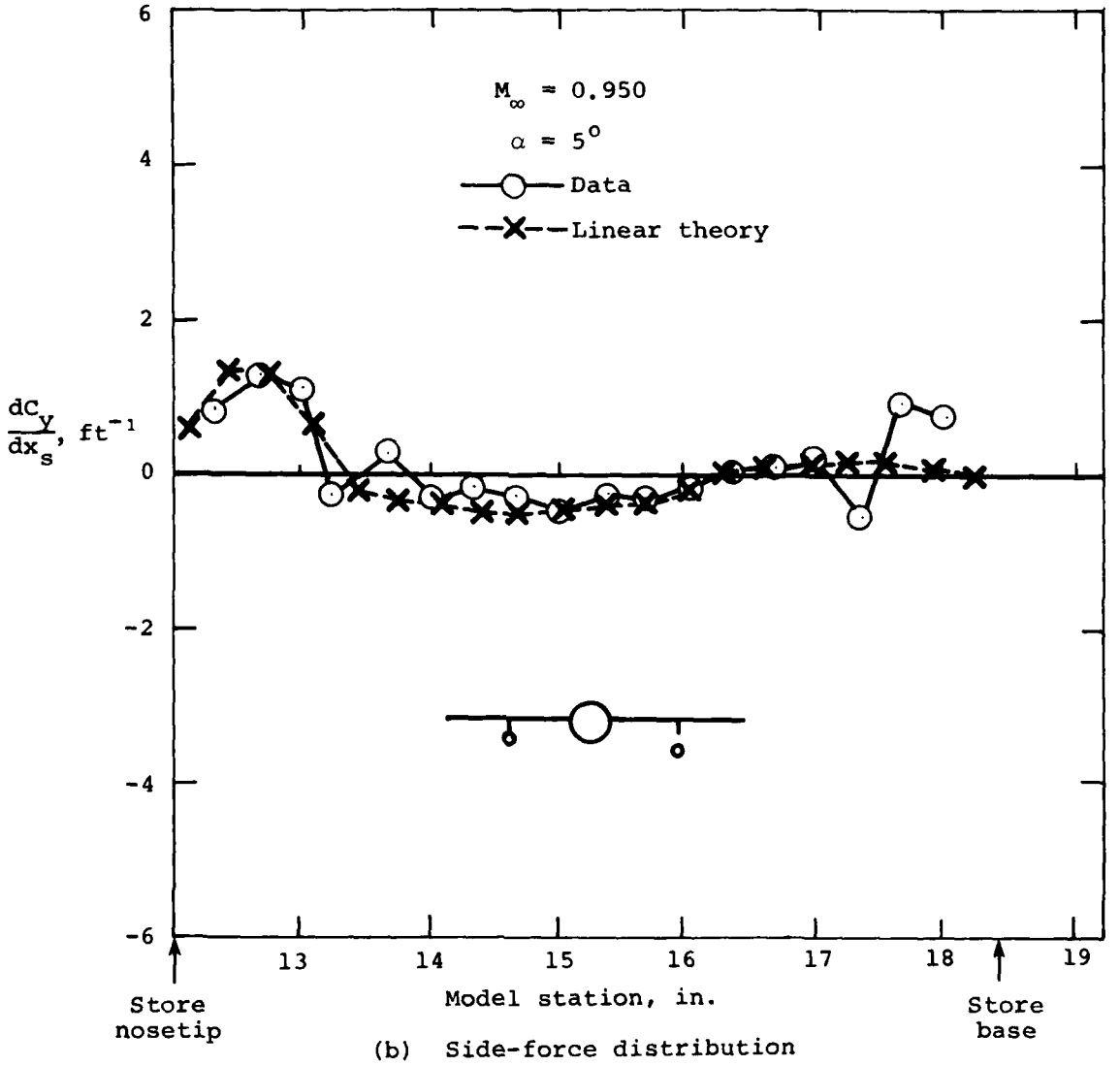

(b) Side-force distribution

Figure 22.- Concluded.

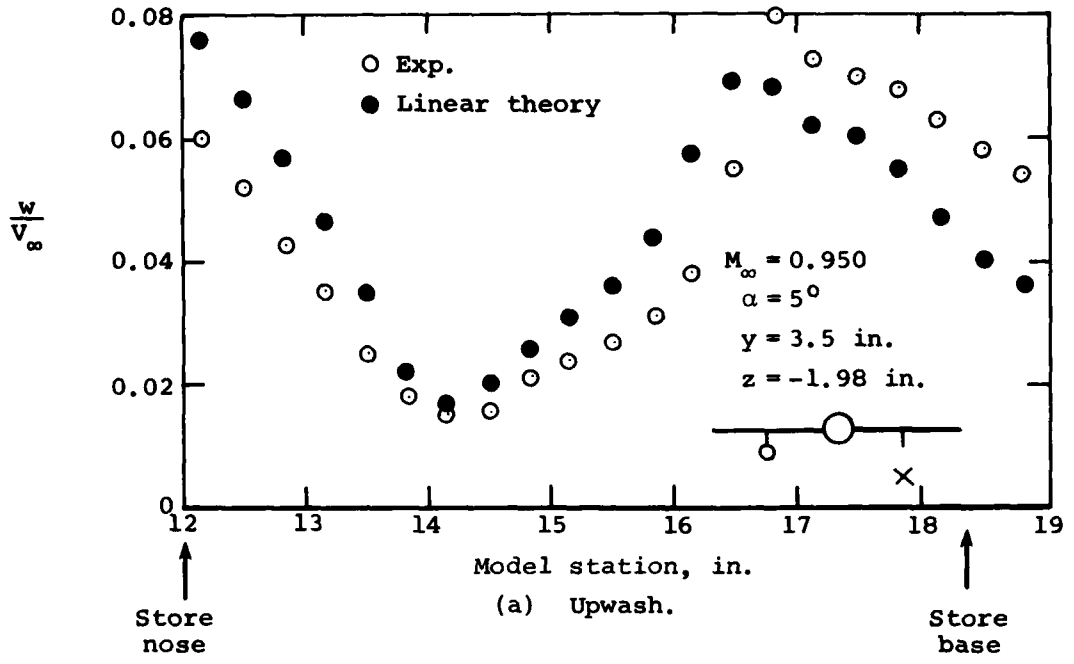

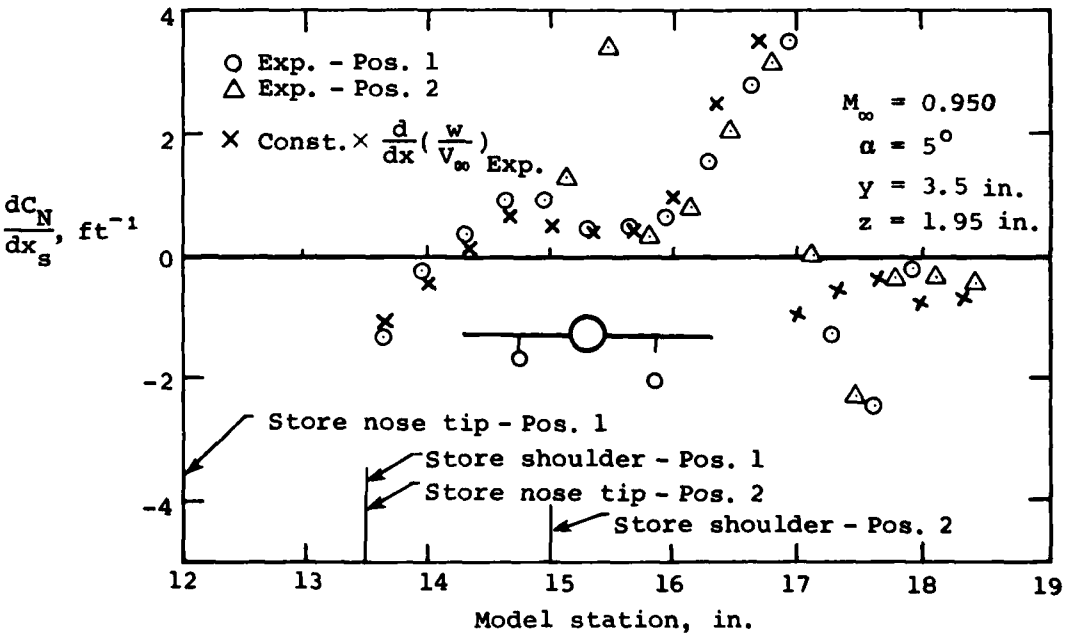

(b) Normal-force distribution.

Figure 23.- Comparison of measured normal-force distributions for stores near wing pylon at two different axial positions with theoretical calculation based on slope of upwash data; $M_\infty = 0.950$, $\alpha = 5^o$.

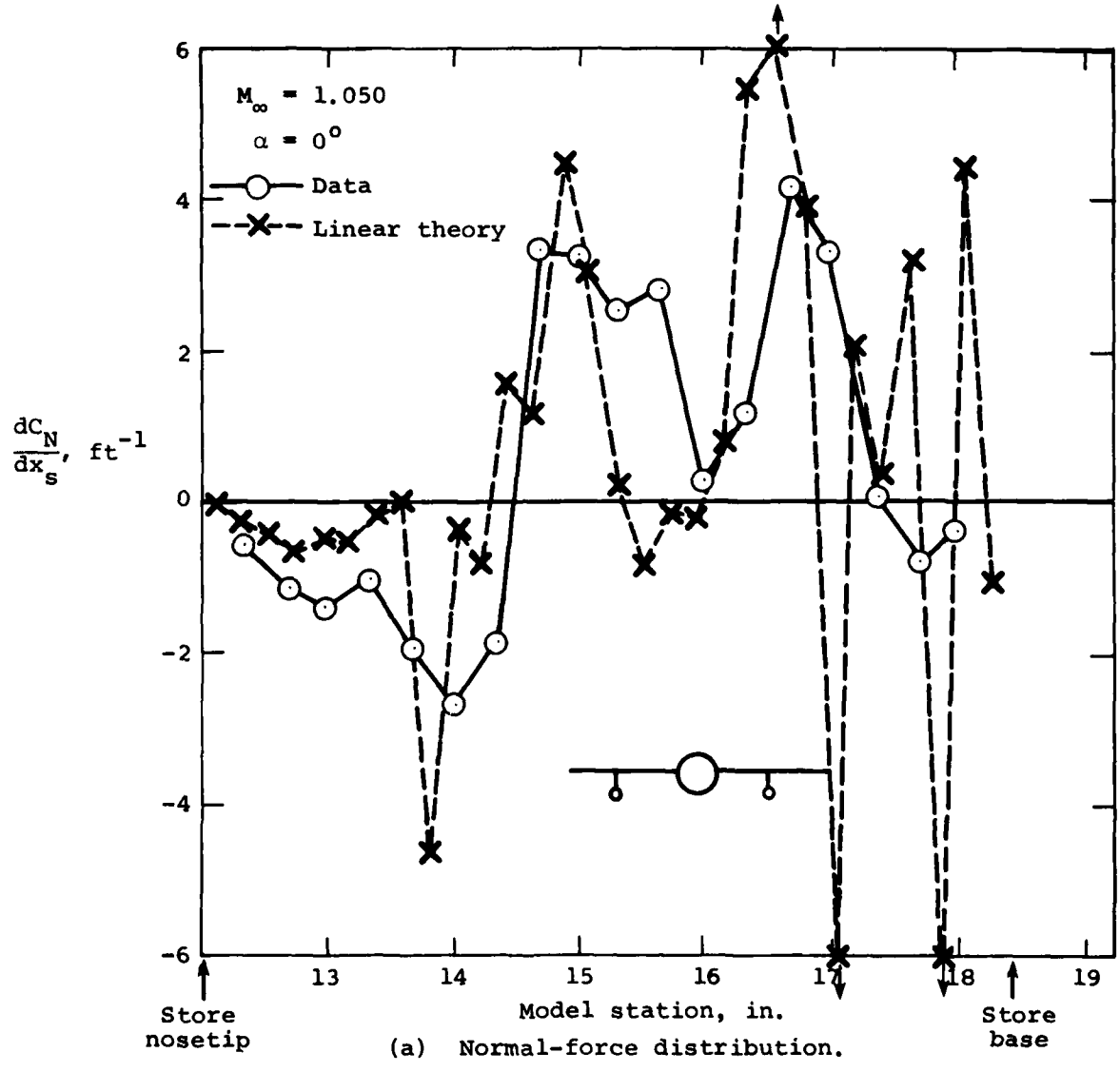

(a) Normal-force distribution.

Figure 24.- Comparison of measured and theoretical loading distributions for store attached to wing pylon; $M_\infty = 1.050$, $\alpha = 0°$, $(y_s, z_s) = (3.5$ in., -1.3 in.).

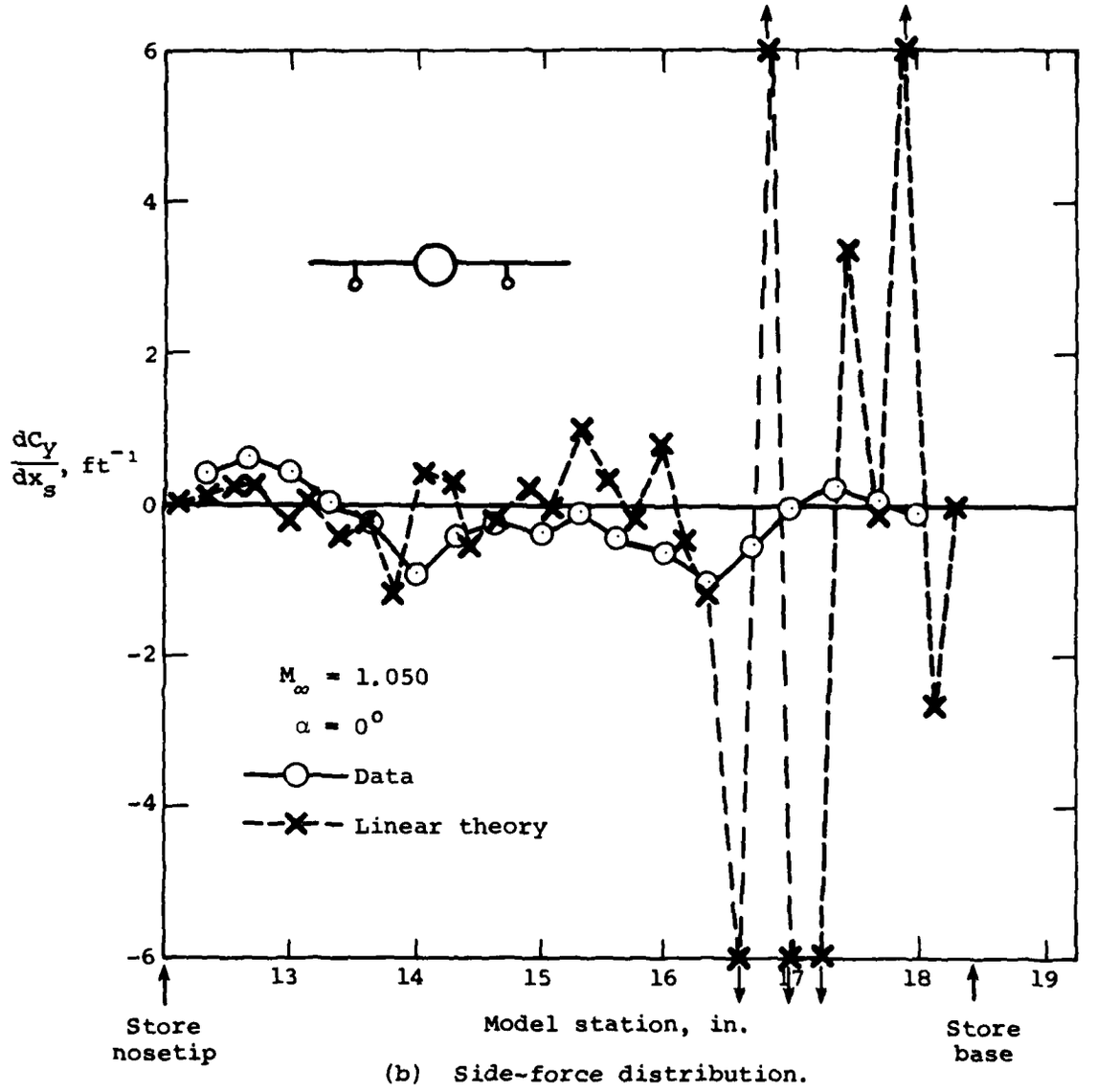

(b) Side-force distribution.

Figure 24.- Concluded.

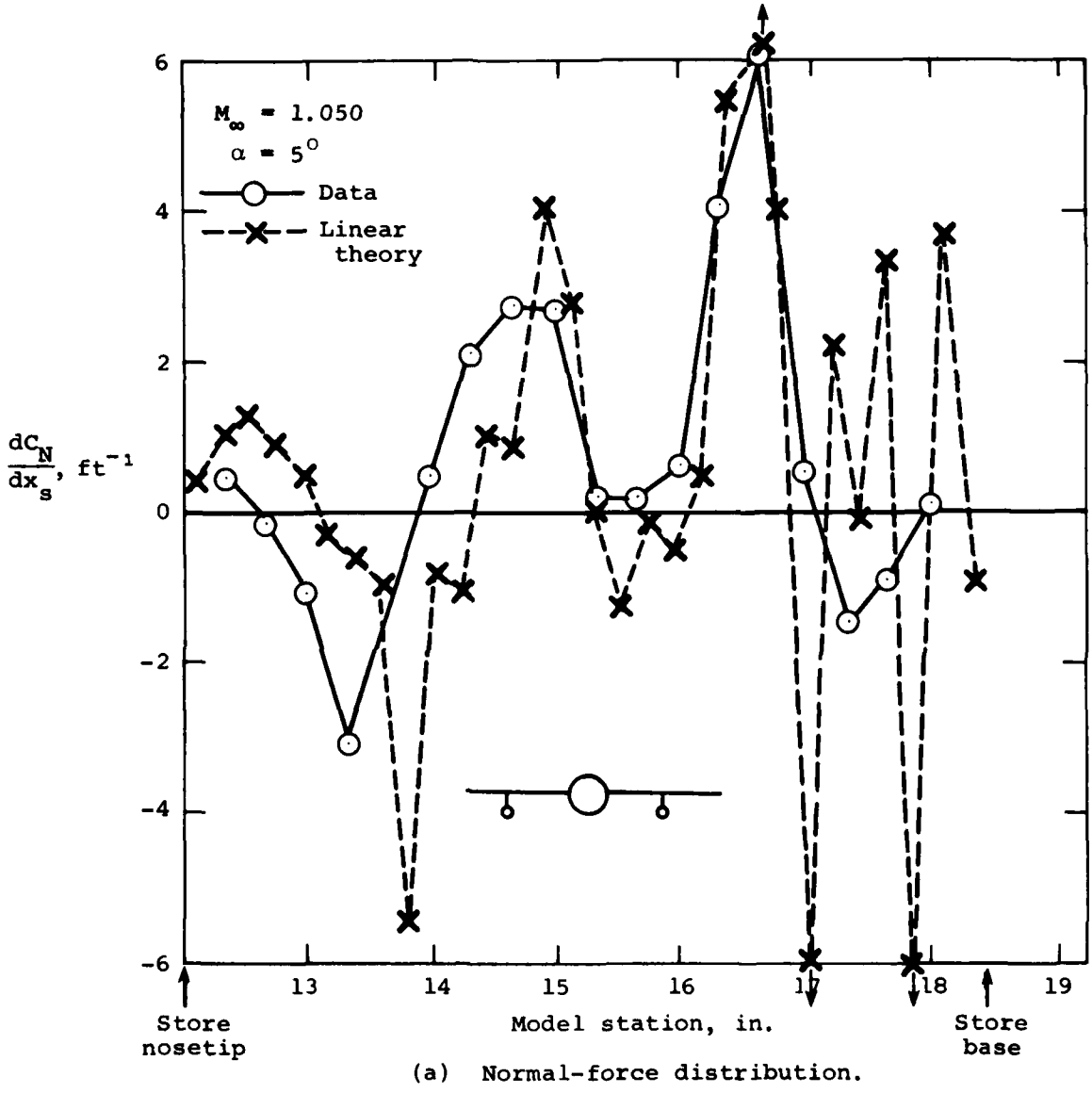

(a) Normal-force distribution.

Figure 25.- Comparison of measured and theoretical loading distributions for store attached to wing pylon; $M_\infty = 1.050$, $\alpha = 5°$, $(y_s, z_s) = (3.5$ in., -1.3 in.$)$.

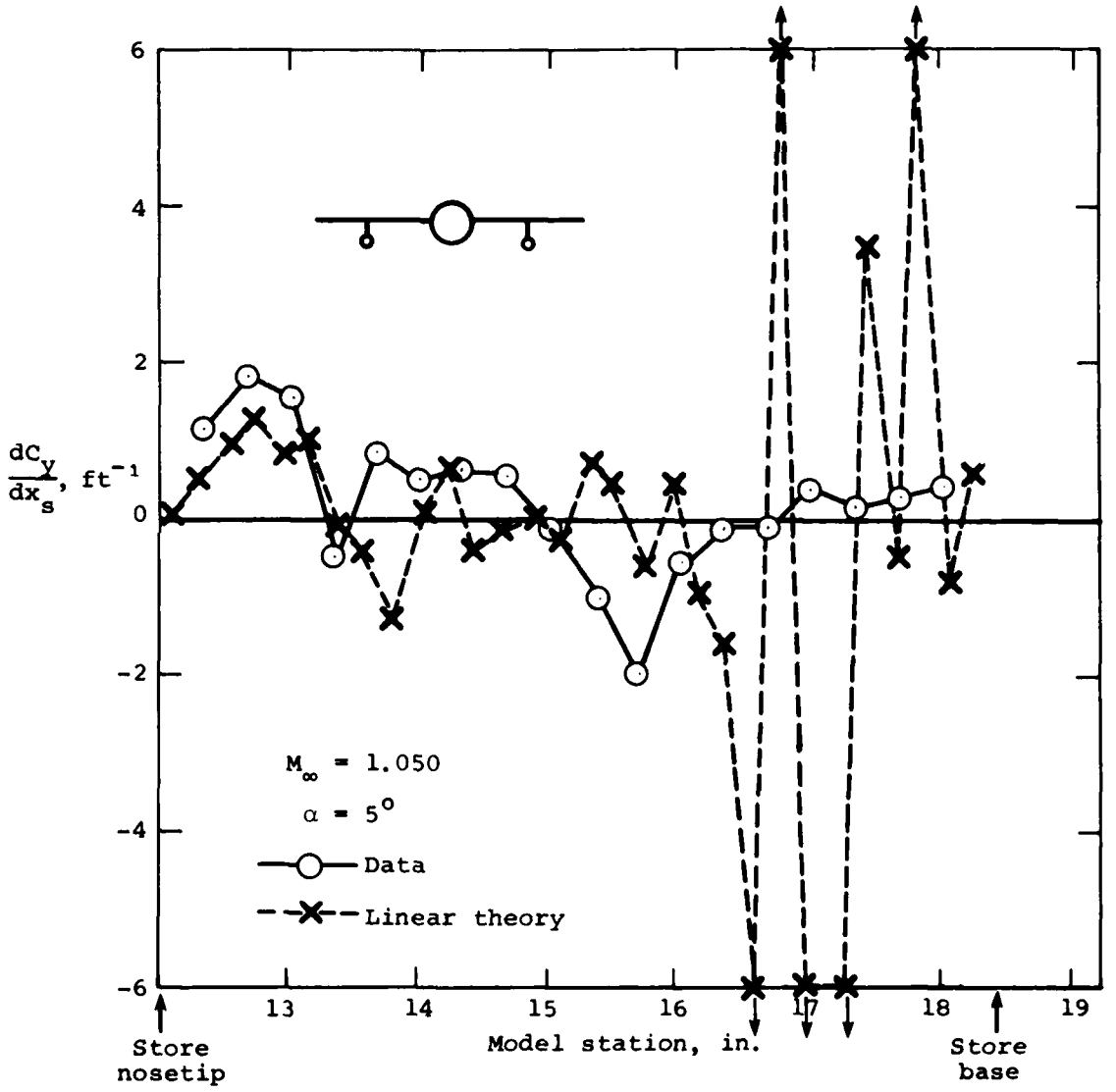

(b) Side-force distribution.

Figure 25.- Concluded.

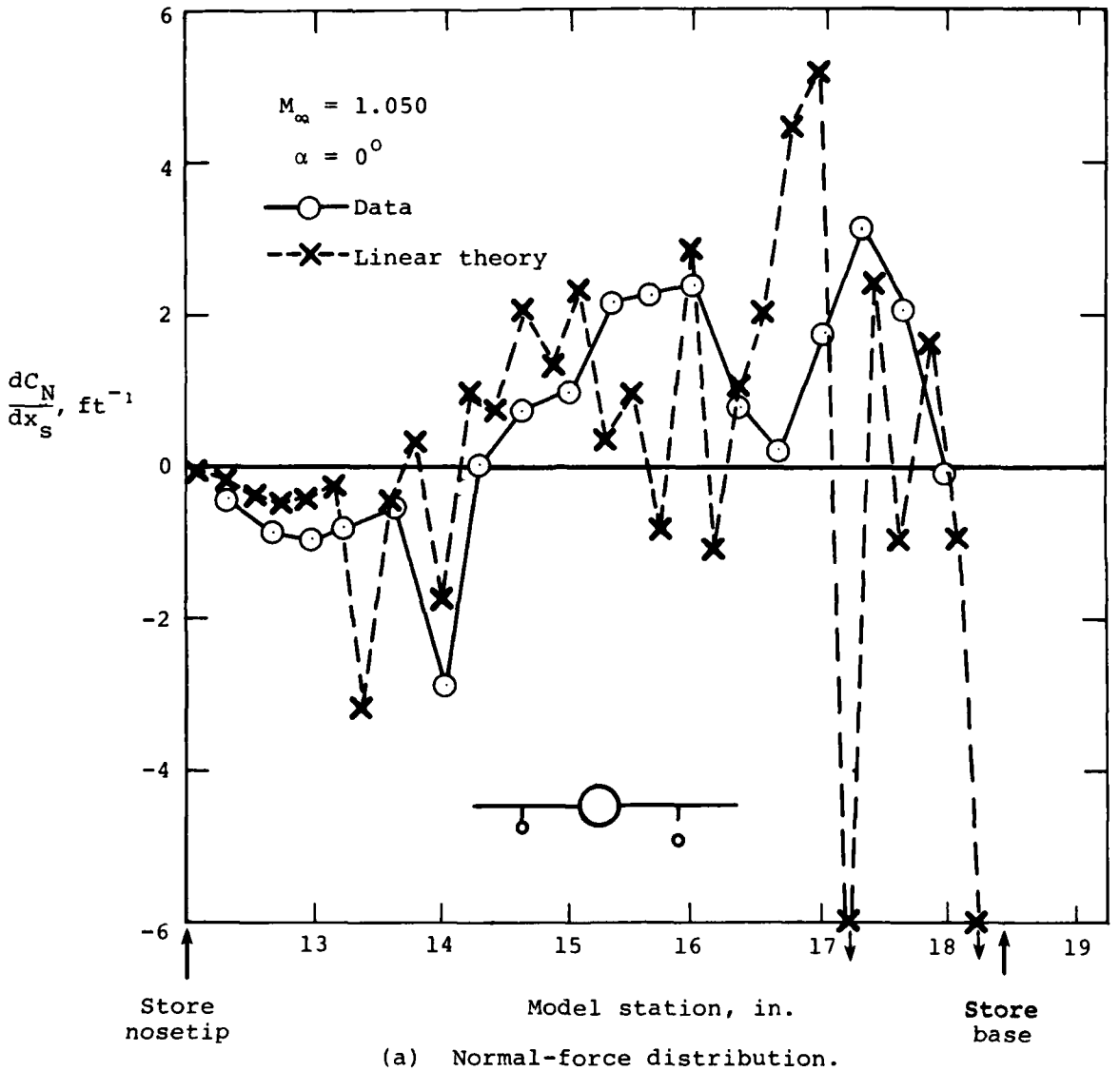

(a) Normal-force distribution.

Figure 26.- Comparison of measured and theoretical loading distributions for store separated from wing pylon; M_∞ = 1.050, α = 0°, (y_s, z_s) = (3.5 in., -1.95 in. .

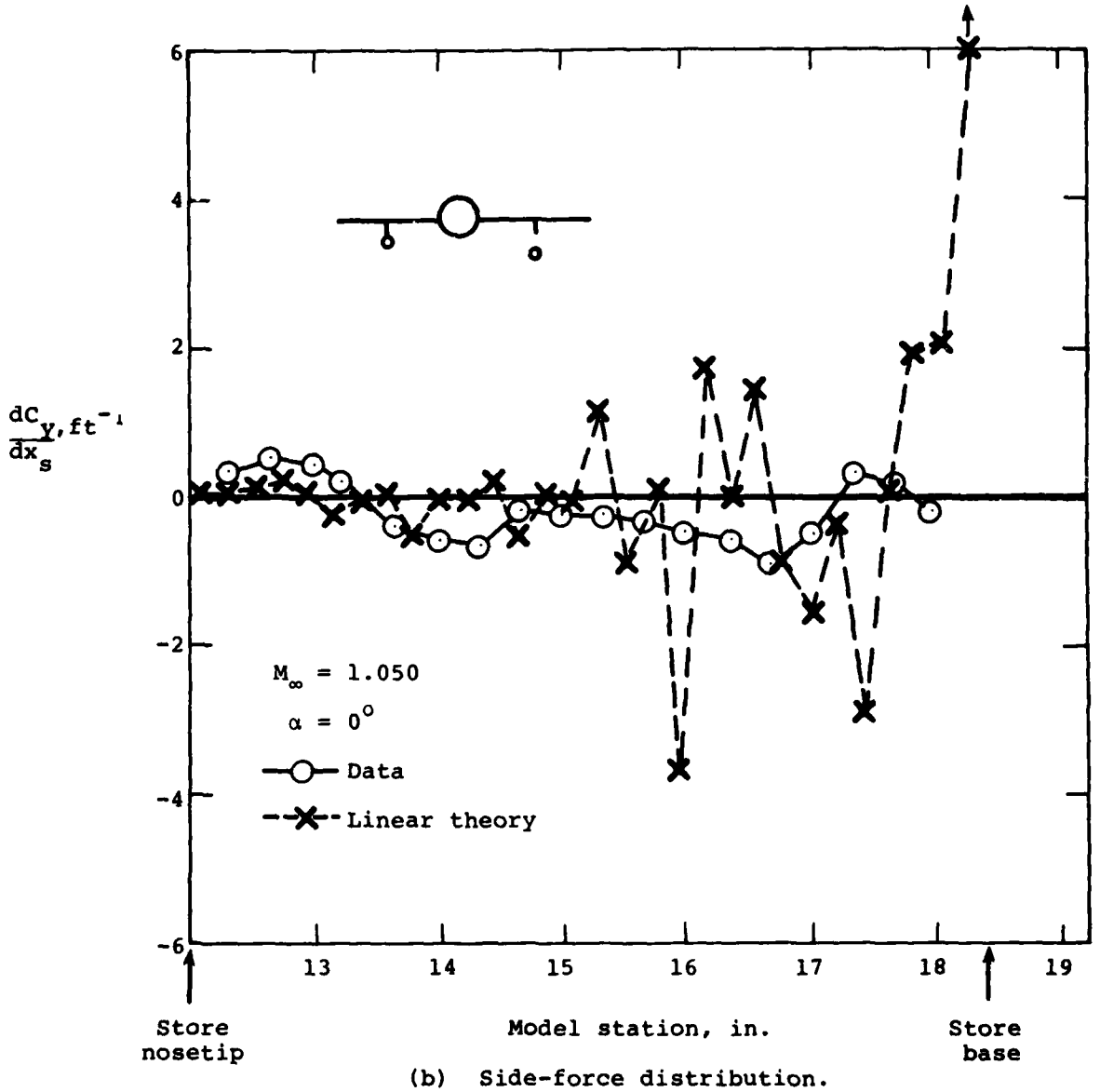

(b) Side-force distribution.

Figure 26.- Concluded.

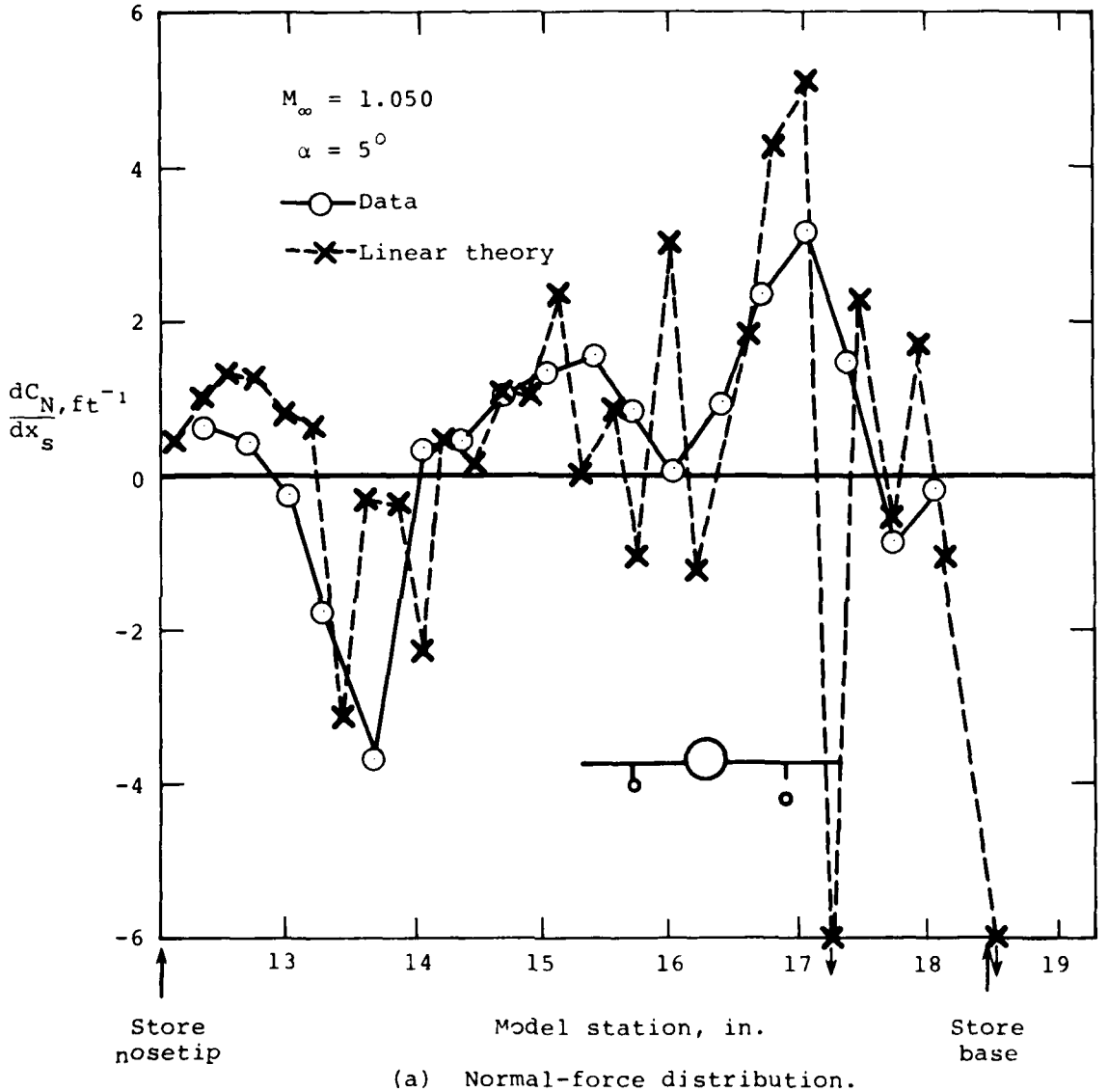

(a) Normal-force distribution.

Figure 27.- Comparison of measured and theoretical loading distributions for store separated from wing pylon; M_∞ = 1.050, α = 5°, (y_s, z_s)=(3.5 in., -1.95 in.).

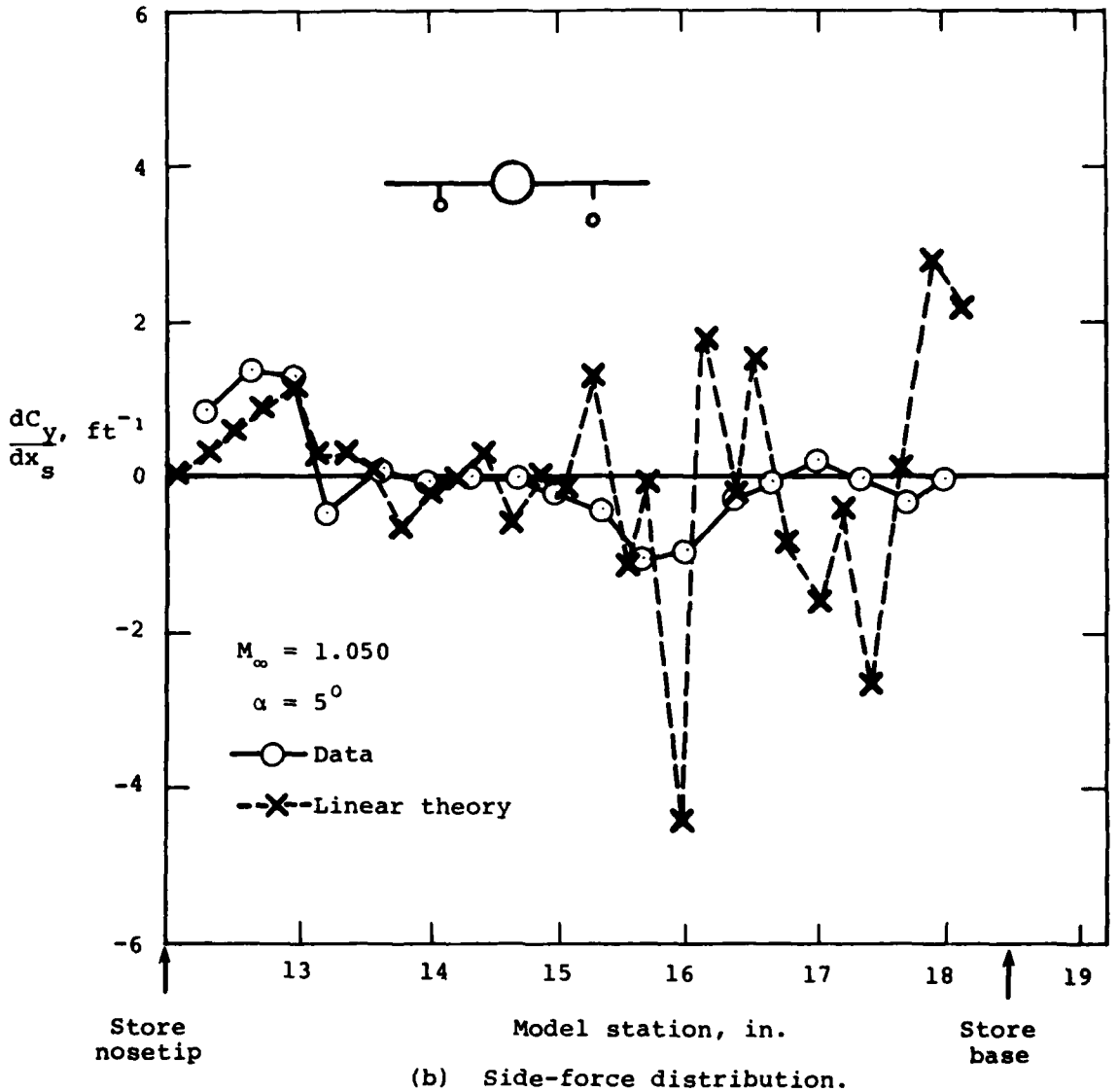

(b) Side-force distribution.

Figure 27.- Concluded.

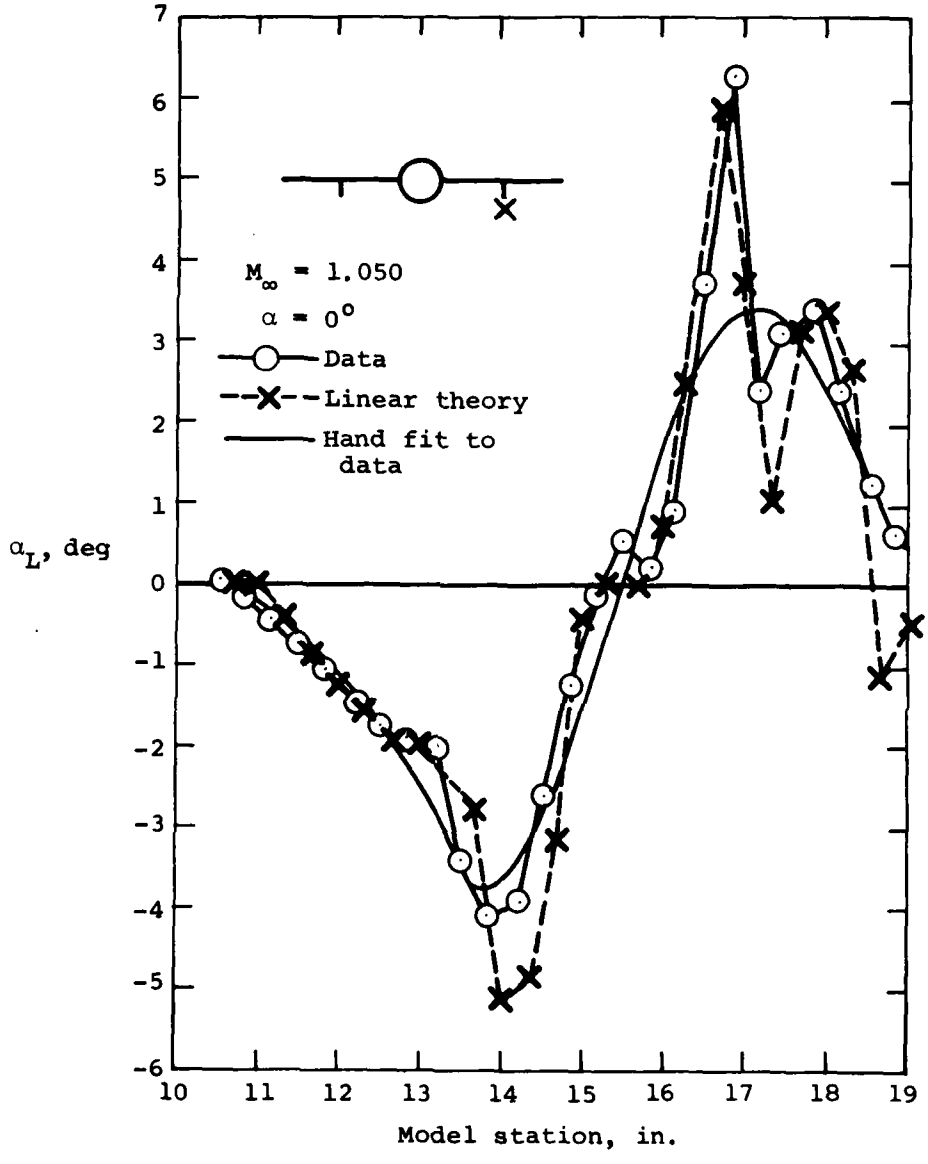

(a) Upwash angle, deg.

Figure 28.- Comparison of measured and theoretical upwash and sidewash for survey near wing pylon; M_∞ = 1.050, α = 0°, (y,z) = (3.5 in., -1.23 in.).

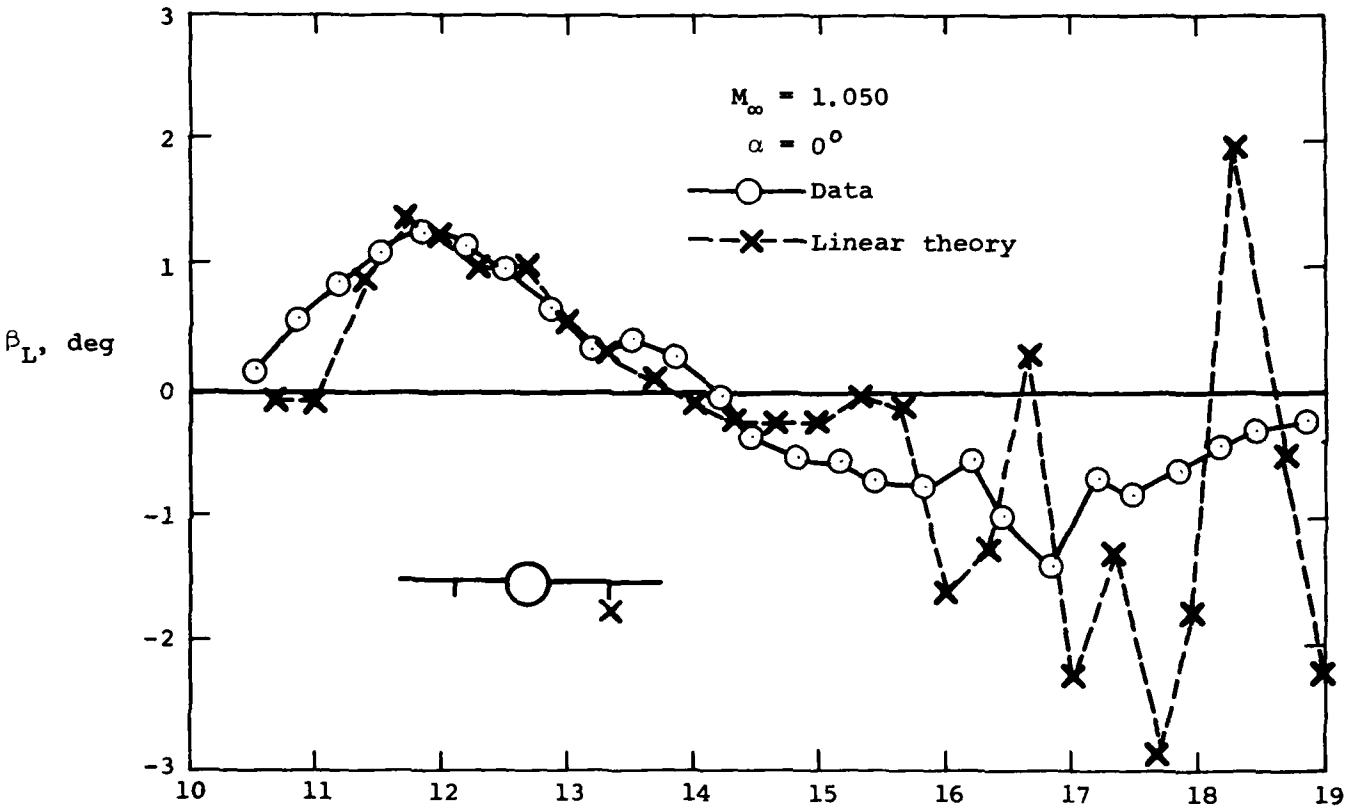

(b) Sidewash angle, deg.

Figure 28.- Concluded.

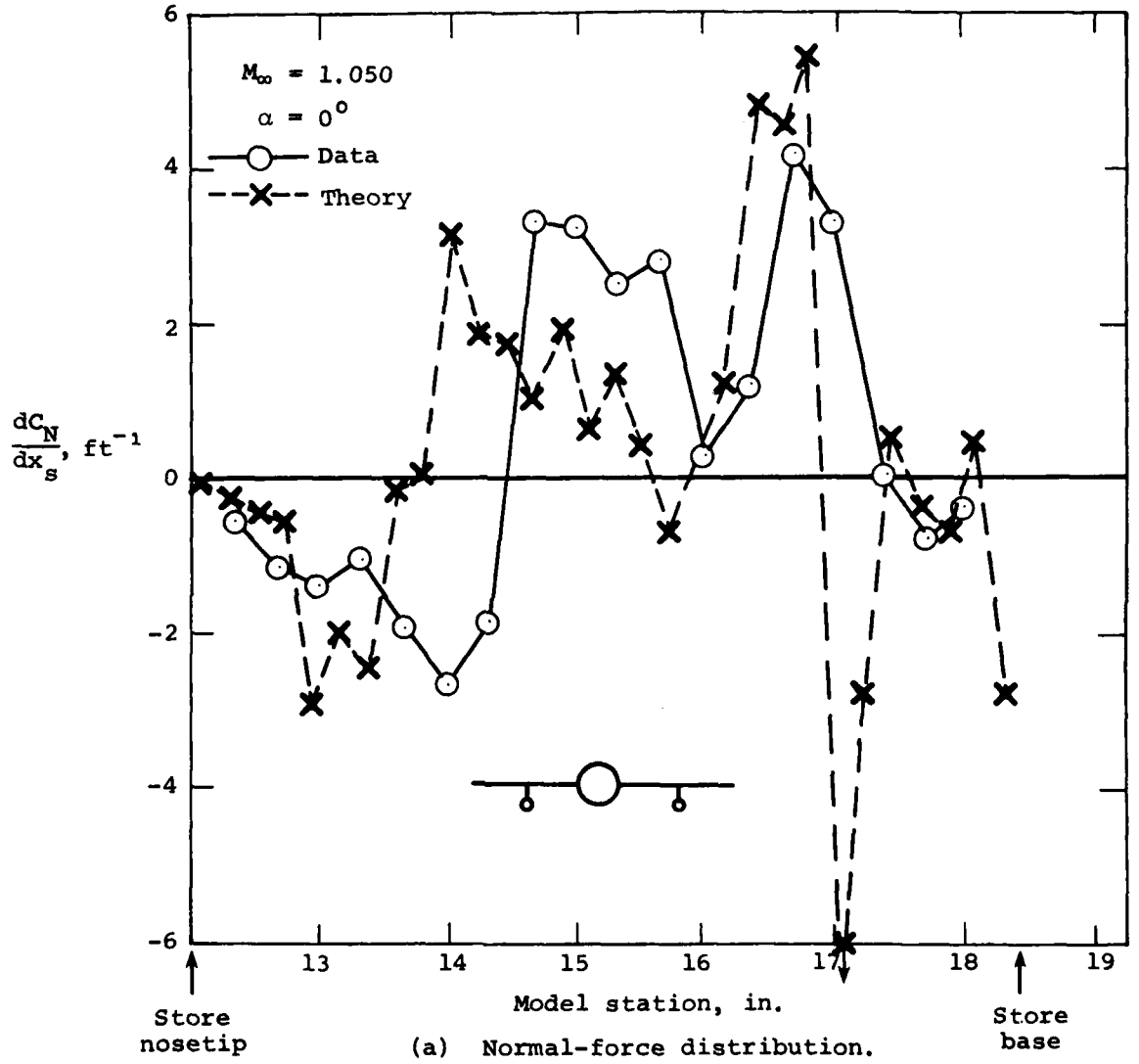

(a) Normal-force distribution.

Figure 29.- Comparison of measured and theoretical loading distribution for store attached to wing pylon. Theory uses flow field data as input to load calculations; M_∞ = 1.050, α = 0°, (y_s, z_s) = (3.5 in., -1.3 in.).

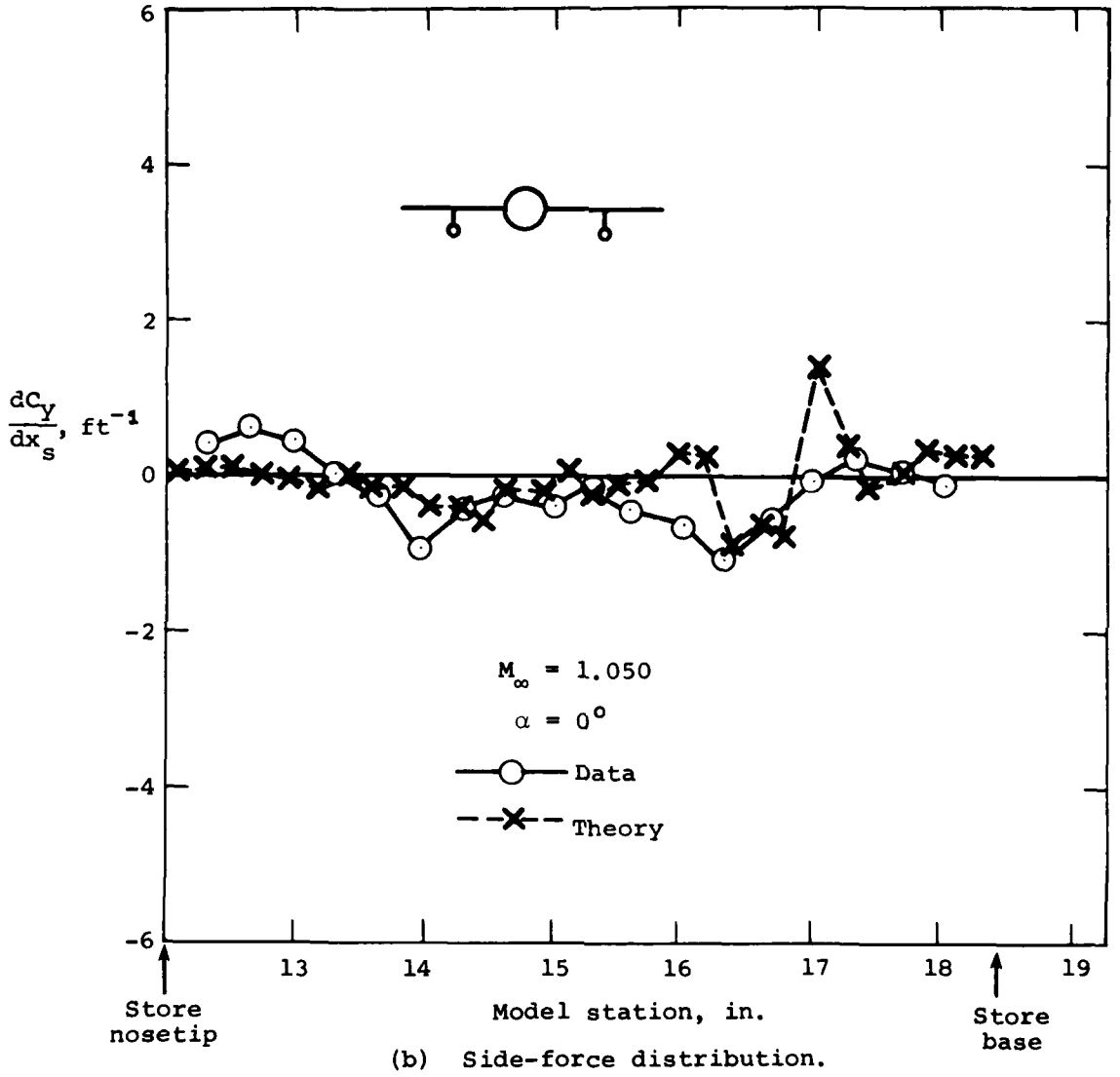

(b) Side-force distribution.

Figure 29,- Concluded.

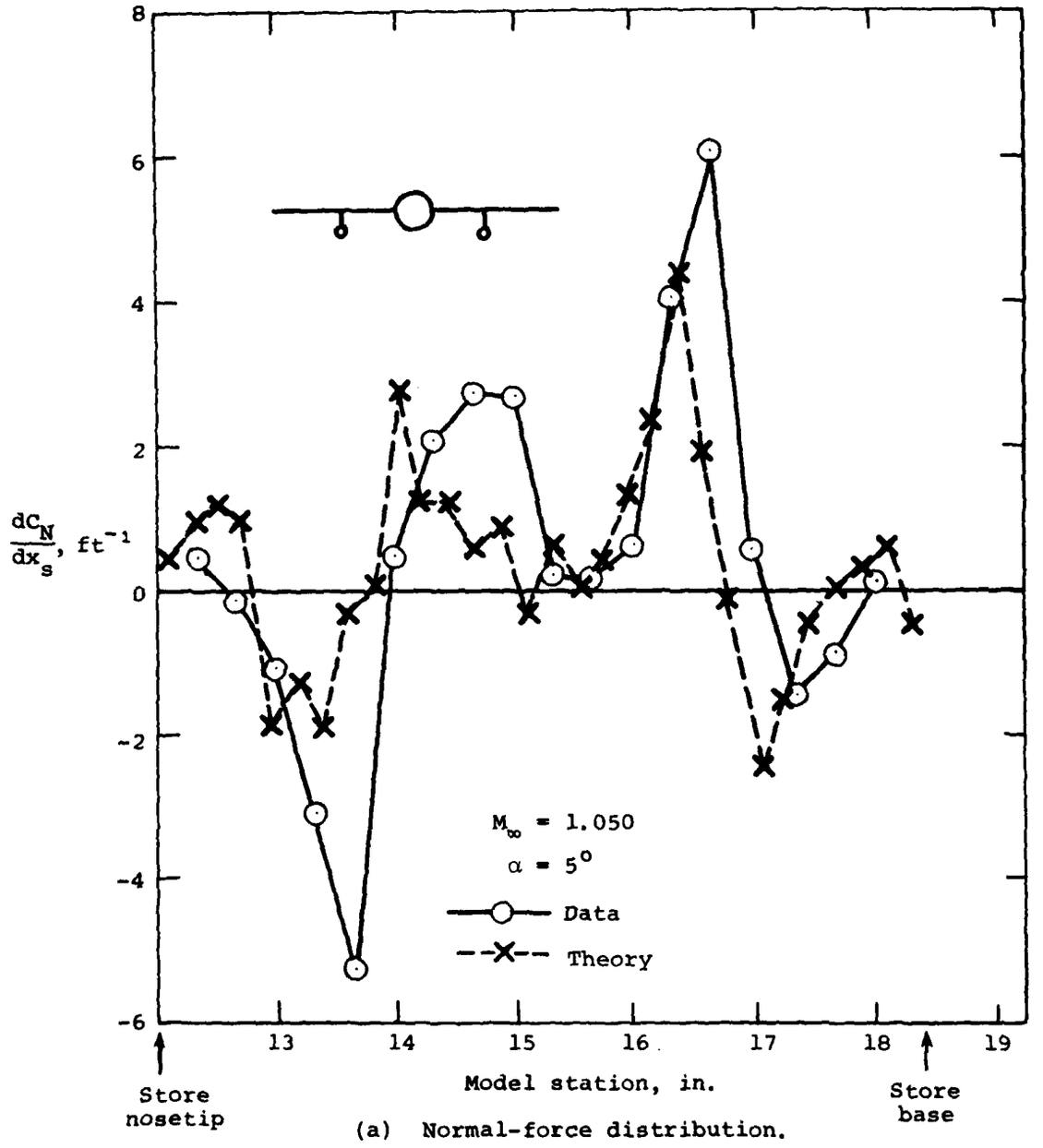

(a) Normal-force distribution.

Figure 30.- Comparison of measured and theoretical loading distributions for store attached to wing pylon. Theory uses flow field data as input to load calculations; M_∞ = 1.050, α = 5°, (y_s, z_s) = (3.5 in., -1.3 in.).

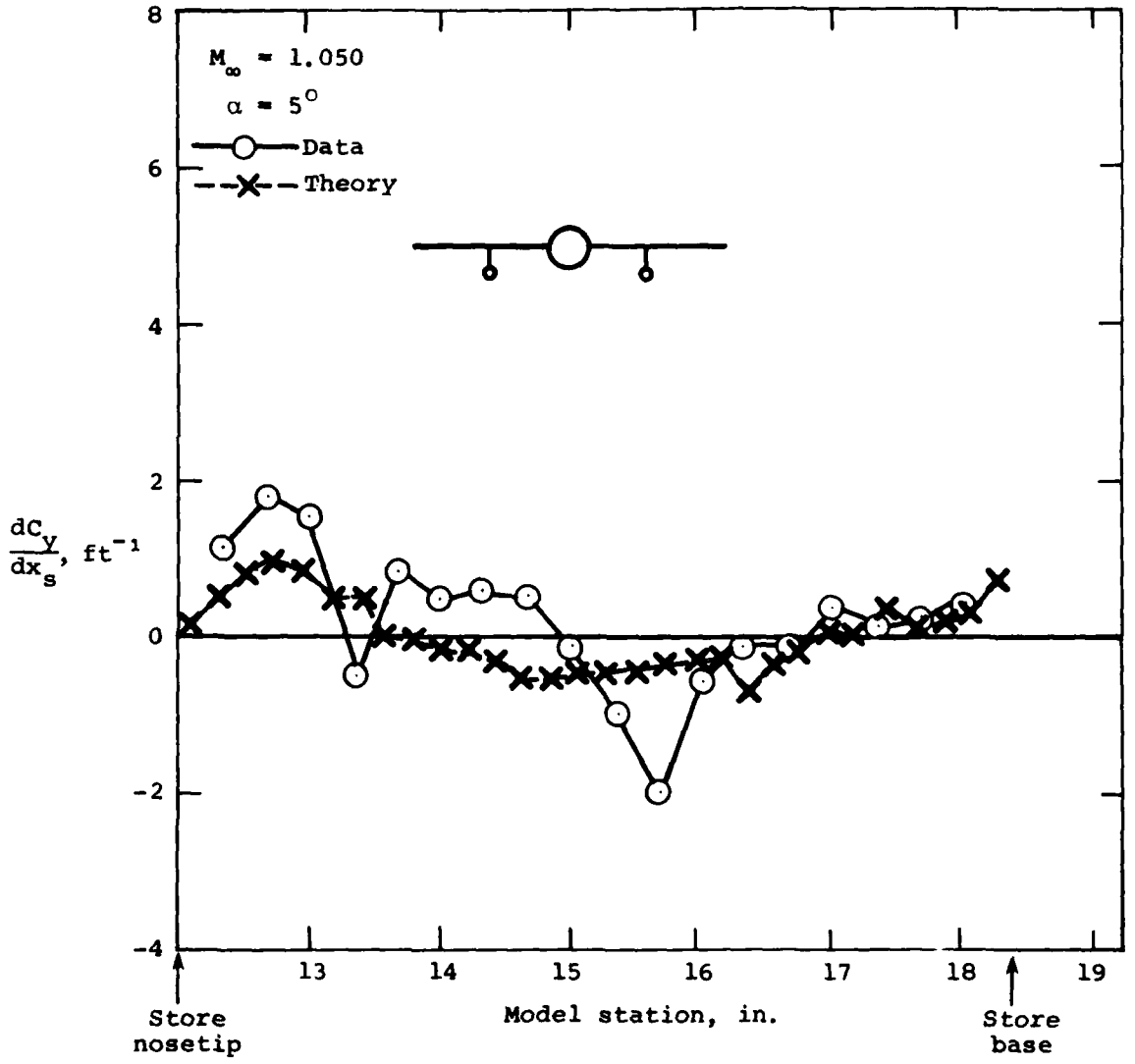

(b) Side-force distribution.

Figure 30.- Concluded.

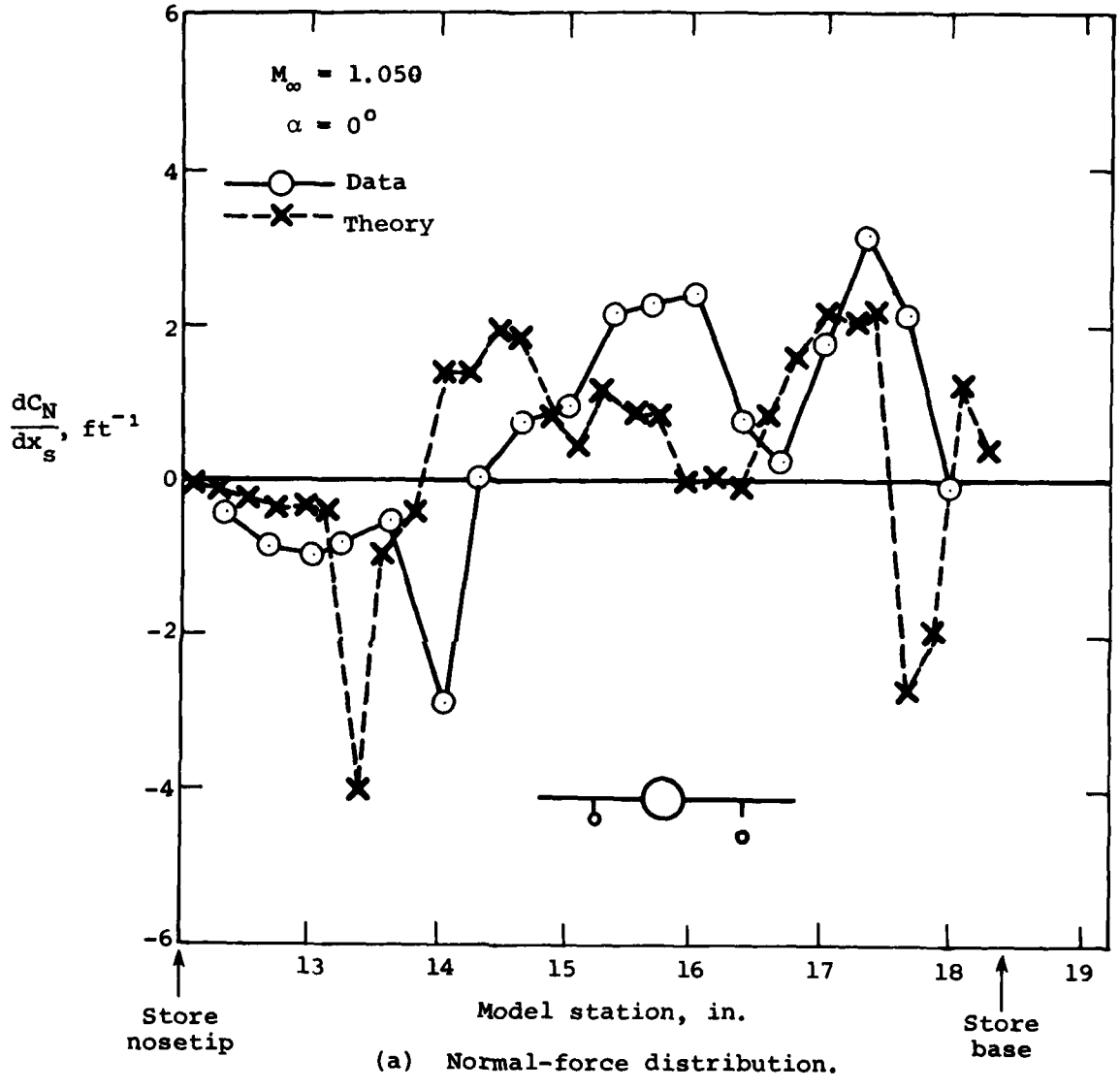

(a) Normal-force distribution.

Figure 31.- Comparison of measured and theoretical loading distributions for store separated from wing pylon. Theory uses flow field data as input to load calculation; M_∞ = 1.050, α = 0°, (y_s,z_s) = 3.5 in., -1.95 in.).

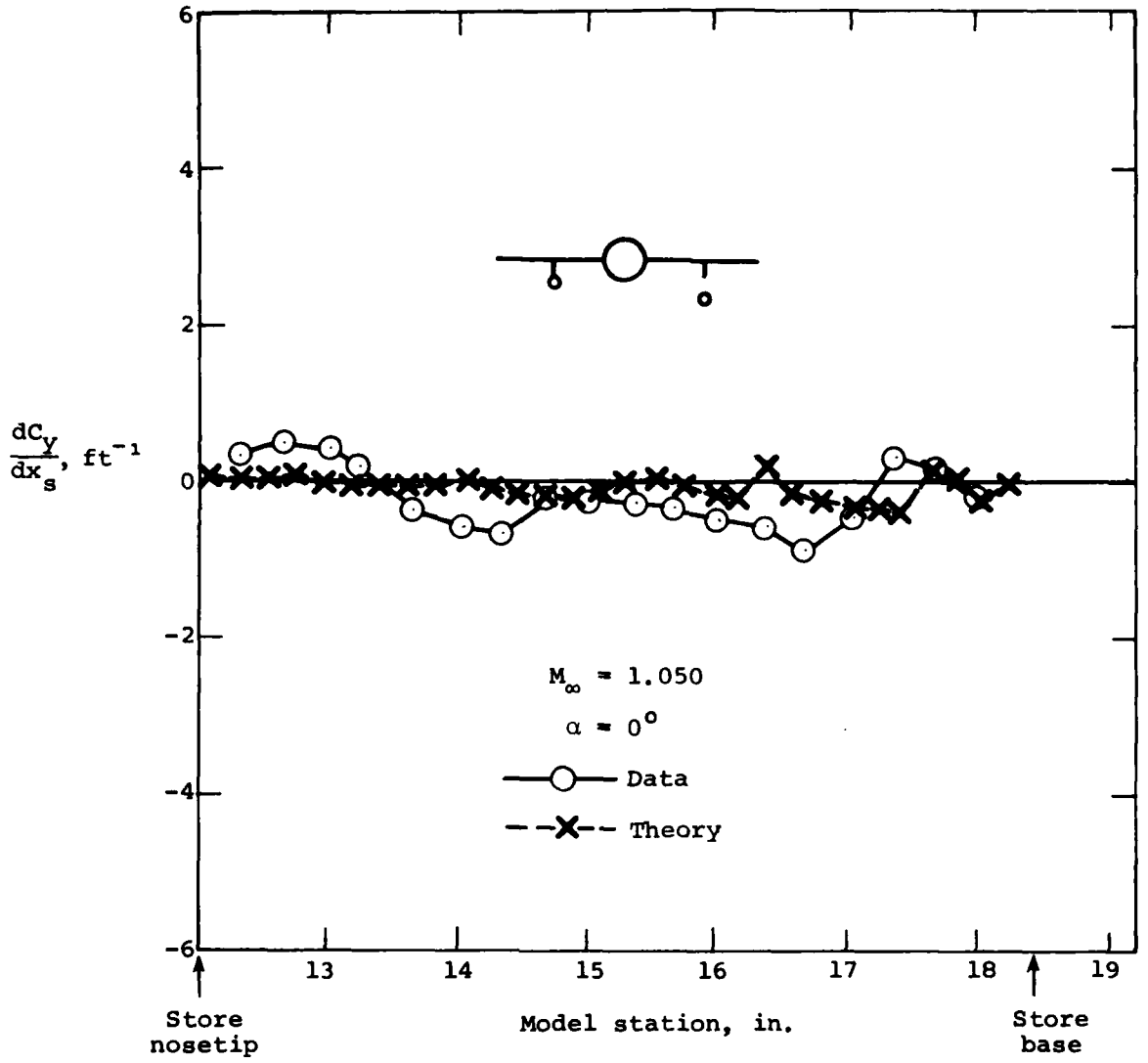

(b) Side-force distribution.

Figure 31.- Concluded.

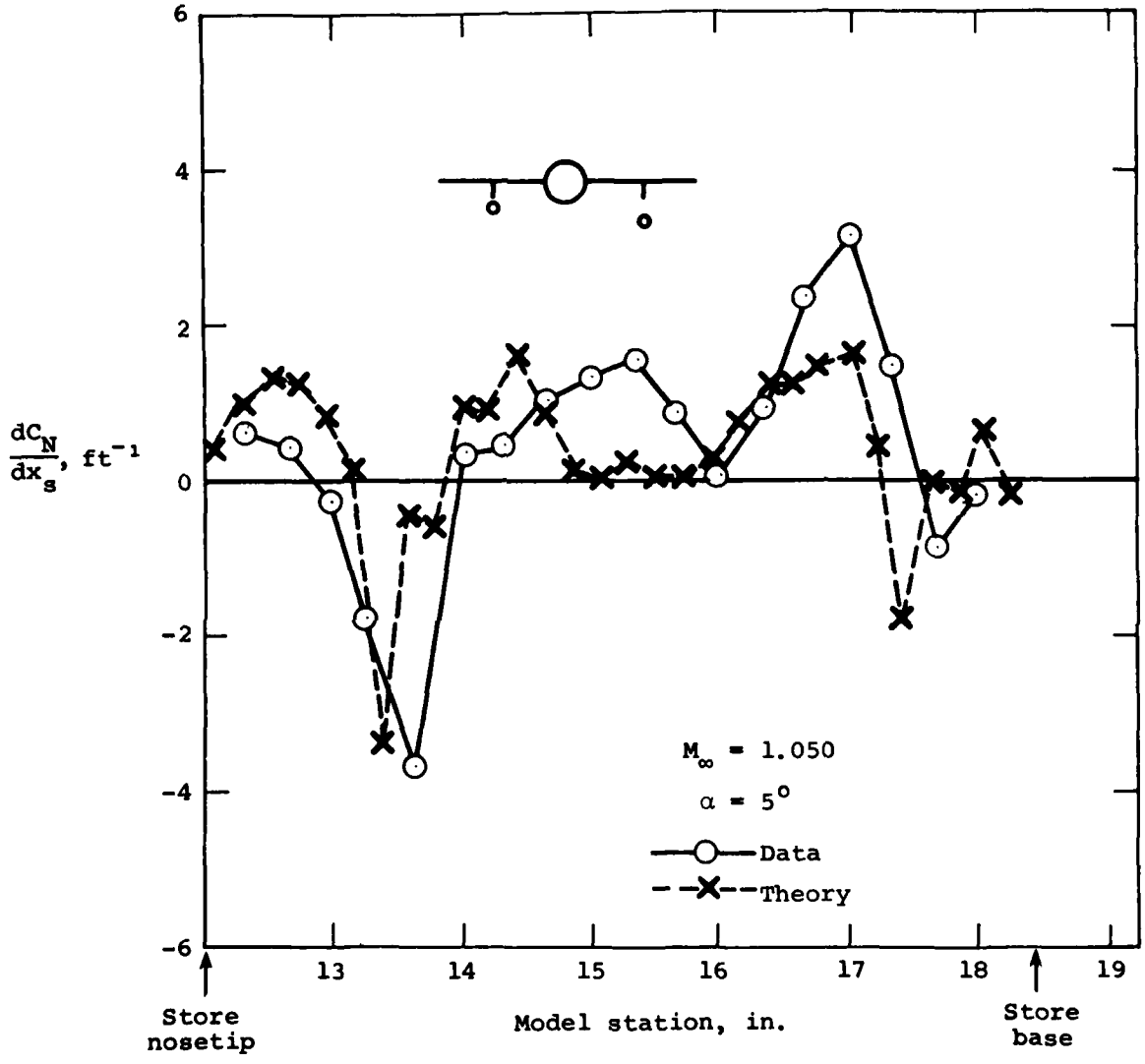

(a) Normal-force distribution.

Figure 32.- Comparison of measured and theoretical loading distributions for store separated from wing pylon. Theory uses flow field data as input to load calculation; M_∞ = 1.050, α = 5°, (y_s, z_s) = (3.5 in., -1.95 in.).

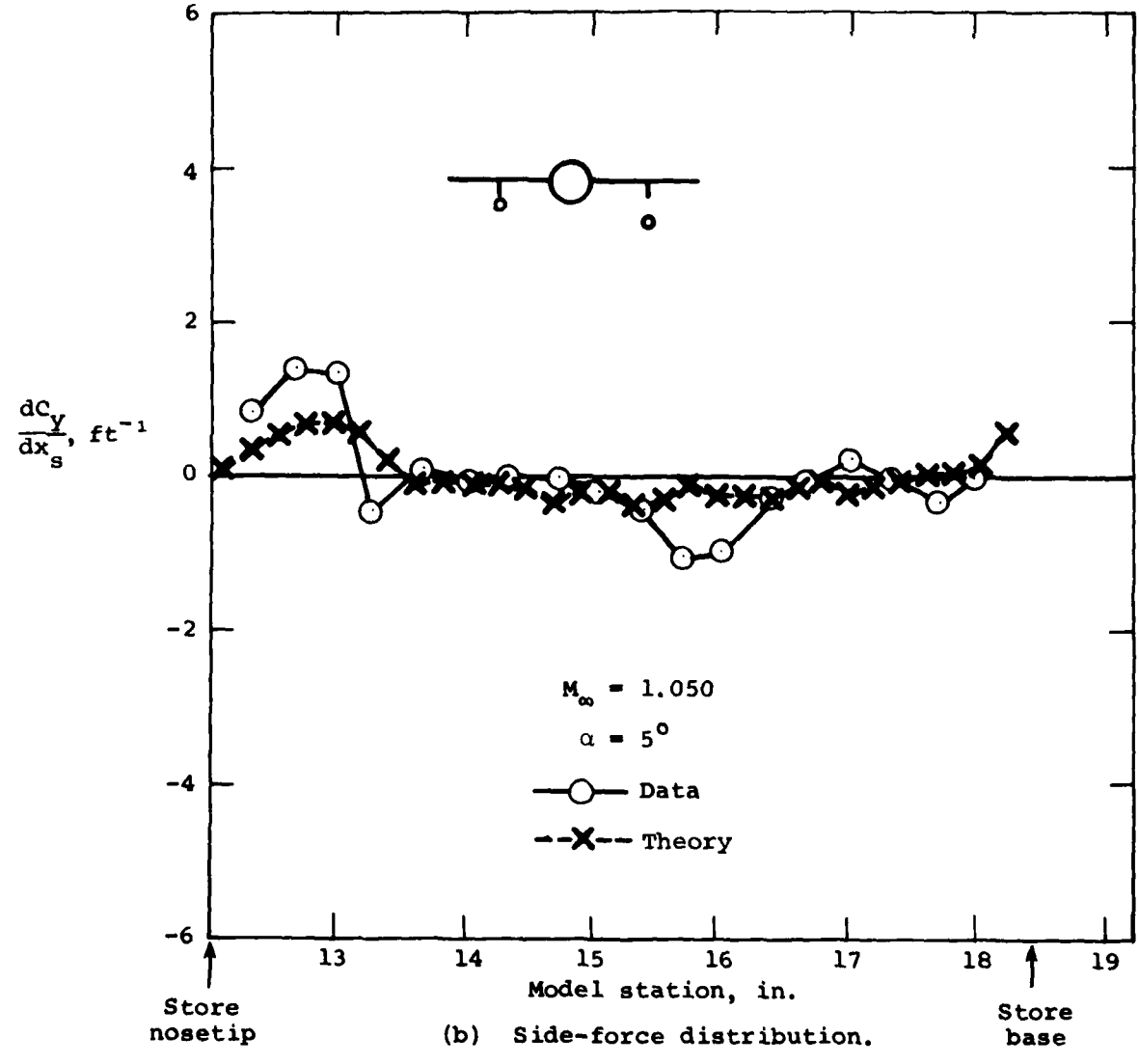

(b) Side-force distribution.

Figure 32.- Concluded.

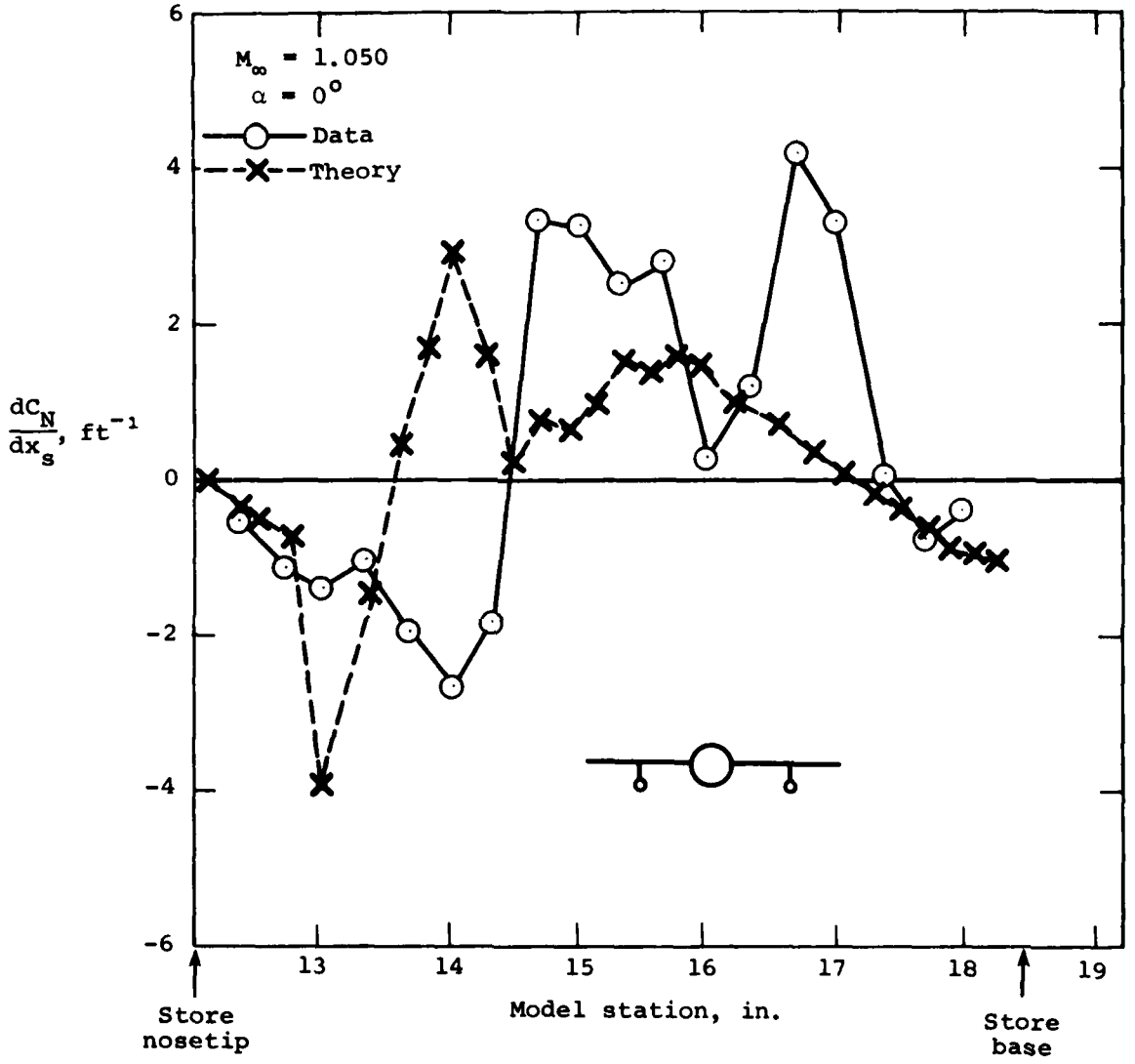

Figure 33.- Comparison of measured and theoretical normal-force loading distribution for store attached to wing pylon. Theory uses smoothed approximation to data of figure 28(a) as input to load calculation. M_∞ = 1.050, α = 0°, (y_s, z_s) = (3.5 in., -1.3 in.).

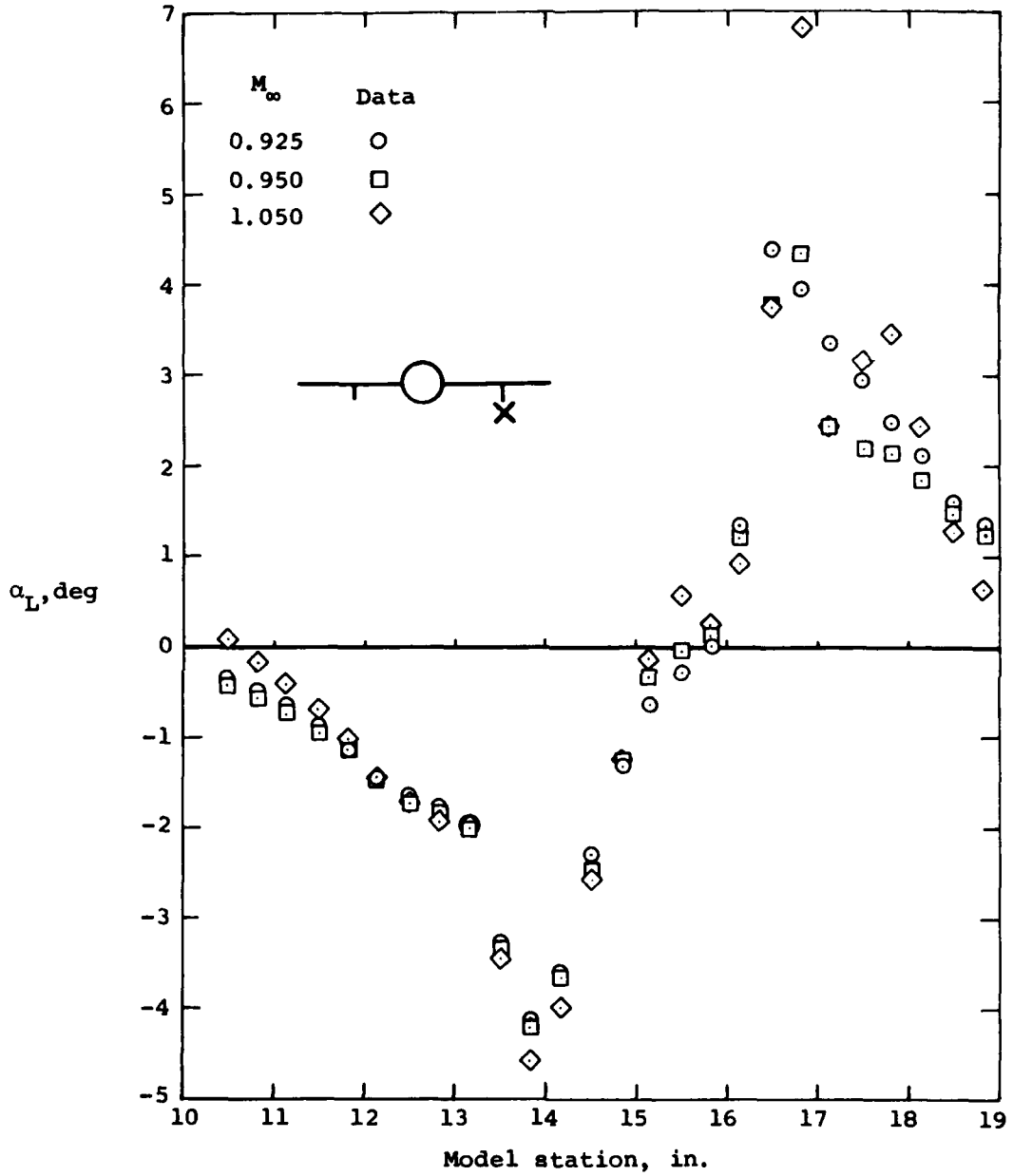

(a) $\alpha = 0^\circ$.

Figure 34.- Measured upwash for three Mach numbers for flow survey location near wing pylon; M_∞ = 0.925, 0.950 and 1.050, (y,z) = (3.5 in., -1.23 in.).

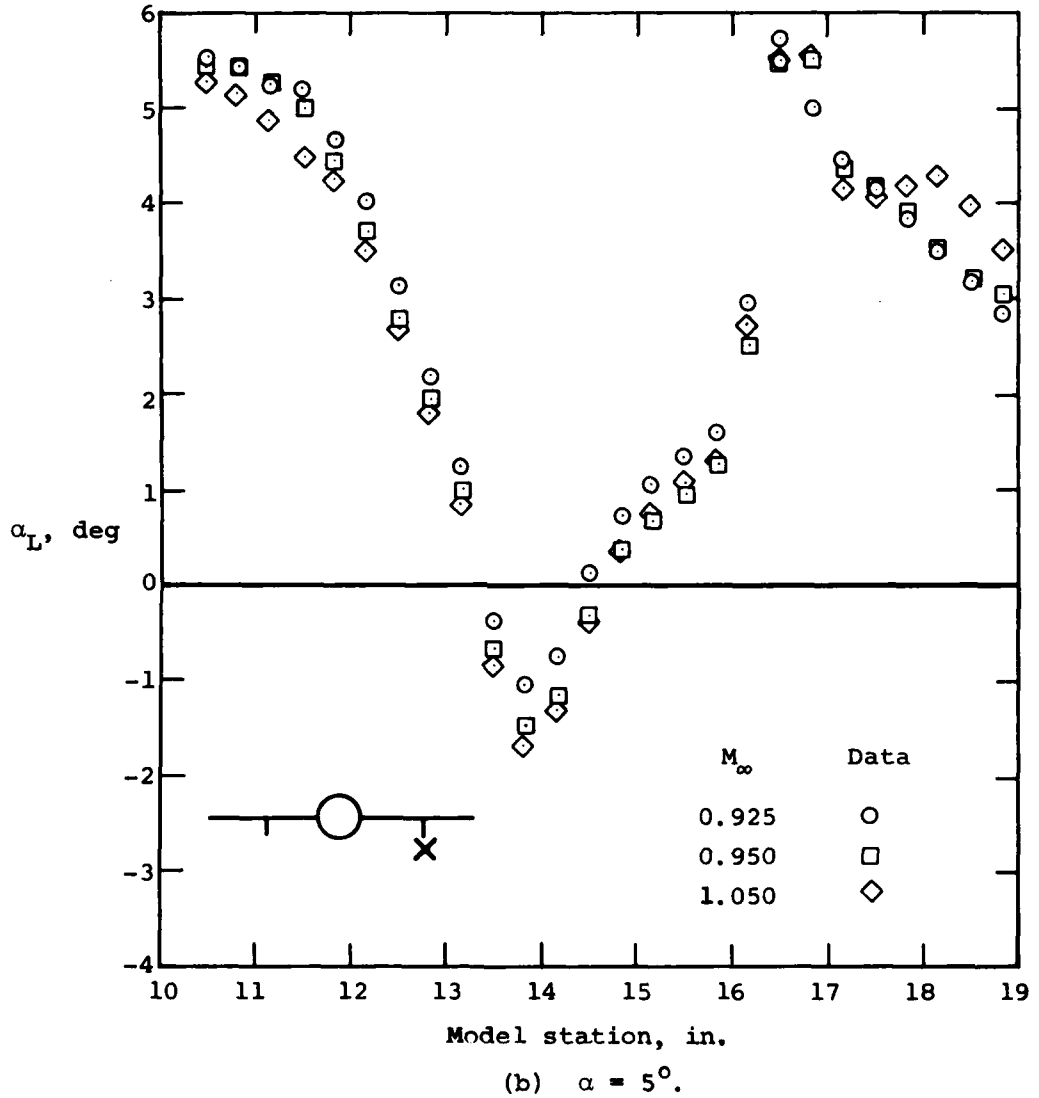

(b) $\alpha = 5^\circ$.

Figure 34.- Concluded.

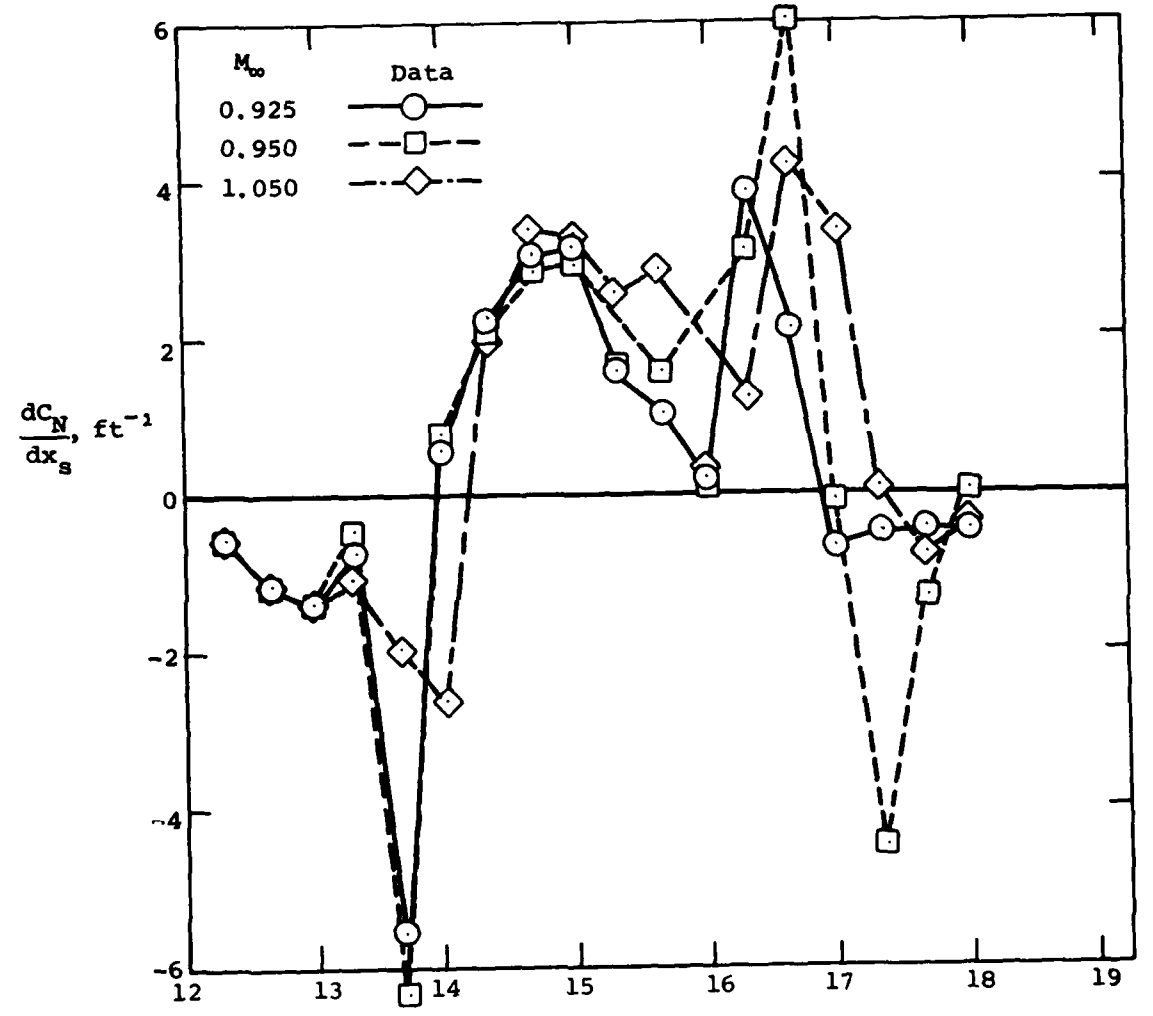

(a) $\alpha = 0^\circ$.

Figure 35.- Measured normal-force distributions for store attached to wing pylon for three Mach numbers; $M_\infty = 0.925$, 0.950 and 1.050, $(y,z) = (3.5$ in., -1.3 in.).

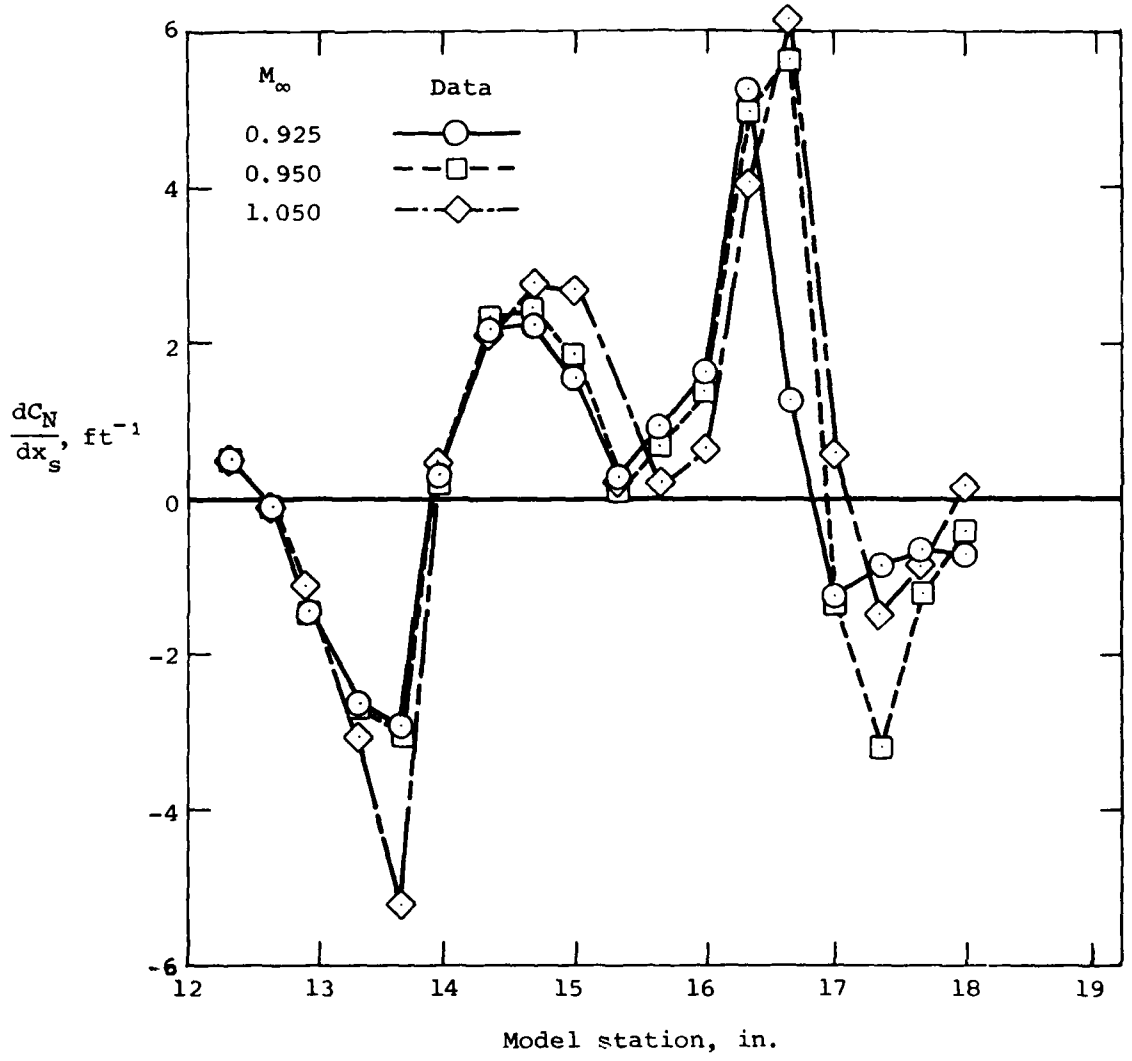

(b) $\alpha = 5^\circ$.

Figure 35.- Concluded.

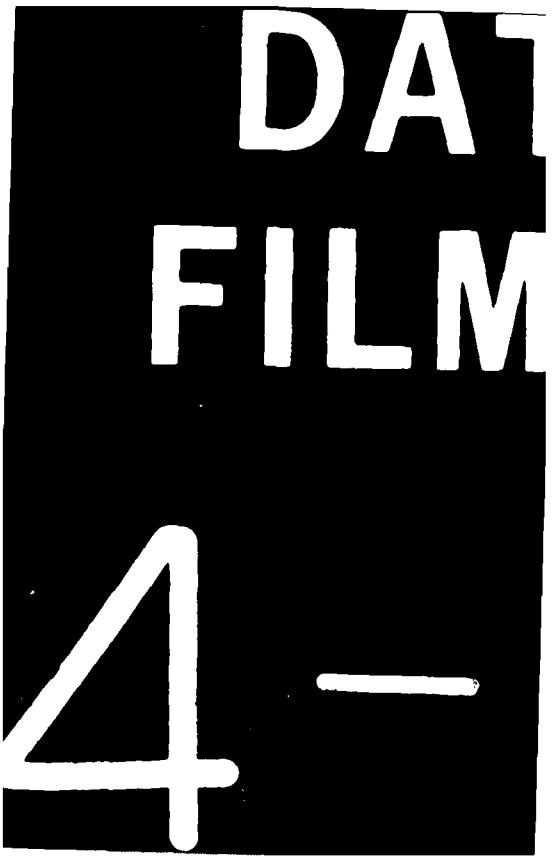
DA
FILM
4 —